

Investigation of Source Rock Potential and Micropaleontology
of the Middle Ordovician Hanadir Member of the Qasim
Formation, Northwestern Saudi Arabia

BY

Assad Hadi Ghazwani

A Thesis Presented to the
DEANSHIP OF GRADUATE STUDIES

KING FAHD UNIVERSITY OF PETROLEUM & MINERALS

DHAHRAN, SAUDI ARABIA

In Partial Fulfillment of the
Requirements for the Degree of

MASTER OF SCIENCE

In

GEOLOGY

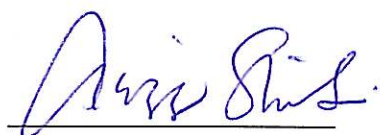
May 2012

KING FAHD UNIVERSITY OF PETROLEUM & MINERALS

DHAHRAN- 31261, SAUDI ARABIA

DEANSHIP OF GRADUATE STUDIES

This thesis, written by **Assad Hadi Ali Ghazwani** under the direction his thesis advisor and approved by his thesis committee, has been presented and accepted by the Dean of Graduate Studies, in partial fulfillment of the requirements for the degree of **MASTER OF SCIENCE IN GEOLOGY**.



Dr. Abdulaziz Al-shaibani
Department Chairman



Dr. Salam A. Zummo
Dean of Graduate Studies

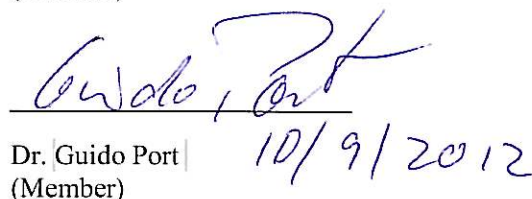
14/10/12
Date

 10-Oct.-12

Dr. Khalid Al-Ramadan
(Advisor)

 Oct. 9. 2012

Dr. Michael Kaminski
(Member)

 10/9/2012

Dr. Guido Port
(Member)

My sincere appreciation is dedicated to my parents, my wife N. Al-Khaldi and three children, Retaj, Mohammed, and Abdulhadi for their patience and support when I was attending MSc. degree courses and working on thesis project.

ACKNOWLEDGMENTS

I am very grateful to ALLAH, who provided me the opportunity, patience and time to accomplish this work. My sincere appreciations are due to all my thesis committee Dr. Khalid Ramadan, Dr. Michael Kaminski, and Dr. Guido Port for their invaluable contributions of the success of this research. Acknowledgment is due to King Fahd University of Petroleum and Minerals for supporting this research. All my course instructors, other faculty members and all staff of the department are thanked for their individual and collective assistance. Thanks go to Saudi Aramco, Exploration resource assessment department, geochemistry unit, geological technical service department, Saudi Aramco palynology lab for encouragement and support. My sincere appreciation to the following people, without the realization of this research would have been much more difficult if not impossible.

- I would like to say big thanks to the team leader of Northern play fairway mapping team leader Dr. William E Chandler for his unlimited support.
- Sincere appreciation due to Dr. Nigel Hooker, Dr. Marco Vecoli, Dr. Ertug Kaya, and Mr. Mohsen Eid for their help and support during palynology analysis work.
- Thanks to Dr. Sami Abdelbagi, Dr. Andreas Fuhrmann, Dr. Peter Jenden, Dr. Henry Halpern, Mr. Ahmed Hakami, Mr. Jaffar Dubaisi, Mr. Khalid Malki, Mr.

- Salman Qathami, and Mr. Ziyad Hellal for their support during geochemical analysis lab work.
- My thanks extended to Dr. Mahdi Abu Ali , Dr. Hong Xio and Mr. Abdulaziz Duaiji for their encouragement
- Great appreciation due to Dr. Lamedee Babola and Dr. Abdullah Al- Sultan for their help and support during the segregation process of foraminifera samples
- Thanks to my friends; Dr. Fawwaz M. Alkhaldi, Mr. Bander Gassal and my brothers Hassan and Mohammed Ghazwani for their great support and interest of this research.

TABLE OF CONTENTS

	Page
TITLE PAGE	i
APPROVAL SHEET	ii
DEDICATION	iii
ACKNOWLEDGEMENTS	iv
TABLE OF CONTENTS	vi
LIST OF TABLES	ix
LIST OF FIGURES	x
ABSTRACT (ENGLISH)	xiv
ABSTRACT (ARABIC)	xvi
CHAPTER ONE	1
INTRODUCTION	1
1.1 INTRODUCTION	1
1.2 OBJECTIVE OF STUDY	2
1.3 LOCATION OF THE STUDY AREA	3
1.4 PREVIOUS WORK AND LITERATUR REVIEW	5
1.4.1 Depositional Environment of Hanadir Member	14
1.4.2 Micropaleontology Review	19
1.4.3 Paleontology Review	22

CHAPTER TWO	25
GEOLOGICAL BACKGROUND	25
2.1 REGIONAL GEOLOGICAL SETTING	25
2.2 PALEOLATITUDE POSTION OF ARABIAN PLATE	27
2.3 HANADIR REGIONAL SOURCE ROCK EQUIVALENTS	30
 CHAPTER THREE	 36
WORKFOLOW AND METHODOLOGY	36
3.1 WORKFOLOW AND METHODOLOGY	36
3.1.1 GEOCHEMICAL ANALYSIS	39
3.1.2 Source Rock Sampling Procedure	39
3.1.3 Rock -Eval Pyrolysis Parameters	44
3.2 PALYNOLOGY SAMPLES PROCESS	48
3.3 MICROPALEONTOLOGY SAMPLES PROCESS	41
3.3.1 Process of Agglutinated Foraminifera Segregation and Selection	49
3.3.1 Agglutinated Foraminifera Description	58
3.4 BASIN MODELING	75
3.4.1 Numerical Simulation 1D Model	75
3.4.2 Input Data to Present Day Model	75
 CHAPTER FOUR	 79
DISCUSSION	79
4.1 HANADIR SOURCE ROCK POTENTIAL	79
4.1.2 Quality of Organic Matter of Well-A	79
4.1.3 Type of Organic Matter and Thermal Maturity of Well-A	84

4.1.4 Quality of Organic Matter of Well-B	87
4.1.5 Type of Organic Matter and Thermal Maturity of Well-B	91
4.1.6 Quality of Organic Matter of Well-C	94
4.1.7 Possible Effect of Contamination Observed in Well-C	97
4.2 FURTHER ELEMENTAL ANALYSIS	101
4.3 MICROPALAEONTOLOGY RESULTS	104
4.3.1 New Approach to Predict Hanadir Kerogen Type	110
4.4 PALYNOLOGY RESULTS	116
4.4.1 Palynology Samples Analysis and Thermal Maturity Interpretation	116
4.5 BASIN MODELING	123
4.5.1 Structural Restoration	123
4.5.2 Calibration Data of Basin Models and Limitation	124
4.5.3 Two Different Scenarios of Heat Flow	124
4.5.4 Thermal and Burial History of Well-A	127
4.5.5 Thermal and Burial History of Well-B	130
4.5.6 Thermal and Burial History of Well-C	133
CONCLUSIONS	138
RECOMMENDATIONS	140
REFERENCES	141
APPENDIX Rock-EVAL Table Results	147
VITAE	149

LIST OF TABLES

	Page
Table 1.1: Regional correlation of Hanadir equivalents in the Arabian plate during MFS O30	18
Table 1.2: Summary of discovered agglutinated foraminifera	21
Table 1.3: Summary of most recovered Acritachs and Chitinozoans assemblages from lower and middle Ordovician Central Arabia	24
Table 2.1: Regional Middle Ordovician source rock equivalents to Hanadir and their hydrocarbon potential	35
Table 3.1: Example of main input data to numerical simulation 1D model	77
Table 3.2: Main input for boundary conditions	78
Table 4.1: Geochemical parameters used to evaluate Hanadir source rock potential of well-A	82
Table 4.2: Geochemical parameters used to evaluate Hanadir source rock potential of well-B	89
Table 4.3: Geochemical parameters used to evaluate Hanadir source rock potential of well-C	95
Table 4.4: Summary of source rock organic facies identified based on relationship between oxygen content and benthic foraminifera environments	113
Table 4.5: Depth of collected samples for palynology analysis	117

LIST OF FIGURES

	Page
Figure 1.1: Location map of study area with three selected wells	4
Figure 1.2: Simplified geological map of Paleozoic distribution rock in the northernwest Saudi Arabia	7
Figure 1.3a: Isopach map showing increased thickness of Qasim Formation	9
Figure 1.3b: Schematic cross section of Qasim Formation showing increased thickness toward Northeast of Al-Jauf graben	9
Figure 1.4: Basement depth map of the Arabian plate	10
Figure 1.5: History of the lithostratigraphic classification within the lower Paleozoic succession of Saudi Arabia	12
Figure 1.6: Generalized lower Paleozoic stratigraphy column of the Qasim and Hail regions	13
Figure 1.7: Depositional model of Hanadir member	15
Figure 1.8: Outcrop photograph of Hanadir and Kahfa members	16
Figure 1.9: playnomorphys occurrence during geological times	23
Figure 2.1: Structural map showing the location of e major tectonic elements of the Arabian plate	26
Figure 2.2: Paleogeogaphic map of Gondwana during late of Ordovician	28
Figure 2.3: Paleolatitude map of the Arabian plate during late Ordovician	29
Figure 2.4: Paleo depositional environment map of Middle Ordovician, representing major shallow marine covered almost entire Arabian plate	31
Figure 2.5: Regional Paleozoic Stratigraphic column of Akkas field in North Iraq correlated with Middle Hanadir in Saudi Arabia	33

Figure 3.1:	Systematic workflow of different methods have been integrated and applied in this study	38
Figure 3.2:	Photos showing the process of identifying source rock zone	40
Figure 3.3:	Correlation of the Hanadir thickness of the three selected wells	42
Figure 3.4:	A core photo taking for recovered core of well-A, reflecting source rock heterogeneity	43
Figure 3.5a:	A photo of rock-eval machine used to conduct rock – eval pyrolysis	47
Figure 3.5b:	Schematic of rock-eval pyrolysis process with different output parameters	47
Figure 3.6:	A photo showing the materials needed for segregation of agglutinated Foraminifera	51
Figure 3.7	A photo showing a process of agglutinated foraminifera segregation	53
Figure 3.8:	A photo showing a process of agglutinated foraminifera microscopic examination	55
Figure 3.9:	A photo showing a process of agglutinated foraminifera description	57
Figure 4.1:	Geochemical log of rock-eval and TOC results from well-A	81
Figure 4.2:	A plot of remaining hydrocarbon potential of Hanadir for well -A	83
Figure 4.3:	A plot of pseudo Van Krevelen diagram of well-A	85
Figure 4.4:	A plot of hydrogen index against Tmax of well-A	86
Figure 4.5:	Geochemical log of rock-eval and TOC results from well-B	88
Figure 4.6:	A plot of remaining hydrocarbon potential of Hanadir for well -B	90
Figure 4.7:	A plot of pseudo Van Krevelen diagram of well-B	92
Figure 4.8:	A plot of hydrogen index against Tmax of well-B	93
Figure 4.9:	Geochemical log of rock-eval and TOC results from well-C	96
Figure 4.10:	A plot of organic matter conversion of well-C	98

Figure 4.22b: Calibration between predicted and measured present day temperature in well-B	131
Figure 4.22c: The evolution of thermal maturity of Hanadir during geological time in well-B	131
Figure 4.23 A burial history of well-A showing the evolution of sedimentary basin through geological time	132
Figure 4.24a: Calibration between predicted and measured vitrinite reflectance in well-C	134
Figure 4.24b: Calibration between predicted and measured Present day temperature in well-C	134
Figure 4.24b: The evolution of thermal maturity of Hanadir during geological time in well-C	134
Figure 4.25: A burial history of well-C showing the evolution of sedimentary basin through geological time and effect of igneous intrusion	135
Figure 4.26a: Geochemical log of rock-eval showing the igneous intrusion and effect of fluid contamination on rock-eval analysis	137
Figure 4.26b: 1D model of predicted vitrinite reflectance at zone of igneous intrusion in well-C	137
Figure 4.26c: A photo showing igneous fragment recognized from cutting samples	137

Figure 4.11: Bimodal histogram of Tmax showing two different temperatures	100
Figure 4.12: Location map showing three sites where source rock samples collected for elemental analysis	102
Figure 4.13: Results of elemental analysis at ternary plot of Qasim Formation	103
Figure 4.14: Conceptual morphogroup model representing the response of agglutinated foraminifera to redox conditions	106
Figure 4.15a: Microscopic photo of recovered Pasammosphera species from Hanadir as Indication to dysoxic condition in well-C	107
Figure 4.16: Systematic approach used to predict Hanadir kerogen type	111
Figure 4.17: Predicted source rock organic facies based on oxygen content and depostional factors	122
Figure 4.18: Color of thermal alteration index	113
Figure 4.19a: Present daytemperature using 52 Mw/m ² scenario for heat flow	126
Figure 4.19b: Present day temperature using 72 Mw/m ² scenari of heat flow	126
Figure 4.20a: Calibration between predicted and measured vitrinite reflectance in well-A	128
Figure 4.20b: Calibration between predicted and measured present day temperature in well-A	128
Figure 4.20c: The evolution of thermal maturity of Hanadir during geological time in well-A	128
Figure 4.21: A burial history of well-A showing the evolution of sedimentary basin through geological time	129
Figure 4.22a: Calibration between predicted and measured vitrinite reflectance in well-B	131

THESIS ABSTRACT

Full Name : [Assad Hadi Ghazwani]
Thesis Title : Investigation of Source Rock Potential and Micropaleontology Of
[Middle Ordovician Hanadir Member Of Qasim Formation,
Northwestern Saudi Arabia]
Major Field : [GEOLOGY]
Date of Degree : [May,2012]

The main purpose of this study is the evaluation of the geochemical source potential of the Middle Ordovician (Llavirnian) Hanadir member of the Qasim Formation in the North West of Saudi Arabia. Cuttings and cores from three wells (A, B, and C) were subjected to Rock-Eval pyrolysis. Additionally, micropaleontological and palynological analyses were conducted to reveal the depositional environment and thermal maturity of the Hanadir. Numerical simulations of 1D basin models were performed for all three wells to support the understanding of the geologic evolution of the Hanadir member. The wells used for this study are located at NE flank of the NW-SE oriented Al Jauf Graben near the border to Jordan. While this tectonic feature was mainly active during the Cretaceous, there is evidence that it already formed during Cambrian times. The average thickness of the Hanadir member in all three wells is about 300 ft. Recently the discovered oldest Paleozoic agglutinated foraminifera analysis suggests the organic matter of the Hanadir member in wells A and B is preserved in anoxic conditions, where in well C it was not preserved in total anoxic bottom water conditions; it may be exposed seasonally to dysoxic conditions. Regionally Hanadir can be correlated with Hiswa

Formation in Jordan because they both representing maximum flooding surface MFSO30 during Middle Ordovician and have similar sediment facies .Geochemically the present day organic matter of Hanadir can be correlated with present day organic matter of Hiswa Formation in Jordan because they are both highly mature type II kerogen with range of total organic carbon between 0.5 -2.98% (TOC) in Hanadir and 1.3 -1.5% (TOC) in Hiswa formation and considered as main source of gas in Jordan. All integrated results obtained from Rock-Eval of wells A and B indicates the source rock of the Hanadir is in gas generation window as indicated by low HI, high Tmax, high vitrinite reflectance and present day temperature which implies the Hanadir member is possibly another candidate Paleozoic source rock to be the main source of gas in Northwest of Saudi Arabia.

ملخص الرسالة

الاسم الكامل: اسعد هادي علي غزواني

عنوان الرسالة: التحقيق في احتمالية وجود صخر مصدر البترول والاحافير الدقيقة لحقبة الأردوفيشي الأوسط لعضو الحنادر من متكون القصيم في شمال غرب المملكة العربية السعودية.

التخصص: الجيولوجيا

تاريخ : مايو 2012 م

الهدف الرئيسي من هذه الدراسة هو التقييم الجيوكيميائي للمواد العضوية لصخر البترول لعضو حنادر من متكون القصيم والذي يمثل حقبة الأردوفيشي الأوسط في شمال غرب المملكة العربية السعودية. لقد اجريت دراسة تحليل الانحلال الانحراري والاحافير الدقيقة والمواد العضوية على كل من الفتات الصخري والعينات اللبية الصخرية للأبار (أ، ب، ت) وذلك للكشف عن بيئته الترسيب ومدى النضج الحراري لعضو الحنادر.

كما اجريت عمليات محاكاة رقمية لنماذج الاحواض الترسيبية لجميع الأبار لفهم التطور الجيولوجي لعضو الحنادر. تقع الآبار المستخدمة لهذه الدراسة في الجزء الشمال الشرقي من حوض الجوف بالقرب من حدود الاردن . هذه الحوض كانت نشطه بشكل رئيسي خلال حقبة الطباشيري وهناك ادلة على انها تشكلت بالفعل خلال حقبة الكامبري. يصل متوسط سماكة عضو الحنادر في الآبار الثلاثة الى 300 قدم.

لقد تم الكشف مؤخرا" على اقدم الاحافير الدقيقة في حقبة الحياة القديمة (المتقبات الملتصقة) في عضو الحنادر. هذه الاحافير تشير الى ان المواد العضوية لصخر الحنادر في البئر (أ و ب) ترسبت في بيئة مختزلة بينما في البئر (ت) تعرضت موسميا" الى بيئة ترسيب شبيه مختزلة . اقليميا" عضو الحنادر يمكن ان يقارن بمكون حسوة في الاردن لإنهما يمثلان اقصى مد خلال حقبة الأردوفيشي الأوسط ولهما نفس سحنة الصخور.

جيوكيميائيا" فإن المواد العضوية في الوقت الحاضر لعضو الحنادر يمكن مقارنتها بمتكون حسوة لإنهما ناضجين حراريا" ويتبعان النوع الثاني من الكيروجين حيث ان المواد العضوية في الحنادر تتراوح ما بين 0.5-2.98 % بينما متكون حسوة تتراوح ما بين 1.3- 1.5 % ويعتبر متكون حسوة مصدر الغاز الرئيسي في الاردن. جميع النتائج المتحصل عليها من الإنحلال الحراري في الآبار (أ وب) كانخفاض مؤشر الهيدروجين وارتفاع درجة الحرارة تؤكد ان صخر المصدر لحنادر في حالة توليد الغاز والتي توحى بأن عضو الحنادر مرشحا" أن يكون احد مصادر الغاز لصخر البترول في حقبة الحياة القديمة في شمال غرب المملكة العربية السعودية.

CHAPTER ONE

INTRODUCTION

1.1 INTRODUCTION

Hanadir, is the lower member of Qasim Formation consists, of graded silty laminae. It represents potential source rock that was not comprehensively sampled and geochemically analyzed. This study investigates the source rock potential of the Middle Ordovician (Llavirn) Hanadir in the North West of Saudi Arabia. Three selected wells are used for this study. These wells are located at NE flank of the NW-SE oriented Al Jauf graben near the border to Jordan. This tectonic feature was mainly active during the Cretaceous. Geochemical analyses using Rock-Eval pyrolysis method has been conducted and integrated with other analyses such as, micropaleontology and palynology to understand the depositional environment and evaluate thermal maturity of Hanadir member. Additionally numerical simulations of 1D basin models were performed for all three wells to support the understanding of the geologic evolution during Middle Ordovician.

1.2 OBJECTIVE OF THE STUDY

Hanadir member of the Qasim Formation represents Middle Ordovician (Llanvirn) age. Hanadir source rock generative potential was not systematically sampled and geochemically analyzed. The main purpose of this study is to assess Hanadir source rock generative potential from three selected wells (A, B, and C) in the Northern west of Saudi Arabia with average thickness is about 300ft. additionally integrate other analyses such as , micropaleontology and palynology and 1D basin models.

The objectives of the thesis study are to:

- Assess source rock potential of Hanadir using Rock-Eval Pyrolysis method.
- Understand Hanadir source rock depositional environment through agglutinated Foraminifera.
- Assess level of maturity of Hanadir shale through several methods, such as *Chitinozoans* and *Acritarchs* color index, and calculated vitrinite reflectance equivalent.
- Create 1D numerical simulation model to understand the geological evolution of stratigraphic layers.

1.3 LOCATION OF STUDY AREA

Three wells (A, B, and C) located on the Northwestern of Saudi Arabia are selected to conduct integrated studies including geochemical, micropaleontological, and basin modeling analysis. These wells are located at NE flank of the NW-SE oriented Al Jauf graben near the border to Jordan. This tectonic feature was mainly active during the Cretaceous (Fig 1.1).

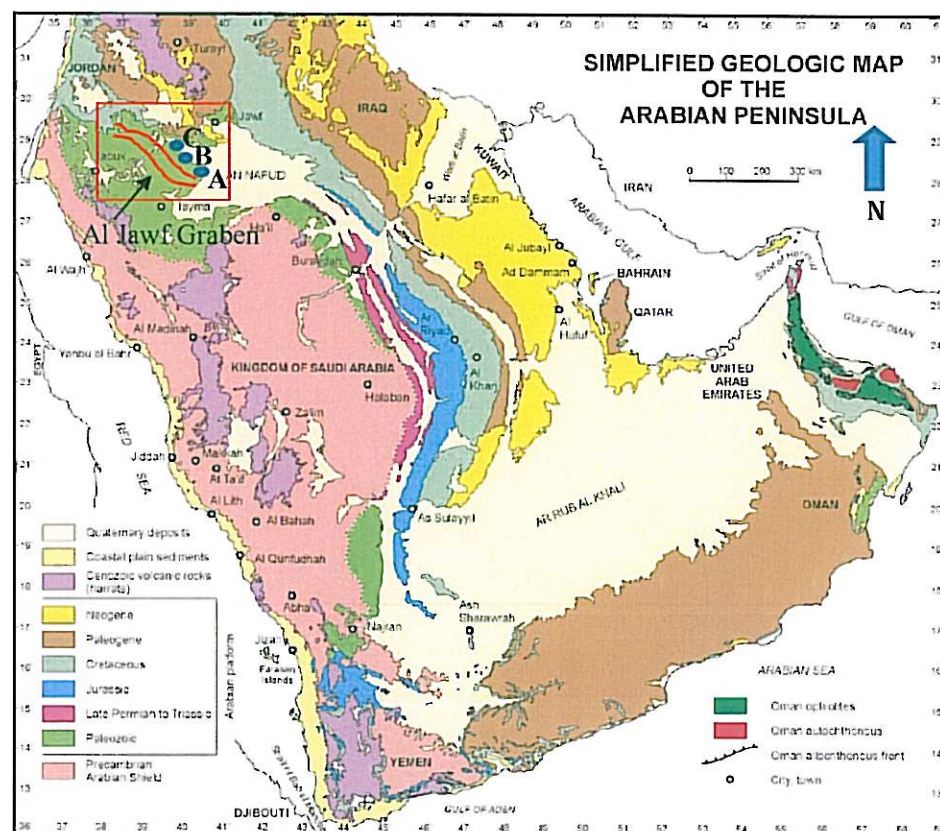


Figure 1.1: Location map of study area showing three selected wells (A, B, and C) are located close to Al Jawf graben, these wells were selected to assess the source rock generative potential of the Hanadir in northwestern Saudi Arabia. (after Le Nindre et al, 2003).

1.4 PREVIOUS WORK AND LITERATURE REVIEW

Qasim Formation was studied by many workers and correlated in subsurface with many wells drilled in the north and east of Saudi Arabia. The Qasim Formation was first defined and published by Williams and others (1968) in the Jabal Habashi quadrangle in Qasim region. As reported by (Janjou et al., 1997), the Early to Late Ordovician marine /shallow marine deposits of the Qasim Formation (Hanadir, Kahafa, Ra'an and Quwarah members) are exposed to the Tayma -Tabuk regions (Fig 1.2). Janjou and others (1997) documented the deposition of the Qasim Formation is locally marked by incised glacial paleovalleys. The upper layers of the Qasim Formation are systematically eroded to variable depths by network of incised paleovalleys that developed during the drop in sea level associated with the onset of the Late Ordovician glaciation. The members of Qasim Formation are arranged in two siliciclastic coarsening and thickening-upward progradational sequences, the two siliciclastic progradational of Qasim Formation sequences started deposition with basal shale/siltstone and an overlying sandstone member.

Vaslet and others, reported 358 m thick section of Qasim Formation in the Tayma quadrangle. In the Qalibah quadrangle, 91m thick section of the Qasim Formation is exposed. The section consists of 69m Ra'an Member and 22m Quwarah Member. The top of Qasim Formation was cut deeply by the Sarah Formation. In the Tabuk quadrangle, (Janjou and others, 1997) included the Qasim Formation in the Tayma

Group. They reported that the Qasim Formation is 308 m thick and all the four members of the formation are well exposed in the entire Tabuk quadrangle. (Janjou and others, 1997) recognized a possible hiatus may exist between Qasim and Saq Formations, as indicated by the lag deposits at the base of Qasim Formation. The depostional environments of the four members of the Qasim were first documented by (Senalp and Al-Duaiji, 1996) and they produced a subsurface isopach map of the Qasim Formation, based on information from 176 wells drilled either for exploration by Saudi Aramco or for water by the Ministry of Agriculture.

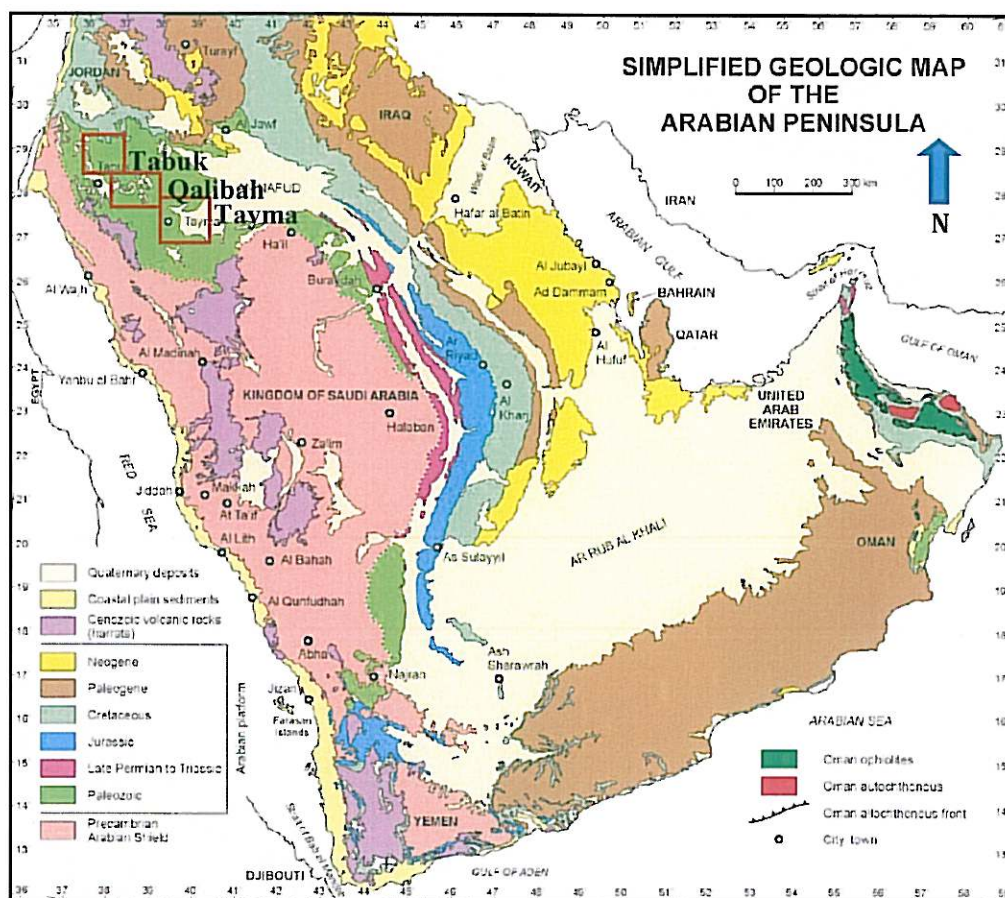


Figure1.2: Simplified geologic Map of the Arabian Peninsula (after Le Nindre et al, 2003). Note the distribution Paleozoic rocks in the Northwest part of Saudi Arabia. The area of study shows the quadrangles of Tabuk, Tayma regions.

Thickness of Qasim Formation increases gradually from northwest toward northeast. It is about reached 500 feet thick at Qalibah regions and reached up to 5500 feet as the maximum thickness at Jalamid region. A schematic cross section illustrates the increased thickness towards northeast (Fig 1.3. a, b). Additionally the Arabian plate depth to basement map indicate basins configuration was developed towards northeast at Jalamid area where the thickest sediments of Qusaiba and Qasim were encountered (Konert et al., 2001) and other areas such as eastern and Rub Alkhali areas (Fig 1.4)

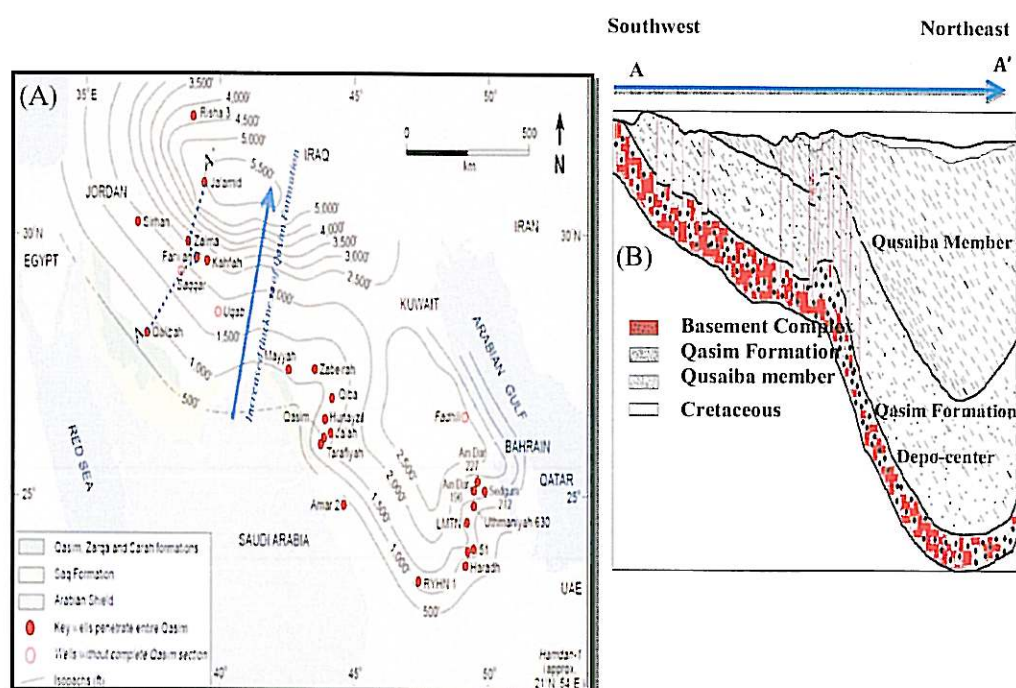


Figure 1.3: Isopach map of increased thickness of Qasim Formation. (A) Isopach map of Qasim Formation created based on information from 176 drilled for exploration or water wells showing increased thickness of Qasim Formation from southwest toward Northeast where it reaches up to 5500 ft as maximum thickness at Jalamid area (Senalp and Al-Duaiji, 2001). (B) a schematic cross section showing the increased thickness toward Qasim depo-center in the Northeast.

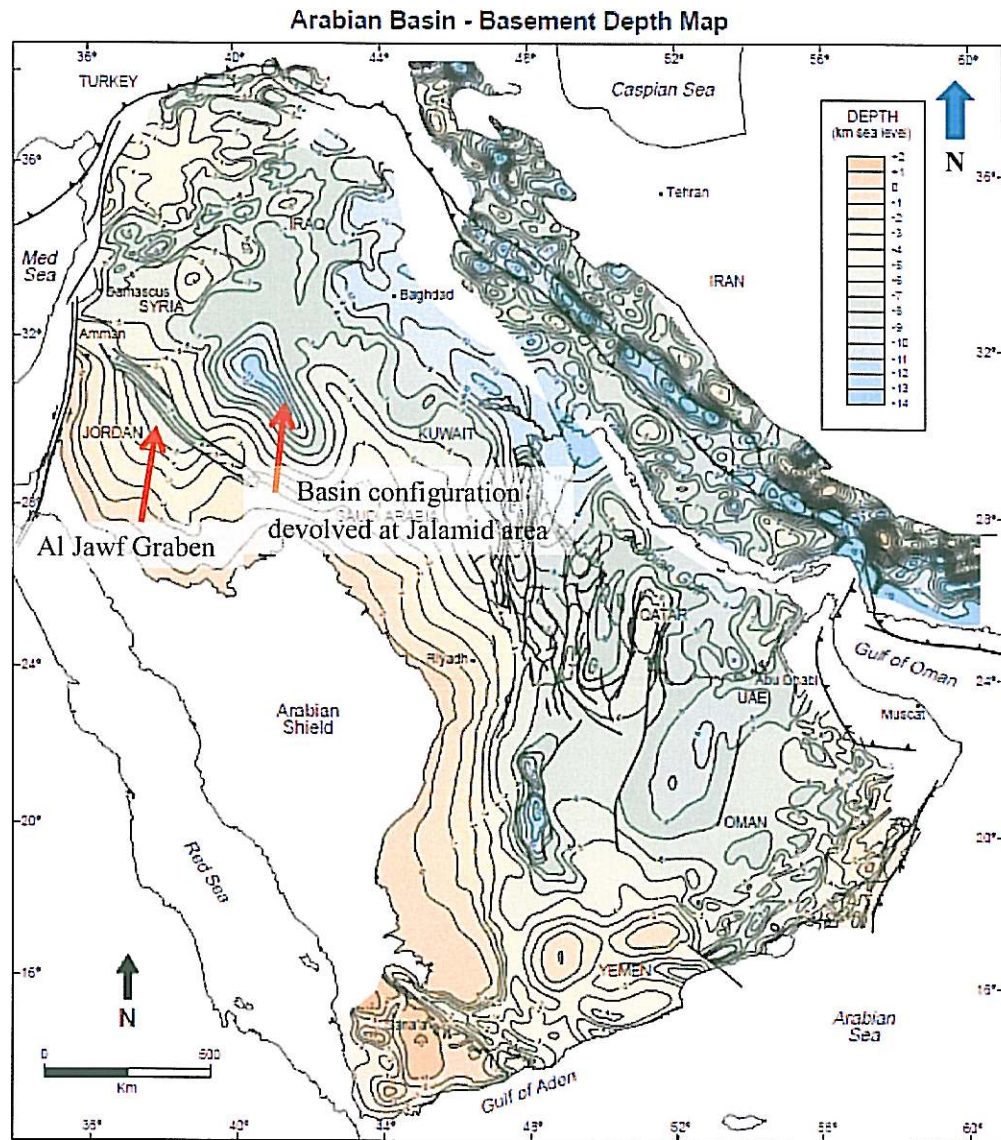


Figure1.4: Basement depth map of the Arabian plate showing basement configuration was developed towards northeast at Jalamid area (after Konert et al, .2001).

Senalp and Duaiji, reported the term of Hanadir was first informally introduced by Holm et al. (1948; unpublished report in Al-Laboun, 1993). Powers (1968) included the “Hanadir Shale member” as the lowermost informal lithologic unit of the Tabuk Formation. The Hanadir member is characterized by occurrence of abundant *Didymograptus protobifidus* fossils. McClure (1978) and Al-Laboun, (1982), Helal (1964, 1965) used the term *Didymograptus* shale member of the same unit. El-Khayal and Romano (1985, 1988) redefined the Hanadir Shale as the Hanadir Formation and raised the Tabuk Formation Williams and others (1986) and Vaslet (1987) proposed that the Tabuk Formation be discarded due to disconformable relationships between rocks of glacial and preglacial origin (Sarah and Zarqa Formations, and the older units of the Tabuk Formation (now Qasim Formation) (Fig 1.5). (Senalp and Duaiji, 2001) approved the formal definitions of Hanadir Member (Fig 1.6). Currently the latest lower Paleozoic stratigraphy column of the Qasim and Hail regions was adopted by Saudi Aramco.

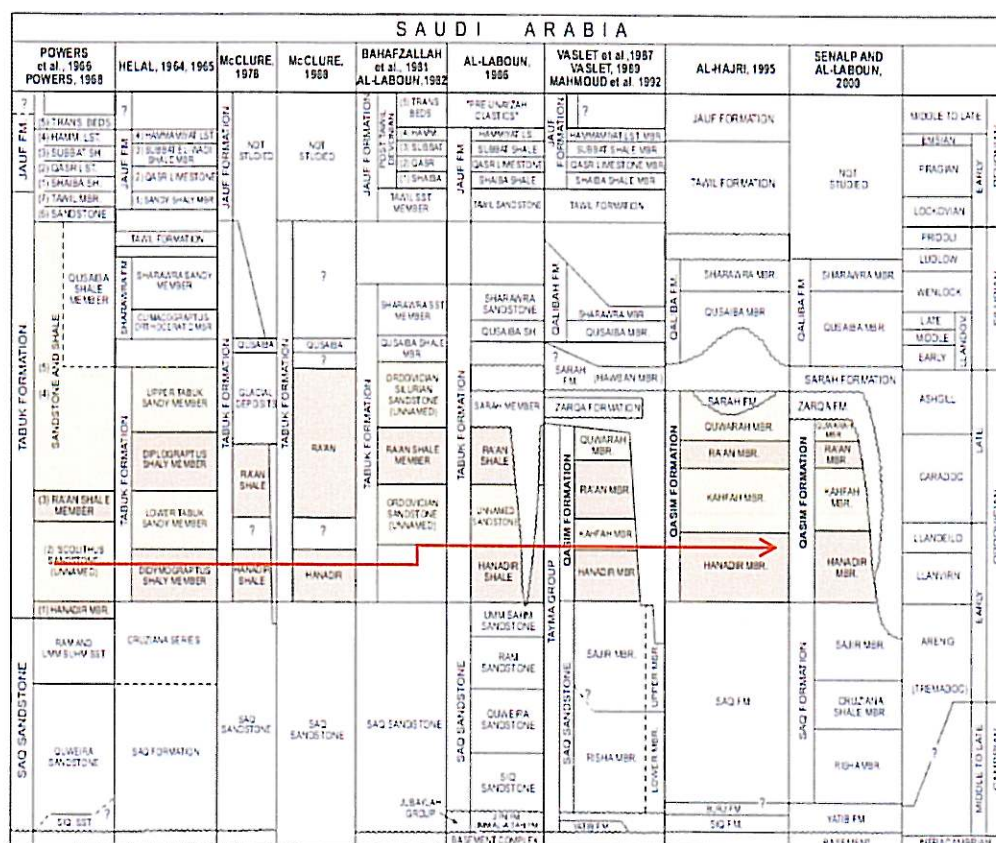


Figure 1.5: History of the lithostratigraphic classification within the lower Paleozoic succession of Saudi Arabia (modified after Vaslet, 1989; Al-Hajri, 1995; Senalp and Al-Laboun, 2000 and Senalp and Duaiji, 2001).

STRATIGRAPHY				DEPOSITIONAL ENVIRONMENT	GENERALIZED LITHOLOGY	SEQUENCE STRATIGRAPHY	
Age	Unit						
DEVONIAN		TAWIL FORMATION		Fluvio-marine			
SILURIAN	Pridoli	QALBAH FORMATION				Pre-Tawil Unc.	
	Ludlow						
	Wenlock		Sharawra Member	Wave-dominated shallow marine			Pre-Sharawra Unc.
			Qusaiba Member	Offshore/shelf			
ORDOVICIAN	Ashgill	SARAH FM.	Boq'a Member	Wave-dominated shallow marine		MFS	
			Hawban Member	Glacial, glaciolacustrine/marine		mfs	
				Glacially/periglacially incised valley			Pre-Sarah Glacial Unc.
			ZARQA FORMATION	Glacial, glaciolacustrine/marine			Pre-Zarqa Glacial Unc.
	Caradoc	QASIM FORMATION	Quwarah Member	Tide-dominated shallow marine			
			Rafan Member	Offshore/shelf		MFS	
						mfs	
			Kahfah Member	Storm-dominated shallow marine			
	Llandeilo						
	Llanvirn						
	Arenig	SAQ FORMATION	Sajir Member	Fluvio-marine (braid delta)			Type-1 Seq. Boundary
			Cruziana Shale Mbr	Open marine			
Tremadoc						MFS	
CAMBRIAN		SAQ FORMATION		Risha Member	Braided stream		
BASEMENT (Arabian Shield)							

Figure 1.6: Generalized lower Paleozoic stratigraphy column of the Qasim and Hail regions. (Senalp and Al-Duaiji, 2001).

1.4.1 Depositional Environment of the Hanadir Member

The Hanadir member of Qasim Formation was described by (Senalp and Al-Duaiji, 2001) as medium gray, fissile, micaceous and fissile (graptolite and trilobite) Some graded silty laminae occur in the lower part of the succession , and some graded very fine –grained sandstone beds in the upper part . The predominately argillaceous sediments were deposited from suspension in open–marine shelf environment below storm wave base (Fig 1.7). The type locality of the Hanadir is located at Jal Al-Aswad (lat. 26 34' 33'' N., long. 43 22' 48'' E.) where the Hanadir member conformably overlying Kahfa Member together showing coursing and thickening–upward progradational sequence of the Qasim Formation (Fig 1.8).

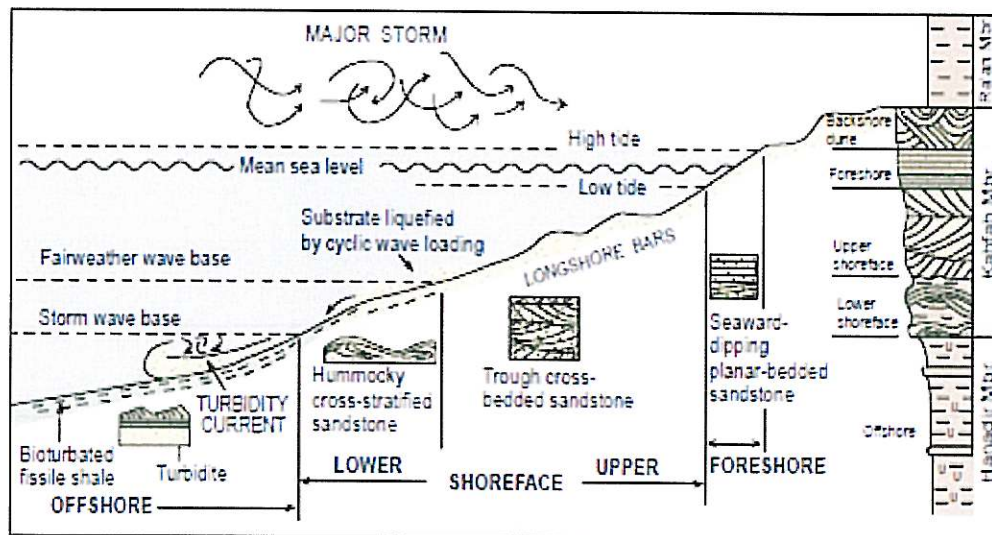


Figure 1.7: Depositional model of the Hanadir member. The sediments were deposited from suspension in open-marine shelf environment below storm wave (Senalp and Al-Duaiji, 2001).



Figure 1.8: Outcrop photograph of the Hanadir Member and lower part of the conformably overlying Kahfa Member of the Qasim Formation at Jal Al-Aswad (lat. 26° 34' 33" N., long . 43° 22' 48" E.) The dashed line represent Hanadir member conformably overlying Kahfa Member together showing coursing and thickening - upward progradational sequence of the Qasim Formation (Senalp and Al-Duaiji, 2001).

According to (Sharlend et al., 2001) the Hanadir member corresponds to O30 maximum flooding event caused deposition of outer black graptolitic shales far into western areas of the Arabian Plate along the whole length of the plate and dated at 465 Ma. Sharlend et al (2001) thought the maximum flooding surface MFS O30 result of environmental change due to increased rate of subsidence caused by a phase of rifting. They consider that the subsidence may have been enhanced by rise in sea level and that marked the transgressive system during Middle to late Ordovician. During MFS O30 the lateral equivalents of the Hanadir member of the Qasim Formation have wide distribution on the Arabian Plate (Table 1).

Syria	Black graptolitic shales near base of Swab Formation
Jordan	Shale near middle of Hiswah Formation.
N .Iraq	Near the base of K7 member of Khabour Formation.
Iran	Shales in lower part of Upper member of Zard Kuh Formation
Saudi Arabia	<i>Didymograptus</i> Shale meber, shale near base of Hanadir
	member of the QasimFormation
Oman	Shales of lowermost Saih Nahyda Formation , or Shales in
	the middle of Shale Member, Amdeh Formation.

Table 1.1: Regional Hanadir (Formation and member) equivalents in the Arabian Plate during MFS O30 (Sharland et al., 2001).

1.4.2 Micropaleontology Review

A few publications documented the discovery of agglutinated foraminifer during Cambrian or Ordovician times, such as (Schroeder, 1985) reported the first discovery of oldest foraminifera and other microfossils (*Astrorbizidae*, *Psammosphera*, *Hemisphaerammina*, *Ammodiscidae*) from the Middle Cambrian of Sardina platform and north Spain. (Riegraf et al., 1996) documented the first recovered the oldest European agglutinated foraminifera from Ordovician (Llanvirnian) of graptolite black shales of Plettenberg in the Sauerland of Northwestern Germany. The foraminiferal fauna consisted of primitive agglutinated species (*Amphitremoida*, *Bathysiphon*, *Raibosammina*, *Thekammina*, and *Thurammina*). These foraminiferal assemblages were cleaned out of an unconsolidated graptolite siltstone represent a reducing environment. Nestell, 2011) reported the first appearance of the Middle Ordovician (Darriwilian) foraminifers in Argentina.

The foraminifers are found together with conodonts of the *Eoplacognathus pseudoplanus*/*Dzikodus tablepointensis* zone that enhance the stratigraphic significance of the foraminifera. The assemblage of foraminifera described includes the agglutinated genera *Lakites*, *Amphitremoida*, *Lavella*, Ordovician and *Pelosina*. The genera *Lakites* and *Levella*, previously known only from lower Ordovician, Floain (*Tetragraptus phyllograptoides* graptolite zone) also the xenophyophore genus *Pelosina* both can be extended to Middle Ordovician.

The foraminiferal fauna recovered from the Hanadir Member contains a well-preserved assemblage consisting entirely of agglutinated taxa. Currently, these are the oldest foraminifera reported from Saudi Arabia. As expected, the middle Ordovician assemblage contains numerous simple forms such as *Rhizammina*, *Psammosphaera*, *Saccammina* and *Lagenammina*, which are found in other Ordovician localities worldwide. In addition to the simple forms, observe a diverse assemblage of lituolids and trochamminids, including the genera *Ammobaculites*, *Bulbobaculites*, *Sculptobaculites*, and diverse trochamminids.

Finding of coiled, multichambered agglutinated foraminifera in the Hanadir Shale of Saudi Arabia pushes back the known stratigraphic range of the suborder Lituolina to the middle Ordovician. The lituolids found in the Hanadir Shale assemblage are diverse, which implies the true first occurrence of this group of foraminifera is even older. Previous reports of these forms placed their origin in the early Devonian (Loeblich and Tappan, 1987). This findings also give increased credibility to previously published reports of trochamminids from the upper Cambrian of Nova Scotia (Scott et al., 2003), which were regarded by some researchers as questionable owing to their poor preservation. Some of the trochamminids from the Hanadir show radially elongated chambers, and likely belong in a new genus (Table 2).

Author	Foraminifera	Period	Type Locality and Country	Remarks
Schroeder.,1985	Astrobizidae Psammosphaera Hemisphaeram Mina Ammodiscidae	Middle Ordovician (Llanvirnian)	Sardina Platform, North Spain	Reported as oldest Foraminifera
Riegraf et al.,1996	Amphitremoida Bathysiphon Raibosammina Thekammina Thurammina	Middle Ordovician (Llanvirnian)	Graptolite black shales of Plettenberg saurland, Northwest Germany	Oldest European Agglutinated Foraminifera
Nestell.,2011	Lakites Ampitremoida Ordovician Pelosina	Middle Ordovician (Llanvirnian)	Upper part of San Juan Formation, Argentina	First appearance of the Middle Ordovician Foraminifera in Argentina
Ghazwani et al., (in press)	Rhizammina Psammosphaera Saccammina Lagenammina Ammobaculites Bulbobaclulites Placopsilina Sculptobaclulites Trochanminids	Middle Ordovician (Llanvirnian)	Hanadir Member of Qasim Formation, Northwest Saudi Arabia	Reported as oldest discovered Paleozoic Agglutinated Foraminifera in Saudi Arabia

Table1.2: Summary of discovered agglutinated foraminifera as reported based on year of publication.

1.4.3 Paleontology Review

Organic-walled microfossils (e.g., acritarchs and chitinozoans) are extremely valuable and have been widely used in age-dating of early Paleozoic rocks. Additionally were utilized in this study as alternative technique of determining level of thermal maturity of the Hanadir member of Qasim Formation. Acritarchs have been recovered from sediments deposited since Pre-Cambrian and they started evolve in abundance, diversity, size and complexity of shape. While the first appearances of Chitinozoans are evolved in late Cambrian rocks, they become most abundant during Ordovician time and extinct by the end of Devonian. They found only on marine rocks unless reworked (Fig 1.9).

A comprehensive Paleozoic palynostratigraphic study was conducted by (Al-Hajri et al., 2000) in Northwestern and Central Saudi Arabia. The results of Al-Hajri study support El-Khayal and Roman's (1988) interpretation that indicate the upper part of Hanadir member possibly is late Darriwilian age.

Paris et al., 2000, conducted another study to investigate the chitinozoan assemblage in Central Arabia. They concluded the age of Middle part of Hanadir is late Darriwilian age, as indicated by age diagnostic taxa *Linochitina pissotensis*, *Laufeldochitina clavata*, *Laufeldochitina striata* and *Pterochitina retracta*. A summary of recovered *Acritarchs* and *Chitinozoans* assemblages from Middle Ordovician in Central Arabia is shown in (Table 3).

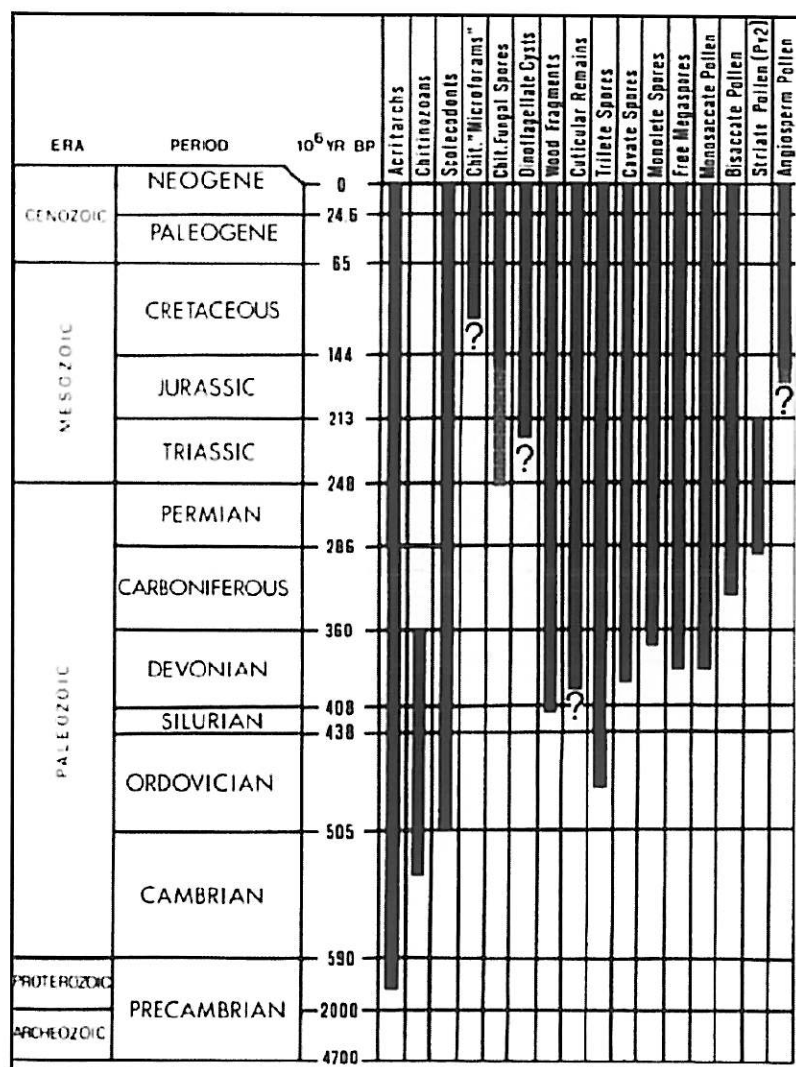


Figure 1.9: palynomorphs occurrence during geological times of all major categories of , notice Acritarchs has the most widespread species during geological time, it started for Proterozoic till present, whereas Chitinozoans spread from late Cambrian and extinct at late Devonian time (Landman et al.,2007).

Assemblage		Age	Remarks
1) <i>Chimerozoans: Lincodina pusiotensis</i>		Late Llanvirn - early Llandefllo	Most distinguishing feature of the palynological assemblages (Paris 1981 and Jenkin 1976)
2) <i>Virgatopores rudis</i>		Lower Ordovician (Arenig-Llanvirn)	Combar 1976, specimen number FA123
3) <i>Dyad</i>		Lower Ordovician (Arenig-Llanvirn)	Specimen number FA124, FA125
4) <i>Laevolamns-like monad</i>		Lower Ordovician (Arenig-Llanvirn)	Specimen number FA126
5) <i>Cymatophylaxia</i>		Lower Ordovician (Arenig-Llanvirn)	Specimen number FA127
6) <i>Sphaeromorph acmarach</i>		Lower Ordovician (Arenig-Llanvirn)	Specimen number FA128
7) <i>Eremichina sp.?</i>		Middle Ordovician (Llanvirn)	(Al-Hajri 1991) Specimen number FA129
All material is housed in paleontological collection of Natural Museum London			
8) <i>Aureoetia diachra</i>		Middle Ordovician (Llanvirn)	Vavrdova 1972, Specimen number FA130
9) <i>Verbachium rubiglobosum</i>		Middle Ordovician (Llanvirn)	Jardine et al. 1974, Specimen number FA131
10) <i>Dicodactyodinium inaequiforme</i>		Middle Ordovician (Llanvirn)	Burman 1970, Specimen number FA132
11) <i>Stellodinium celestem</i>		Middle Ordovician (Llanvirn)	(Marion) Turner 1984, Specimen number FA133
12) <i>Scriatotheca quies</i>		Middle Ordovician (Llanvirn)	(Marion) Rauscher 1973, Specimen number FA134
13) <i>Villoracapsula setozapellucula</i>		Middle Ordovician (Llanvirn)	Loeblich and Tappan 1976, Specimen number FA135
14) <i>Stellodinium belorum?</i>		Middle Ordovician (Llanvirn - Caradoc)	Turner 1984, Specimen number 136
15) <i>Stelliferidium</i>		Ordovician ?	Specimen number 137
16) <i>Jenkinodinium leptia</i>		Upper Ordovician	(Jenkins 1969), Specimen number FA139
17) <i>Cocochina sp.</i>		Late - Middle Ordovician	(Al-Hajri 1991)
18) <i>Tanuchina fimbriata</i>		Late - Middle Ordovician	Tanguerideau and de Jekhorvsky 1960
19) <i>Belonechima micracantha</i>		Late - Middle Ordovician	Eisenack 1931
20) <i>Laufeldochima rotata</i>		Late - Middle Ordovician	Eisenack 1937, broken section of the chamber wall, detail of anti-apertural end showing carina
21) <i>Fungochima fungiformis</i>		Late - Middle Ordovician	Eisenack 1931
22) <i>Lincodina pusiotensis</i>		Late - Middle Ordovician	Paris 1981
23) <i>Petrochima retrata</i>		Late - Middle Ordovician	Eisenack 1955
24) <i>Laufeldochima clavata</i>		Middle Ordovician	Jenkins 1976
25) <i>Laufeldochima clavata</i>		Middle Ordovician	Jenkins 1976
26) <i>Angochima sp.</i>		Middle Ordovician	Detail of "alpha spines"
27) <i>Belochima sp.</i>		Middle Ordovician	Detail of imperfect crest pattern made of short spiny ridges
28) <i>Lagenochima cf.</i>		Middle Ordovician	Pirum Achab 1982, detail of granulous chamber
29) <i>Cocochima minusotensis</i>		Middle Ordovician	Sauffer 1933
30) <i>Eucocochima sp.</i>		Middle Ordovician	Paris 1981

Table 3: Summary of most recovered *Acrirarchs* and *Chitinozoans* assemblages from lower and Middle Ordovician of Qasim Formation in Central Arabia. (Al-Hajri et al., 2000 and Paris et al., 2000)

CHAPTER TWO

GEOLOGICAL BACKGROUND

2.1 REGIONAL GEOLOGICAL SETTING

Arabian plate is bounded by major tectonic activities includes:

1. In the west and southwest of Arabian plate a divergent margins are forming spreading centers of Red Sea and Gulf of Aden.
2. South and southeast of the Arabian plate is bounded by the Owen-Sheba intra-oceanic transform fault.
3. Active margin occurred to the north and northeast with Turkey sutures.
4. In the east the Arabian plate is thrusting beneath the Eurasian plate.
5. Dead Sea represents a transform strike-slip fault zone to the northwest of the Arabian Plate. (Fig 2.1).

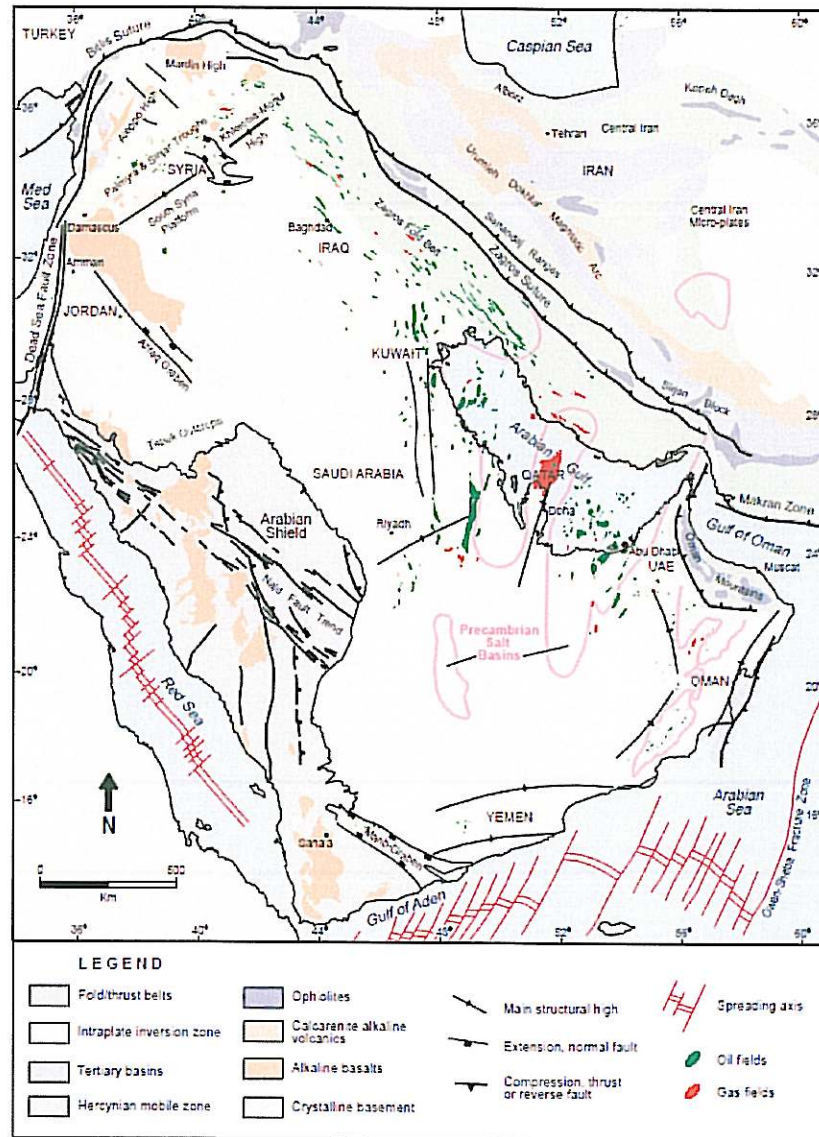


Figure 2.1: Structural map showing the location of the major tectonic elements of the Arabian plate. The present-day Arabian plate is bordered in the north by the collision zone of the Zagros and Bitlis sutures, and by subduction along the Makran zone. To the south, southwest and west, the Arabian Plate boundaries are defined by the Owen-Sheba transform fault, the rift system with sea floor spreading in the Gulf of Aden and Red Sea, and the Dead Sea transform fault zone.

2.2 PALEOLATITUDE POSITION OF ARABIAN PLATE

The glaciation period of Late Ordovician was the coldest period on Earth where the Ice covered much of the southern region of Gondwana (Mckerrrow and Scotese., 1990) the ice cap covered entire North Africa from Morocco to Arabia (Fig 2.2). (Mckerrrow and Scotese., 1990). The Middle Ordovician corresponds to Hanadir (Llanvirn) and was dated at 465 Ma by (Sharlend et al, 2001). During that glaciation period Arabian plate was in anticlockwise rotation when it reached the most southern part at 55°S (Konert et al., 2001) (Fig 2.3).

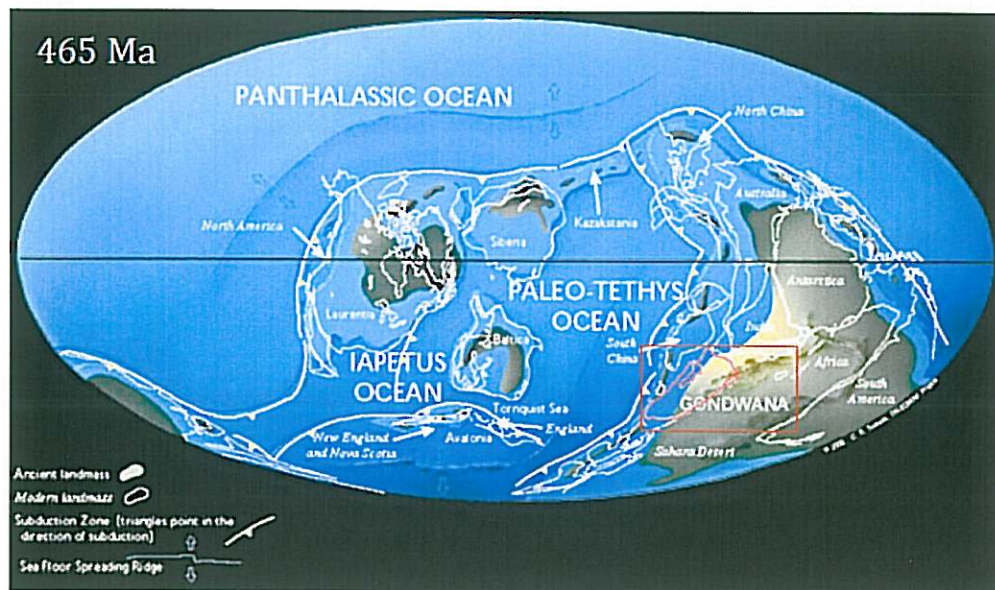


Figure 2.2: Paleogeographic map of Gondwana during late of Ordovician, Gondwana reached to South Pole, where the ice cap covered most of entire North Africa to Arabia. The period of late Ordovician was one of the coldest times in the Earth history (Soctese, 1990).

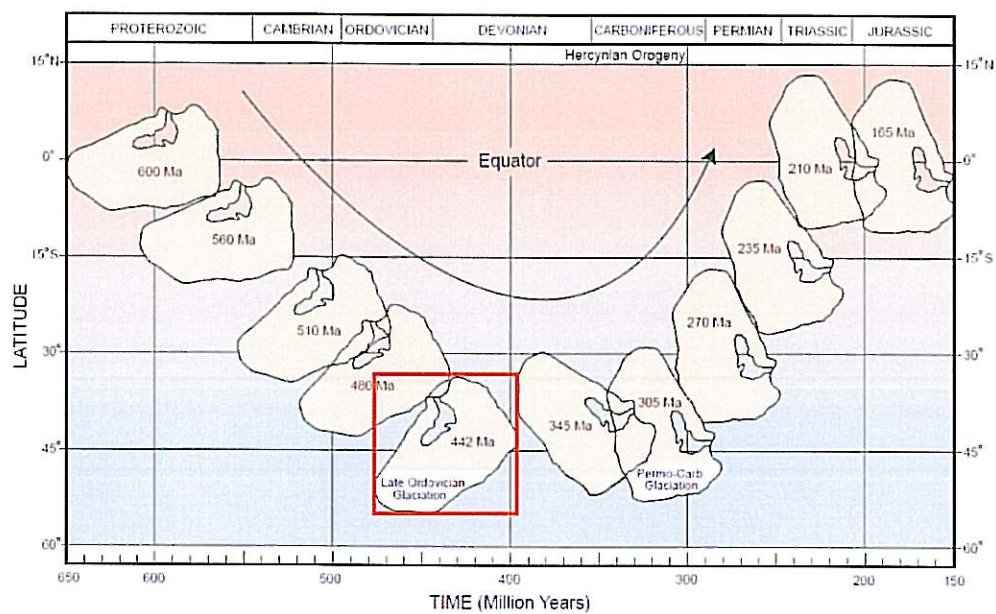


Figure 2.3: Paleolatitude map of Arabian plate during late Ordovician. The position of Arabian plate was about 55° south where the period of glaciation covered most of western margin of the Arabian Plate (Konert et al., 2001).

2.2 HANADIR REGIONAL SOURCE ROCK EQUIVALENTS

During Middle Ordovician, major shallow marine prograding clastic sequences covered almost the entire Arabian Plate (Fig2.4). These sediments were deposited in inner-neritic to estuarine or deltaic environments. The primary maximum flooding surface of this sequence is of Llanvirn age [MFS O30 dated at 465 Ma] (Sharland et al., 2001), and equivalents to the Hanadir Member of the Qasim Formation in Saudi Arabia. Localized rich organic shale may indicate the preservation occurred in restricted water conditions in the Arabian Plate (Konert et al., 2001).

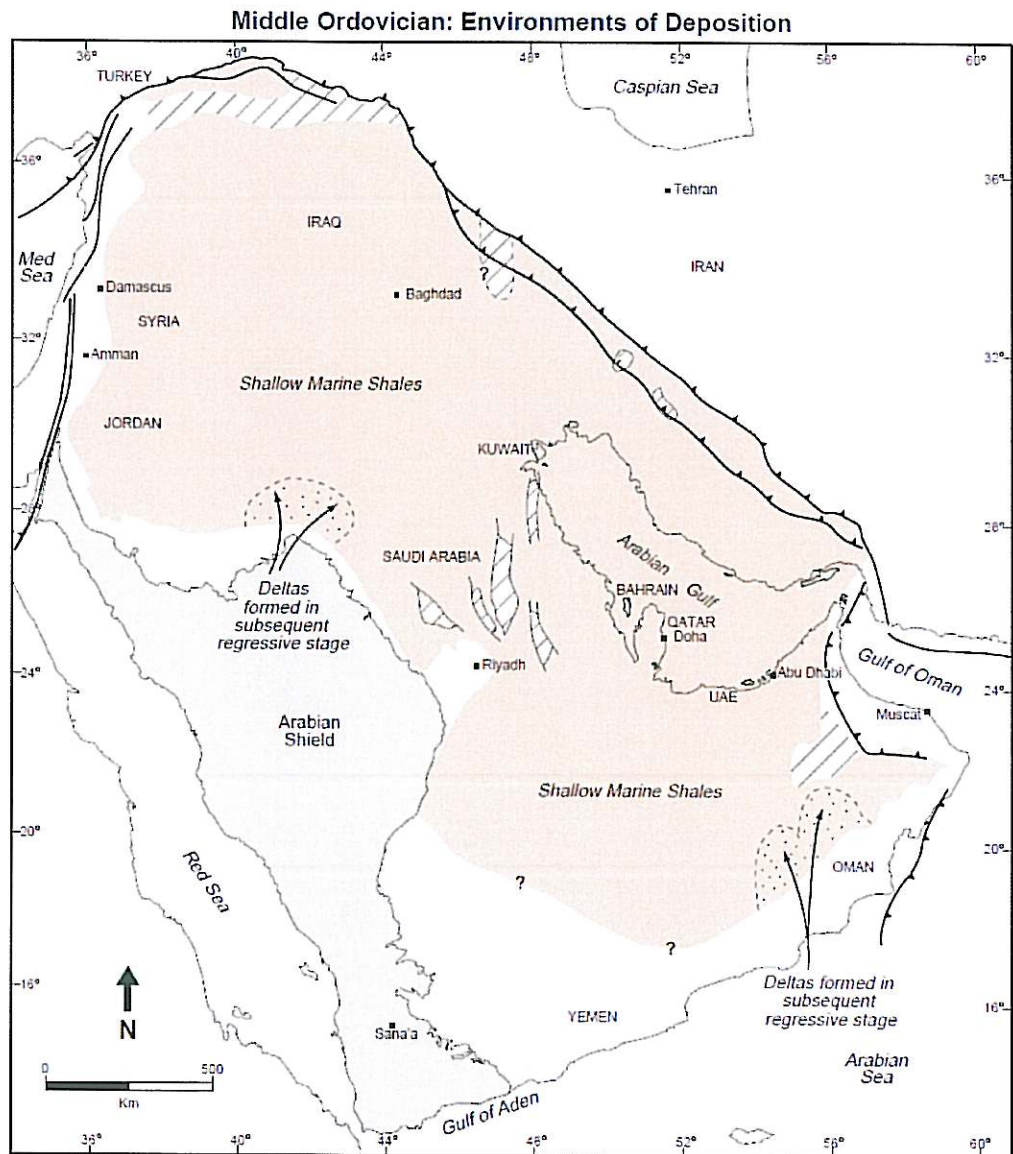


Figure 2.4: Paleodepositional environment map of Middle Ordovician, represent a major shallow marine prograding clastic sequence covered almost the entire Arabian Plate; Localized rich organic shale may indicate the preservation occurred in restricted water condition in some regions of Arabian Plate (Konert et al., 2001).

Hiswa Formation in Jordan was reported by Powell (1991) is stratigraphically correlated with Hanadir in (Al Jafr, Sirhan, Azraq and Risha basins). It is considered to be the possible source rock in Risha basin, it represents highly mature Type II kerogen with a range of total organic carbon between 0.5 -1.5% (TOC). In Syria, the main principle source rock of Middle Ordovician is black graptolitic bituminous shale, siltstone and fine grained sandstone of near the base of Sawab Formation, with average thickness around 590.55ft. Geochemically the Swab shales and Siltstone are mostly very mature type II kerogen and provide the main source of gas in western and central areas.

In Iraq, the K7 member of Khabour Formation probably correlates to Hanadir member of the Qasim Formation in Saudi Arabia (Senalp and Al-Duaiji, 2001). Khabour K7 the lower thick shale member was encountered in Akkas-1 well, and is greater than 2,060 ft thick (Al-Hadidy, 2007), it consists of homogeneous black shales, with dominant mica content and irregular pyrite blotches. The great thickness, pyrite content and lack of bioturbation may reflect deposition in reducing conditions. Al-Hadidy, 2007, reported Khabour K7 Shales are highly mature, marine organic - rich rocks. It contains total organic carbon content (TOC wt. %) of 0.9-5% in Kheleisia-1 and Akkas-1. (Fig 2.5).

Regional Paleozoic correlations												
GEOLOGICAL TIME SCALE: GTS 2004			SAUDI ARABIA	IRAQ	JORDAN	SYRIA						
Early Triassic			Khuff Formation	Mirga Mir Formation								
Permian	Lopingian	Changhsingian		Chia Zairi Formation	Darani Member	Umm Ima Formation	Amanus Formation					
		Wuchiapingian			Satina Anhydrite							
		Capitanian			Zinnar Member							
	Guadalupian	Wordian	Unayzah Formation	Ga'ara Formation								
		Roadian										
		Kungurian										
	Cisuralian	Artinskian										
		Sakmarian										
		Asselian										
		Gzhelian										
Kasimovian												
Moscovian												
Carboniferous	Pennsylvanian	Late					Berwath Formation	Hiatus		Markada or Doubayat Formation		
		Middle	Raha Formation									
		Early	Khleisia Group									
	Mississippian	Late	Harur Formation									
		Middle	Ora Formation									
		Early	Kaista Formation									
Devonian	Late	Famennian	Jubah Formation	Pirispiki Formation								
	Middle	Frasnian										
		Givetian										
	Early	Eifelian										
		Emasian										
	Pragian											
Silurian	Llandovery	Lochkovian	Tawil Formation	Hiatus								
		Pridoli										
	Wenlock	Ludfordian	Qalibah Formation				Sharawra Member	Akkas Formation	Qaim Member	Kisha Formation	Tanf or Abba formations	
		Gorstian					Gusaiba Member					Hoseiba Member
		Homerian					"Hot Shale"					
Ordovician	Llandovery	Rhuddanian	Uqlah Formation	Hiatus	Risha Fm	?						
		Aeronian					Sarah Formation					
		Telychian										
	Middle	Himantian	Qasim Formation	Quwarah	Khabour Formation	K1 Member	Dubaydib Formation	Afandi				
		Katian		Ra'an		K2-K4 Member						
		Sandbian		Kahlah		K5-K6 Member						
Early	Darmwilian	Saq Sandstone	Hanadir	K7 Member	Hiswah Fm	Khanaser Formation						
	"Llanvini"		Sajir	Umm Sahm Formation								
Late Cambrian			Risha		Disi Fm	Sosink Formation						

Figure 2.5: Regional Paleozoic Stratigraphic Column showing correlation from Akkas field in North Iraq with adjacent countries. Note Middle Ordovician of Hanadir shale stratigraphically correlated with K7member of Kabour Formation,Hiswa formation and basal of Swab Formation. The proposed correlation is based on (Lababidi and Hamdan 1985), (Aqrabi, 1998), (Konert et al., 2001), (Sharland et al., 2001, 2004) and (Al-Hadidy, 2007).

The summary of regional source rock equivalents of Middle Ordovician Hanadir shale is provided in (Table 2.1). Geochemically the present day organic matter of Hanadir can be correlated with present day organic matter of Hiswa formation in Jordan because they both are highly mature type II kerogen with range of total organic carbon between 0.05 -2.98% (TOC) in Hanadir and 0.5 -1.5% (TOC) in Hiswa Formation and consider to be the main source of gas in Jordan (Al-Sharhan et al., 1997). Rock – eval data indicates the source rock of the Hanadir is in gas generation window, which implies Hanadir member is possibly another Paleozoic source rock candidate to be the main source of gas in Northwestern of Saudi Arabia.

Regional Hanadir Hydrocarbon Equivalents in Adjacent countries				
Country	Hanadir Equivalents	Kerogen Type	(TOC.wt.%)	Remarks
Jordan	Hiswa Formation	Type II Kerogen	0.5 -1.5	Highly mature source , consider the main source of gas
Syria	Base of Sawab Formation	Type II Kerogen	*N/A	Main principal source rock , black shale , graptolitic highly mature , provide main source of gas
N Iraq	K7- member of Khabour formation at Akkas Field	Type II Kerogen	0.9-5	Highly mature organic -rich marine shale in Akkas Field
NW Saudi Arabia	Hanadir Member	Type II Kerogen	0.05 - 2.98	Highly mature shale

Table 2.1 Regional Middle Ordovician source rock equivalent to Hanadir member with their hydrocarbon potential. The result of the Hanadir Rock-Eval analysis of the current study indicates the organic matter of is undergone high level of thermal maturity .This imply Hanadir member is possibly another Paleozoic source rock candidate to be main source of gas in Northwest of Saudi Arabia(after AL-Sharhan et al.,1997).

CHAPTER THREE

3.1 WORKFLOW AND METHODOLOGY

The main objective of this study is to investigate Hanadir source rock potential in three selected wells (A, B, and C) in the northwest are of Saudi Arabia. This approach is going to be applied to this study to investigate Hanadir hydrocarbon potential and micropaleontology as following:

1. Collect source rock samples (cores and cuttings) for Rock-Eval pyrolysis, micropaleontology and palynology analyses. All analyses required amount of 30-50g of rock sample.
2. Conduct Rock-Eval pyrolysis to assess Hanadir source rock potential (quantity and quality).
3. *Acritarchs* and *Chitinozans* analysis was conducted to estimate the age of Hanadir and determine the stage thermal maturity.
4. Micropaleontology analysis will be provided information about depositional environment and anoxia.
5. Agglutinated foraminifera color index provide a supportive evidence of igneous intrusion.
6. Numerical simulation 1 D models for wells (A, B and C) illustrate the basin evolution through geological time.

7. All the integrated results of Rock-Eval pyrolysis, micropaleontology, palynology and 1D numerical simulation collaborate to understand the type of depositional environment and organic matter, richness and thermal maturity of Hanadir. This approach can be applied for over mature source rock similar to Hanadir source, where determining the kerogen type is an extremely challenging assignment. (Fig 3.1).

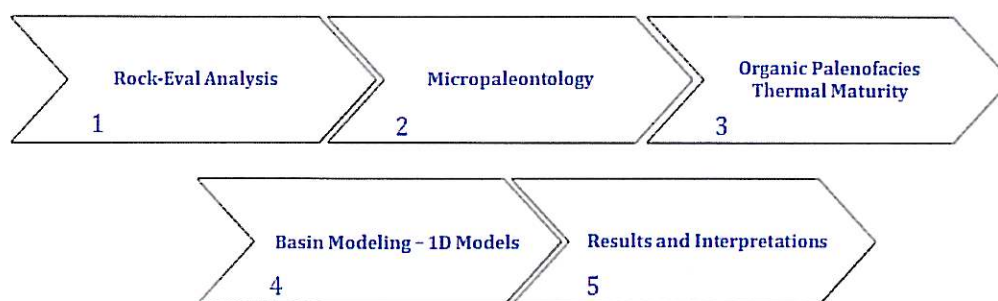


Figure 3.1: Systematic workflow of different methods have been integrated and applied in this study such as geochemistry, micropaleontology, palynology and basin modeling to investigate Hanadir source rock potential.

3.1 GEOCHEMICAL ANALYSIS

3.1.1 Source Rock Sampling Procedure

The approach that has been adopted in this study for geochemical analysis is starting with identifying source rock zone using combination of logs response such as gamma ray, density and resistivity. It is important to use delta Log R program to identify the different source rock zones. This method basically utilized the log signature of gamma ray, density and resistivity to identify source rock interval and can calculate the predicted present day total organic carbon (TOC wt. %). After the source rock zone was identified the next important step must be the collection of the samples themselves. It is fundamental that the studied source rock samples are representative and uncontaminated. In sampling wells, different lithologies are encountered, and as source rock are rarely homogeneous. Consideration must be made for the sampling of all lithologies (with evaluation of their relative proportions). Contamination is a common problem with cuttings and core samples, with various types of mud additives interfering with geochemical analysis. (Fig 3.2)

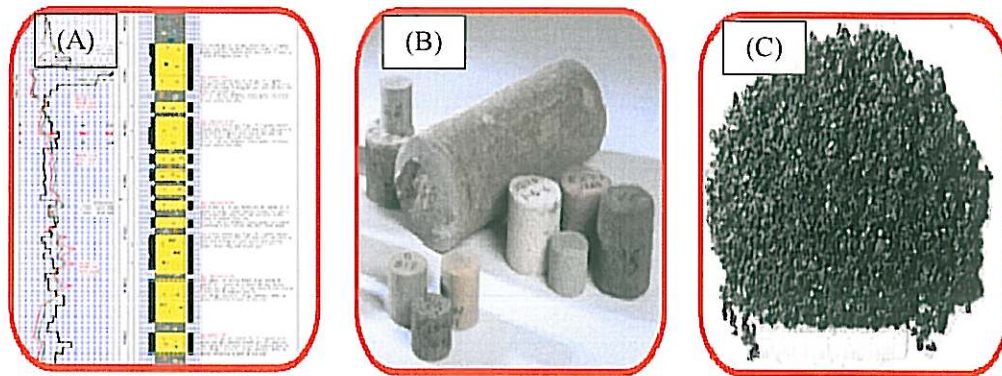


Figure 3.2: Photos showing the process of identifying source rock zone. A) Example of log data showing gamma ray, density and resistivity with lithology description. B) Photo showing some different type of core samples. C) Photo showing cutting sample of dark source rock. The process of identifying source rock zone begins with looking for log signature using delta Log R.

Sixty cuttings and cores samples were collected from three wells (A,B,and C) to conduct Rock-Eval analysis of Hanadir. The Hanadir thickness in the well-A is about 316ft around 96.31m. The collected source rock samples from Well-A represent both cuttings and cores. In the Well-B the maximum thickness of the Hanadir is 333ft, which is equivalent to 101.49m, most of collected source rock samples are cuttings. The thickest section of the Hanadir member is encountered in Well-C. It reaches up to 373 ft. which is about 113.69m. The total thickness of the Hanadir member encountered in both wells is 1022 ft, equivalent to 311.50m (Fig 3.3). The description of recovered core from well-A was gray to dark gray, black, silty in part, sub-fissile – fissile, sub-blocky, abundant of graptolites and trilobites, moderately hard and occasional calcite veins (Fig3.4).

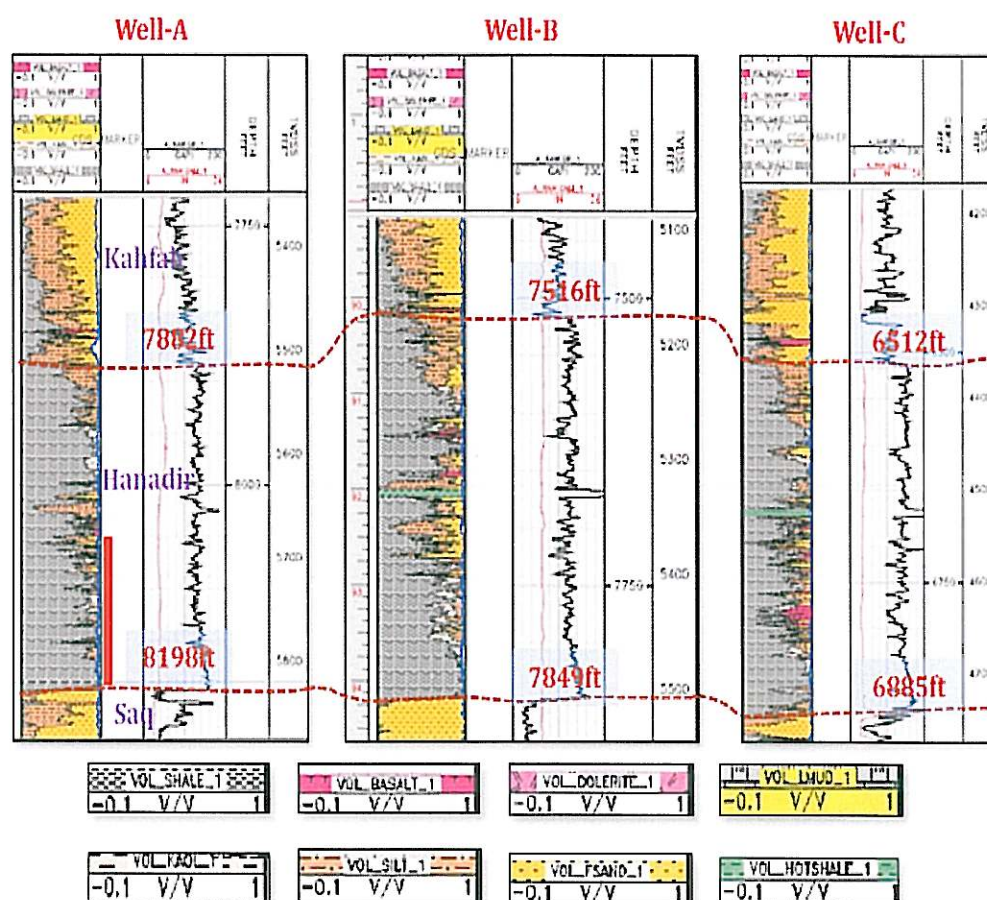


Figure 3.3: Well correlation of the Hanadir source rock bounded by red dashed line in both wells, Noet Hanadir contained some igneous intrusions most likely basalt or diorite.

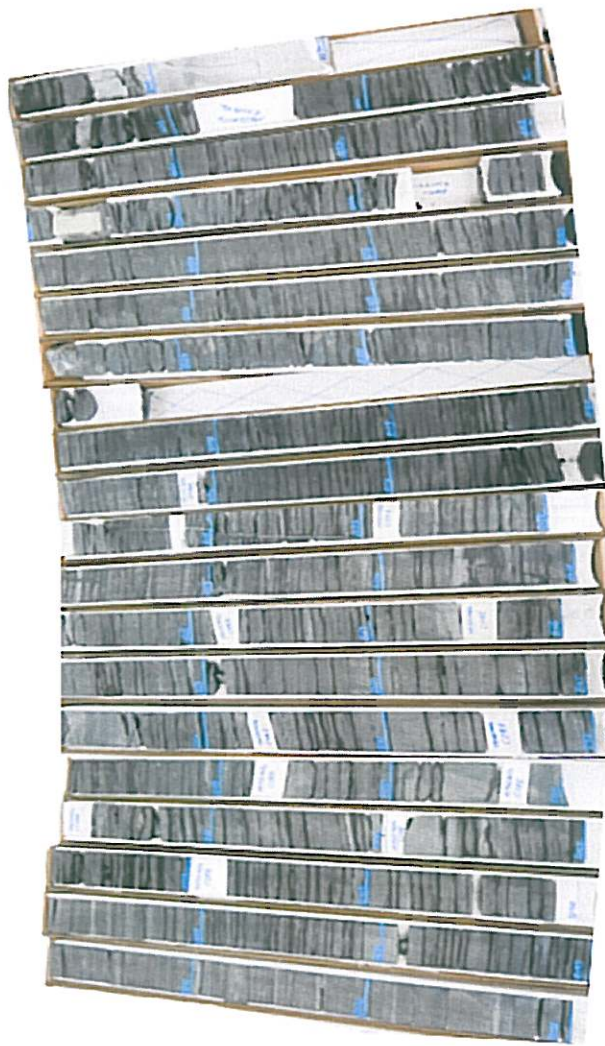


Figure 3.4: A core photo taken for Hamadir recovered core of Well-A showing source rock heterogeneity which may reflect source rock redox condition

3.1.2 Rock-Eval Pyrolysis Parameters

Hanadir source rock samples were analyzed using the Rock-Eval pyrolysis method. This method was conducted utilizing Saudi Aramco geochemistry unit (pyrolysis lab). Rock-Eval pyrolysis used to investigate the petroleum generative potential of Hanadir source rock. It provides information about type of organic matter, quantity, and thermal maturity.

The main function of pyrolysis is heating organic matter in the absence of oxygen, to distilled free organic compounds (bitumen), and then cracking pyrolytic products from kerogen. The source rock analyzer machine was designed to deliver several measurements for both source and reservoir rocks by heating geologic samples (i.e., outcrops, cuttings, conventional cores and sidewall cores). To start the Rock-Eval pyrolysis, the source rock samples (cores, cuttings) should be crushed by grinder into powder. The amount of source rock required for Rock-Eval pyrolysis is ranging between 65 – 75 mg/g of rock.

The source powder should be weight by sensitive balance, the next step is to drop the sample into clean crucible (not contaminated with other materials), then the crucible should be inserted into the machine's crucibles tray. The source rock analyzer machine (SRA) should be calibrated and ready to run the analysis.

The Rock- Eval pyrolysis method consists of a programmed temperature heating (in a pyrolysis oven) in an inert atmosphere (helium) of a small sample of source rock (~100 mg). The pyrolysis temperature program is as follows: the oven is kept isothermally at 300°C for three minutes; the volatilized free hydrocarbons are measured as the S_1 peak and detected by flame ionization detector (FID). The volatilization of the very heavy hydrocarbons compounds ($>C_{40}$) as well as the cracking of nonvolatile organic matter is produced when temperature is increased from 300° to 550°C (at 25°C/min). The hydrocarbon released from this cracking is measured as the S_2 peak (by FID). The temperature at which S_2 reaches its maximum is called T_{max} . The CO_2 produced from kerogen cracking is trapped in the 300°-390°C range and during the cooling of the pyrolysis oven S_3 peak is detected (Fig 3.5). The measurements obtained from Rock-Eval pyrolysis are the following:

S_1 = is the free hydrocarbons in the sample (in milligrams of hydrocarbon per gram of rock). If $S_1 > 1$ mg/g abnormally high value of S_1 is due to contamination of samples by drilling fluids and mud.

S_2 = residual hydrocarbons generated through thermal cracking of nonvolatile organic matter. S_2 is an indication of the quantity of hydrocarbons that the rock has the potential to produce with continued burial and maturation.

S_3 = is an indication of the amount of oxygen exists in the kerogen. It is used to calculate the oxygen index.

T_{\max} = the maximum temperature at which hydrocarbons release from cracking of kerogen occurs during pyrolysis (top of S_2 peak). T_{\max} is one of the maturity thermal indications of the organic matter.

TOC= total organic carbon remaining in the sample after pyrolysis (in an oxidation oven kept at 600°C). The TOC is then calculated by adding the residual organic carbon detected to the pyrolyzed organic carbon, which in turn is measured in weight percent (wt %).

HI = hydrogen index is calculated using residual hydrocarbon and total organic carbon content ($HI = [100 \times S_2]/TOC$).

OI = oxygen index is calculated based the amount of oxygen exists in the kerogen ($OI = [100 \times S_3]/TOC$).

PI = production index ($PI = S_1/[S_1 + S_2]$). PI is used to characterize the evolution level of the organic matter. Maturation of the organic matter can be estimated by the location of HI and OI. T_{\max} range of 400°-430°C represents immature organic matter; $T_{\max} = 435^\circ$ -450°C represents mature or oil zone; $T_{\max} > 450^\circ$ C represents the over-mature zone.

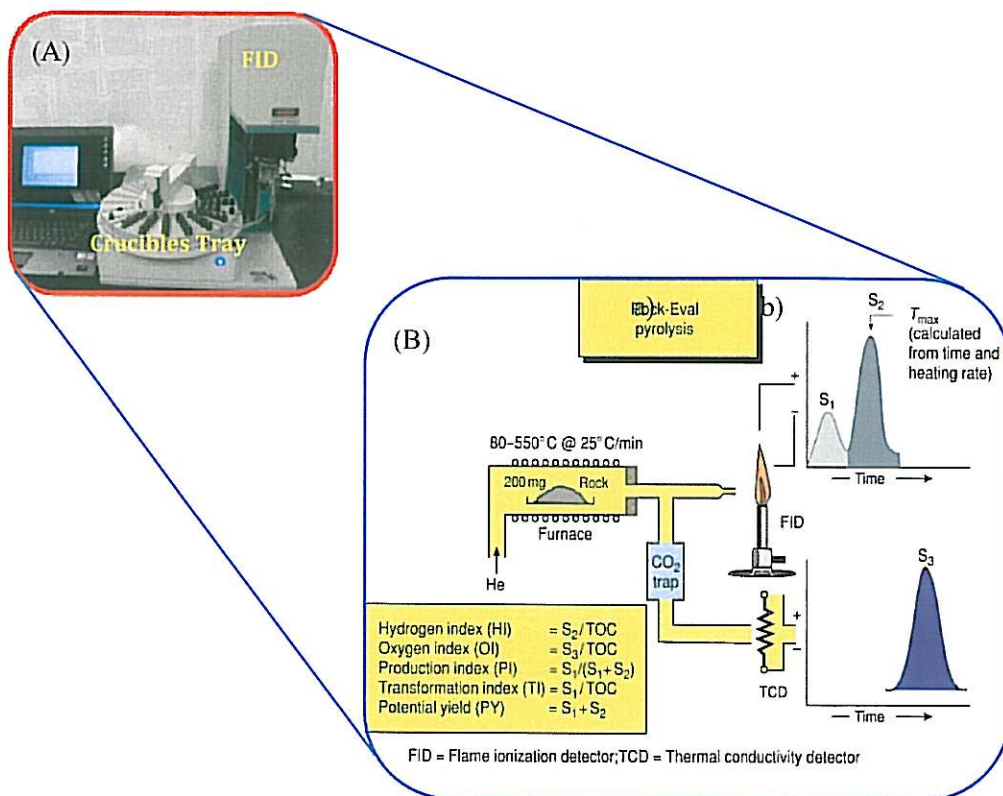


Figure 3.5: (A) photo of Rock-Eval machine used to conduct source rock Rock-Eval pyrolysis analysis in Aramco Pyrolysis lab. (B) Schematic of Rock-Eval pyrolysis process with different output parameters (Cornford, 2005).

3.2 PALYNOLOGY SAMPLES PROCESS

All samples were processed according to standard palynological laboratory methods (Streel, 1965). Each sample was crushed and 10-25 grams were demineralized in 10% HCl and 40% HF. The residue of the most poorly-preserved samples was oxidized in 65% HNO₃ and KClO₃ and sieved through a 10 µm mesh. Subsequently, a hot bath in 25% HCl eliminated the remaining fine mineral particles. The residue of all samples was rinsed through a 10 µm mesh. The final residue was mounted on palynological slides using Euparal[®].

3.3 MICROPALEONTOLOGY SAMPLES PROCESS

3.3.1 Process of Agglutinated Foraminifera Segregation and Selection

Agglutinated foraminifers are widespread in terrigenous clastic sedimentary basins. They are common in shallow water facies, in deltaic facies, and in deep-water facies. Foraminifera can be divided into two groups, one constructed by agglutinated detrital grains, the other constructed secreted calcite, both forams utilize organic matter in the construction of their test. The foraminiferal fauna recovered from the Hanadir Member of Qasim Formation contains a well-preserved assemblage consisting entirely of agglutinated taxa. Currently, these are the oldest foraminifera reported from Saudi Arabia. The presence of these fauna cannot be established without multistage of segregation process. Twenty seven samples represent both core and cuttings were collected from wells (A, B, and C) in the northwestern Saudi Arabia. All samples were picked and placed into simple zip-lock plastic pages. Well name and depth of the samples was labeled on yellow envelopes. The main objective of this process is to isolate agglutinated foraminifera from the sediment grains that surrounded them in this case from Hanadir shale.

Some soft rocks will break down after soaking in water for a few hours, whereas harder rocks such as Hanadir member may first require crushing and then boiling and the whole process took around four months to segregate 30 samples of Hanadir member. The best approach is to utilize the simplest technique that will provide the preferred results. Initially breaking the sediment or rock into fragments slightly larger, will

accelerate the process. The facility of rock analysis lab at King Fahd University (Research Institute) was utilized to conduct the segregation process. The materials needed for segregation process as following:

1. Yellow envelope labeled with the well name and depth where the samples were collected.
2. Zip lock plastic bags to hold the samples
3. Teflon pots to use as containers for the samples
4. Chemicals Lacquer thinner or Hydrogen Peroxide (H_2O_2)
5. Standard Sieve No 230 with mesh openings of 63 microns
6. Hot Plate for boiling the samples
7. Grinder to crush the hard core samples
8. Source of water

After the materials are prepared the segregation process starts with soaking the samples in the lacquer thinner and keeps the samples overnight, this process is to segregate the fine sediments (muds) and to see how long any given sample needs to be soaked. (Fig 3.6)

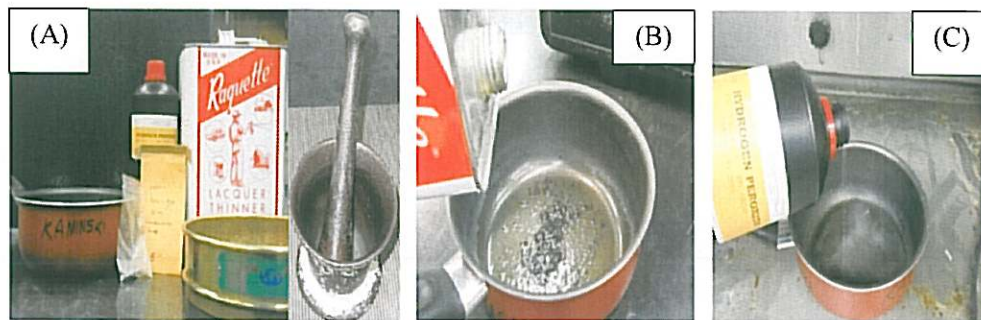


Figure 3.6: A) Photo showing the materials needed for segregation process such as Lacquer thinner or Hydrogen peroxide and grinder to crush the core sample into small pieces. B) Process of soaking the sample with lacquer thinner, the samples response to lacquer thinner was extremely slow .C) Photo showing using Hydrogen peroxide as another chemical, the samples response to Hydrogen Peroxides was ideal. It was the most effective chemical that help to segregate Hanadir samples.

As a result of soaking the samples into lacquer thinner, it took long time to segregate the samples; therefore we tried another method to accelerate the process of segregation by using 6-15% concentration of hydrogen peroxides (H_2O_2). A lot of hydrogen peroxide bottles were used and the results were promising and within an acceptable period of time. The samples soaked in hydrogen peroxide (H_2O_2) solution and were kept overnight at room temperature.

By heating the solution containing sample for 15 to 20 minutes, then stirring frequently and taking care that the solution does not boil over; finally the sample can be washed through a sieve stainless steel U. S. Standard Sieve No. 230 with mesh openings of 63 microns. Stir water/sediment mixture gently, onto the sieve, and wash under a gentle stream of water, the muds will pass through the sieve and be discarded (Fig3.7)

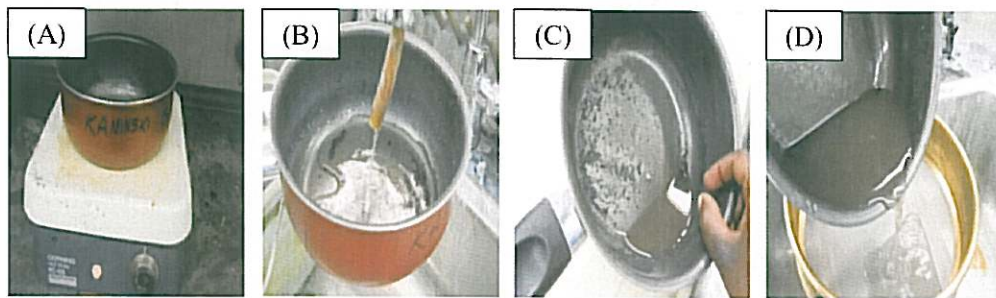


Figure 3.7: Showing the process of segregation after soaking the samples with Hydrogen Peroxide and become muddier. A) Boiling the samples using hot plate, using around 100 °C temperature for 3-5 minutes. B) Washing the sample using source of water. C) Cleaning the samples and examine the sediment mixture if the mud still exist. D) Gently decant water/sediment mixture onto the sieve, and wash under a gentle stream of water. Not, the segregation process need to be repeated for more three to four times till the foraminifer's assemblage clearly observed under the microscope.

The remaining materials on the sieve contain a concentration of sand-sized materials, including foraminifers. Allow the sample to drain in a dry place and safe from contamination and breezes. The grains should not stick to one another. If they do, some mud still remains and the soaking, boiling and sieving procedure should be repeated till the sample is dried, the dried sample should be stowed in a properly labeled vial until ready for microscopic analysis (Fig3.8).

The sample is then scattered across a picking tray and examined under a binocular microscope. Picking trays with a grid of rectangular subdivisions is used by professionals. A binocular microscope with reasonably good optics and the power to magnify 30 to 40 times will be acceptable for the study of foraminifera.



Figure 3.8: Photo of microscopic examination for samples from well A, B and C were properly stored and labeled vials ready for microscopic examination; some forams were examined in the black brass picking tray.

During examining, separate foraminifera samples are scattered across the picking tray can be picked and mounted with water - soluble glue (e.g., Tragacanth) for permanent reference. The cardboard slides should be labeled with well name and sample depth. More than thirty cardboard slides of Hanadir shale agglutinated foraminifera were recovered after segregation process from wells (A,B,and C) . The advanced microscopic lab at King Fahd University of Petroleum and Minerals (KFUPM) was utilized to take photos for agglutinated foraminifers and prepared them for foraminiferal identification and description (Fig3.9).

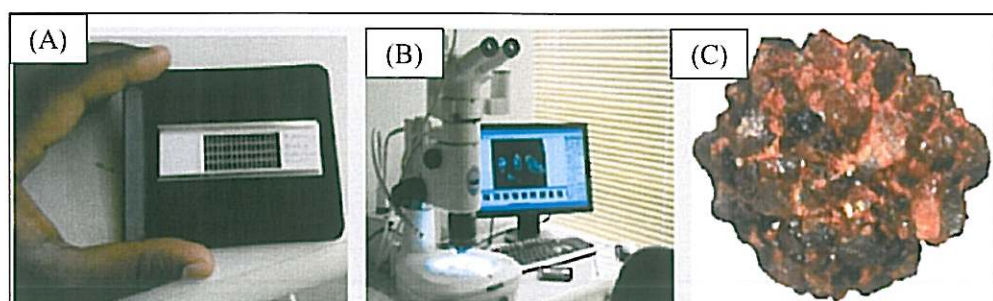


Figure 3.9: Photos of the process of agglutinated foraminifera description. A) photo showing cardboard slide of agglutinated recovered from Well-A, coated with water - soluble glue. B) photo showing cardboard slide of agglutinated foraminifera placed under the lens of advanced microscope to take a photo of foraminifera. C) Photo of *Psammosiphonella* species is ready for description.

3.3.2 AGGLUTINATED FORAMINIFERA DISCRIPTION

The foraminiferal fauna recovered from Middle Ordovician (Llanvrin) Hanadir member of Qasim Formation contains a well-preserved assemblage consisting entirely of agglutinated taxa. Currently, these are the oldest foraminifera reported from three selected wells (A, B, and C) in Northwestern Saudi Arabia.

The Light microscope photographs of taxa recovered at depth 8103.9ft from Well –A represented in Plate 1.

1,2. *Psammosiphonella* sp. 1

Test large, elongated tube with a thick, coarsely agglutinated wall, comprised of well-sorted quartz grains. No visible constrictions.

3, 4. *Trochammina* sp.1 (with triangular final chamber)

Test large, rounded-triangular in outline, coiled in a very low trochospire, with a closed umbilicus, three chambers in the final whorl. Wall comprised of equidimensional quartz grains. Aperture a short basal slit, extraumbilical in position, but closer to the peripheral margin.

5. *Ammobaculites* sp. 3 (with tapered last chamber)

Test free, robust, initially planispiral with five or six poorly visible chambers, later uncoiled and rectilinear. Coiled portion is short, with the last chamber tapering toward the neck. Wall thick comprised of medium-coarse sized agglutinated grains. Aperture terminal.

6.9. Trochammina sp. 5 (with stellate chambers)

Test free, medium size, coiled in a very low trochospire with five chambers per whorl. Spiral side evolute, flat or elevated slightly in the center, with a flat ventral slide. Chambers increase in size rapidly; early chambers are rounded, but rapidly become petaloid then radially elongated with a subtriangular shape after the first whorl. Chamber elongation in the final whorl is perpendicular to the previous whorl. Chamber extensions gradually tapering from the chamber of origin, and are situated between the locations of the sutures. Sutures radial flush with the surface of the test. Wall coarsely agglutinated, comprised of mineral grains that include quartz and some heavy minerals. Aperture obscured, likely interiomarginal and extraumbilical in position.

Remarks: With its radially elongated chambers, compressed test and nearly planispiral coiling, this species closely resembles specimens of *Leupoldina*, a planktonic foraminifer known from the Early Cretaceous. Chamber shape is subtriangular in the adult stage, and shows no sign of tapering into a tubulospine as in the planktonic foraminiferal genus *Schackoina*. Occasionally a larger agglutinated grain protrudes from the distal tip of the elongated chamber.

7.12. Trochammina sp. 2 (with square chambers)

Test free, compressed, coiled in a very low trochospire to planispire, Spiral side evolute, flat or elevated slightly in the center, with a flat ventral slide with four chambers in the last whorl. Outline quadrate. Chambers increase in size rapidly, and have a truncated-triangular shape. The final chamber is well separated from the others. Wall medium-

coarsely agglutinated, comprised of quartz grains. Aperture obscured owing to the coarse wall – possibly a short slit umbilical in position.

Remarks: With its triangular chambers, this species is best compared with the Eocene planktonic foraminifer *Truncorotaloides rohri*. The test wall is medium to coarsely agglutinated, which generally obscures the apertural characteristics.

8,10,11. Trochammina sp. 4 (with digitate final chambers)

Test free, medium to large size, compressed to the point that specimens become watch glass-shaped, coiled in a very low trochospire, Spiral side evolute, flat or elevated slightly in the center, with a flat to concave ventral side with six to eight chambers in the last whorl. Outline of the test is originally circular, but the last chambers become digitate with tangentially oriented subcylindrical projections of the chambers, producing a strongly lobate outline in the adult stage. The final chamber is sometimes strongly digitate. Chambers increase in size slowly. Wall coarsely agglutinated, comprised of mineral grains that include mafic minerals. Aperture an interiomarginal slit, extraumbilical in position.



Plate.1. Microscopic photo of agglutinated foraminifera recovered from Well-A represents Hanadir shale member of Qasim Formation: 1,2. *Psammosiphonella* sp; 3,4. *Trochammina* sp; 4. *Bulbobaculites* sp. 5. *Placopsilina* sp. 6. *Ammobaculites* sp. 7. *Ammobaculites* sp. 8-9. *Ammobaculites* sp

The Light microscope photographs of taxa recovered at depth 7560ft -7570ft from Well -B represented in **Plate 2.**

1. Psammosphaera sp. 1

Test free, slightly compressed and circular in outline. Wall made of angular, poorly-sorted quartz grains with a rough surface. No visible aperture

2. Psammosiphonella sp. 1(description on plate 1, p.74)

3. Lagenammina sp. 1.

Test large, flask-shaped, compressed slightly, gradually tapering towards the aperture. Wall made of medium to coarsely agglutinated quartz grains.

4. Bulbobaculites sp. 1

Test free, laterally compressed, with few rapidly-enlarging chambers. Early part coiled irregularly, comprised of 3–4 chambers, then uncoiled and rectilinear, comprised of two chambers with horizontal sutures. Wall comprised of equidimensional quartz grains. Aperture terminal on a slightly produced neck.

5. Placopsilina sp. 1

Test probably attached, with one side flat or slightly concaves the other side more convex. Coiling planispiral with approx. six chambers in the last whorl. Sutures indistinct. Wall coarsely agglutinated with some larger grains. Aperture indistinct.

6. Ammobaculites sp. 1.

Test free, robust, laterally compressed, initially planispiral with six or more poorly visible chambers, with only a slight tendency to uncoil. Wall thick, comprised of coarse agglutinated grains. Aperture indistinct.

7. Ammobaculites sp. 2.

Test free, laterally compressed, initially planispiral with four visible chambers, later uncoiled and rectilinear. Coiled portion involute, with radially-elongated chambers producing an irregularly lobate outline. Wall comprised of medium-sized agglutinated grains. Aperture terminal.

8-9. Ammobaculites sp. 3. (with tapered last chamber)

Test free, robust, initially planispiral with five or six poorly visible chambers, later uncoiled and rectilinear. Coiled portion is short, with the last chamber tapering toward the neck. Wall thick comprised of medium-coarse sized agglutinated grains. Aperture terminal.



Plate.2. Microscopic photo of agglutinated foraminifera recovered from Well-B represent Hanadir shale member of Qasim Formation: 1. *Psammospaera* sp ; 2. *Psammosiphonella* sp; 3. *Lagenammina* sp. 4. *Bulbobaculites* sp. 5. *Placopsilina* sp. 6. *Ammobaculites* sp. 7. *Ammobaculites* sp. 8-9. *Ammobaculites* sp.

The Light microscope photographs of taxa recovered at depth 7560ft -7570ft from Well -B represented in **Plate3**.

1a-3b. Placopsilina sp. 2

Test attached, with one side flat or slightly concave, the other side convex and two-sided with a median ridge, forming a rounded-triangular transverse section. Initial portion comprised of few rapidly-enlarging chambers, then uncoiled and rectilinear. A round depressed umbilicus may be present on the attached side. Sutures in the uncoiled portion chevron-shaped, with the final chamber tapering towards the aperture.

Remarks. The species is clearly attached to something flat because on the attached side the agglutinated grains have a terrazzo arrangement, whereas on the dorsal side the coarse agglutinated grains give the test a rough surface. Some coarser grains are present along the median ridge. The umbilicus may be filled with pyrite

4a-b. Trochammina sp.1 (with triangular final chamber) (description on plate 1, p.77)

5. Trochammina sp. 3 (petaloid chambers)

Test free, medium to large size, compressed, coiled in a very low trochospire, Spiral side evolute, flat or elevated slightly in the center, with a flat ventral side with four chambers in the last whorl. Outline of the test is petaloid. Chambers increase in size rapidly. Wall coarsely agglutinated, comprised of quartz grains. Aperture probably an interiomarginal slit, extraumbilical in position.

Remarks. With its rounded, petaloid chambers that have their elongation axis perpendicular to the last whorl, this species is best compared with the Cretaceous planktonic foraminifer *Pseudoclavhedbergella* Georgescu, 2009. The test wall is medium to coarsely agglutinated, which generally obscures the apertural characteristics.

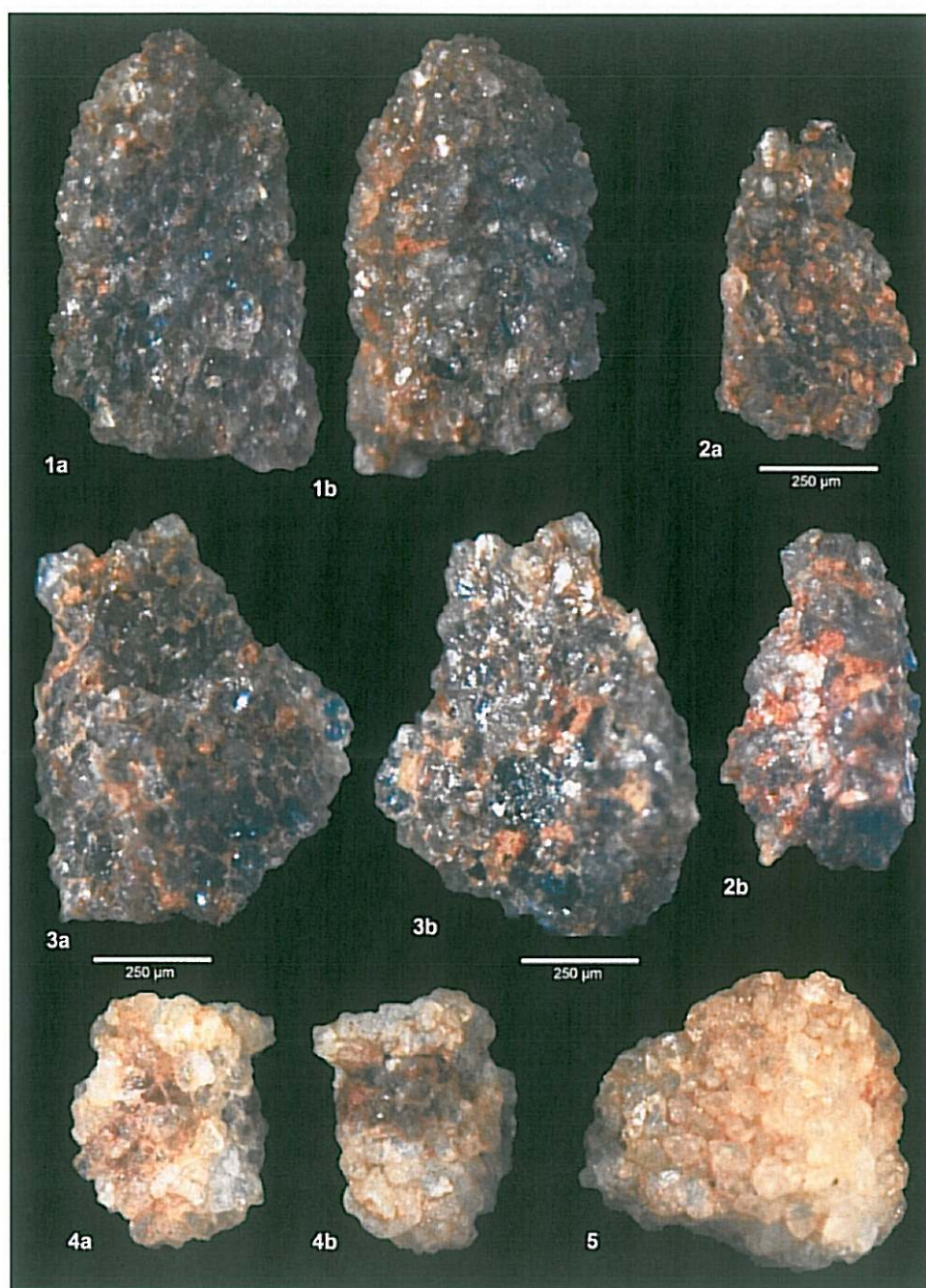


Plate.3. Microscopic photo of agglutinated foraminifera recovered from Well-B represent Hanadir shale member of Qasim Formation: **1a-3b.***Placopsilina* sp; **4a-b.***Trochammina* sp;**5.** *Trochammina* sp

The Light microscope photographs of taxa recovered at depth 7560ft -7570ft from Well -B represented in **Plate 4.**

1a-b Trochammina sp. (large, with four chambers in the final whorl)

Test free, medium to large size, compressed, coiled in a very low trochospire, Spiral side evolute, flat or elevated slightly in the center, with a flat ventral slide with four chambers in the last whorl. Outline of the test is petaloid. Chambers increase in size rapidly. Wall coarsely agglutinated, comprised of quartz grains. Aperture probably an interiomarginal slit, extraumbilical in position.

Remarks: with its rounded, petaloid chambers that have their elongation axis perpendicular to the last whorl, this species is best compared with the Cretaceous planktonic foraminifer *Pseudoclavibergella* Georgescu, 2009. The test wall is medium to coarsely agglutinated, which generally obscures the apertural characteristics.

2. Trochammina sp. 5 (with stellate chambers) (description on plate 1, p.75)

3a-b. Trochammina sp. 4 (with digitate final chambers) (description on plate 1, p.77)

4a-b. Trochammina sp. 2 (with square chambers) (description on plate 1, p.76)

5a-b. Trochammina sp. 6 (with “spiky” periphery)

Test free, medium size, flattened, coiled in a very low trochospire with four or five chambers per whorl and a rectangular outline. Spiral side slightly elevated slightly in the center, with a flat ventral slide. Chambers increase in size rapidly. Wall very coarsely agglutinated, with larger pointed quartz grains extending outward from the periphery,

much like spines or tubulospines in some Cretaceous or Paleogene planktonic foraminifera. Aperture is indistinct.

Remarks: This species shows the remarkable ability to select triangular quartz grains and use them as spines or spikes that extend outward from the periphery. The positioning of these grains appears to be very deliberate, as they are also positioned at the corners of the rounded-rectangular test.

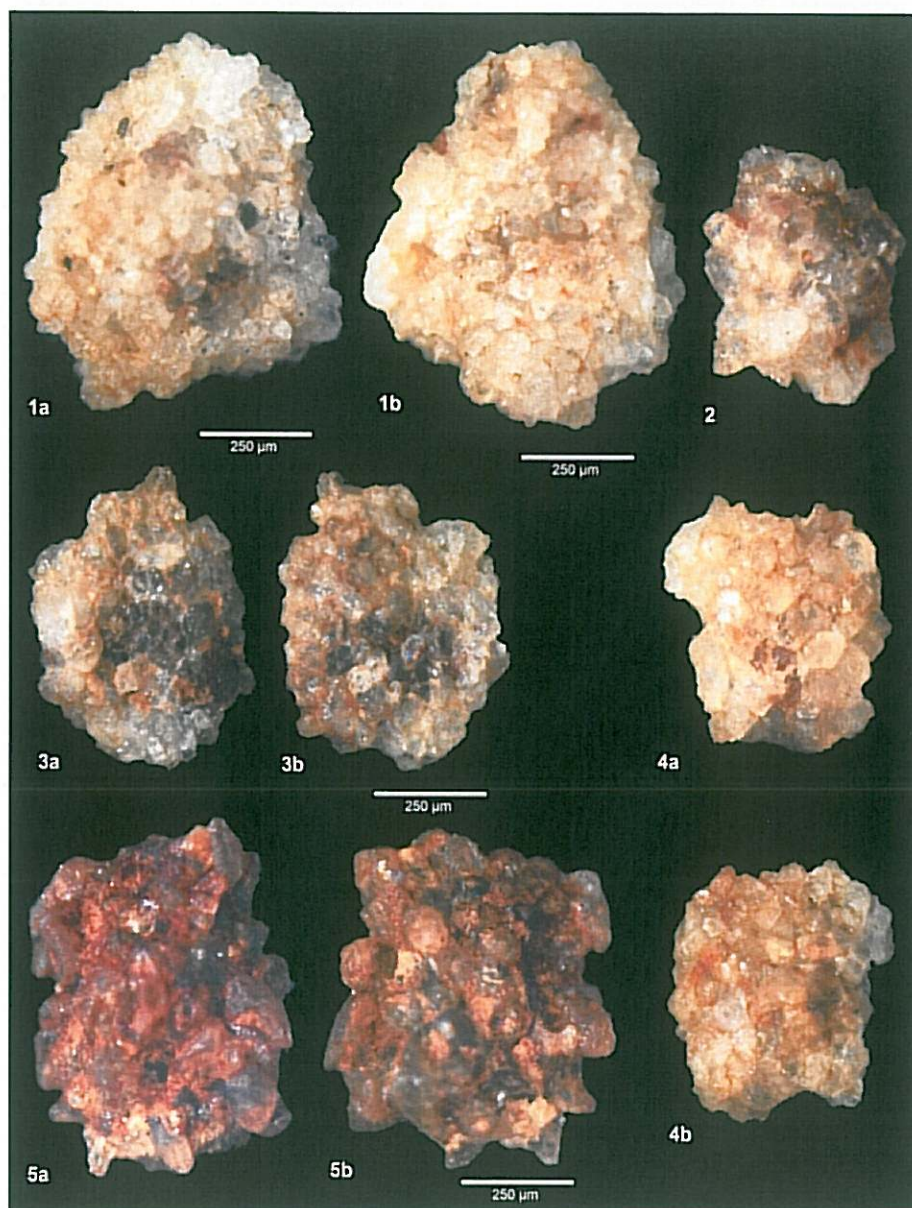


Plate.4.Microscopic photo of agglutinated foraminifera recovered from Well-B represent Hanadir shale ember of Qasim Formation; **1a-b.** *Trochammina* sp; **2.** *Trochammina* sp; **3a-b.** *Trochammina* sp; **4a-b.** *Trochammina* sp;**5a-b.***Trochammina* sp

The Light microscope photographs of taxa recovered at depth 6640ft -6650ft from Well -C represented in **Plate 5.**

1-2. Psammosiphonella sp.1 (description on plate 1, p.74)

3. Psammosphaera sp.1 (description on plate 2, p.79)

4. Ammobaculites sp.1 (description on plate 2, p.80)

5a, b. Placopsilina sp. 1

Test probably attached, with one side flat or slightly concaves the other side more convex. Coiling planispiral with approx. six chambers in the last whorl. Sutures indistinct. Wall coarsely agglutinated with some larger grains. Aperture indistinct.

6. Placopsina sp. 2 (description on plate 1, p.82)

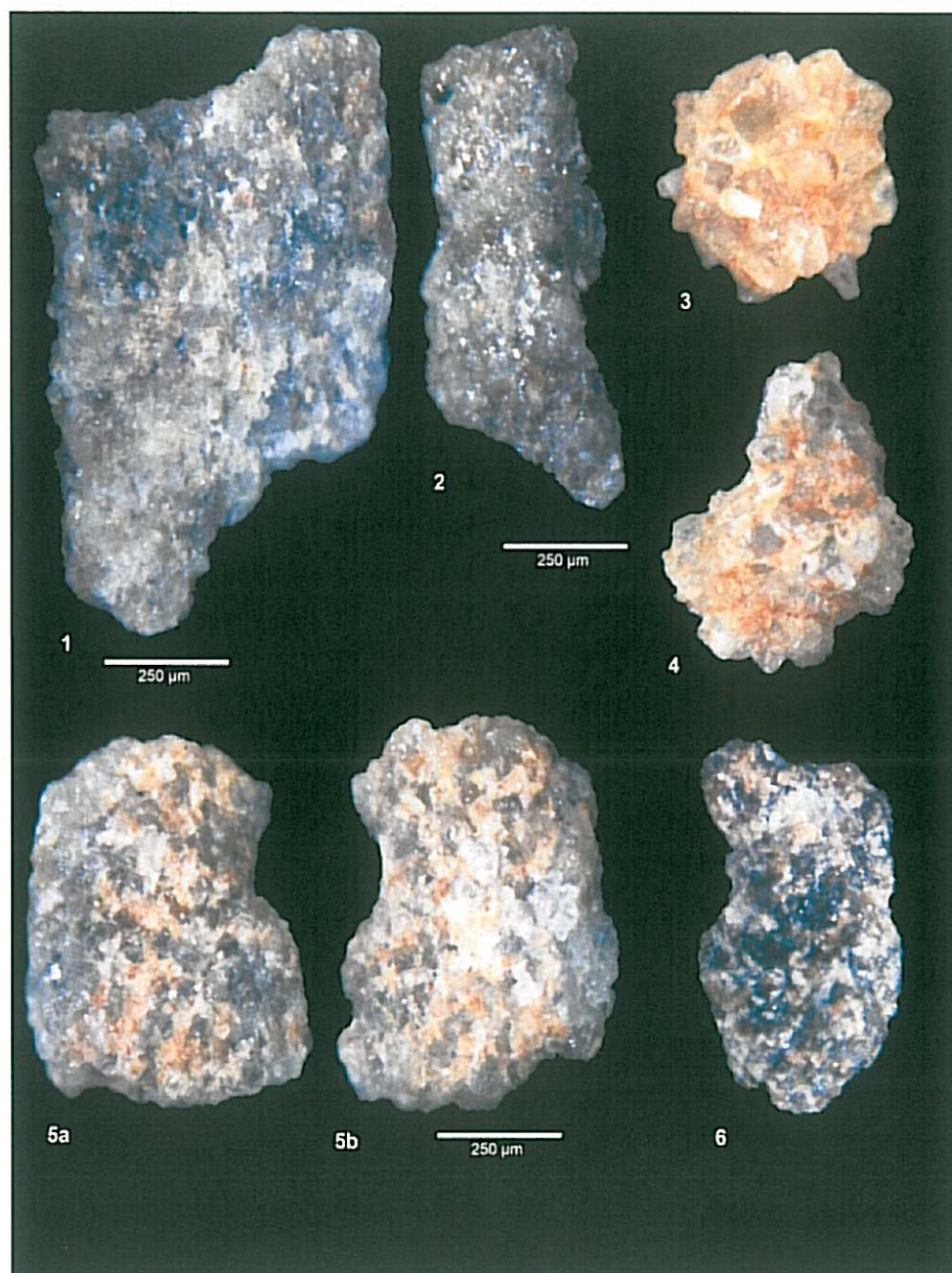


Plate .5. Microscopic photo of agglutinated foraminifera recovered from Well-C represent Hanadir shale member of Qasim Formation;; **1-2.** *Psammosiphonella* sp; **3.** *Psammosphaera* sp; **4.** *Ammobaculites* sp; **5a-b.** *Placopsilnia* sp; **6.** *Placopsina* sp.

The Light microscope photographs of taxa recovered at depth 6640ft -6650ft from Well -C represented in **Plate 6.**

1. Trochammina sp.3 (large with petaloid chambers) (description on plate 3, p.83)

2. Ammobaculites sp.2 (description on plate 2, p.80)

3. Bulbobaculites sp.1 (description on plate 2, p.79)

4, 6. Placopsilina sp.1 (description on plate 2, p.80)

5a-b. Ammobaculites sp.2 (with triangular final chamber) (description on plate 2, p.80)

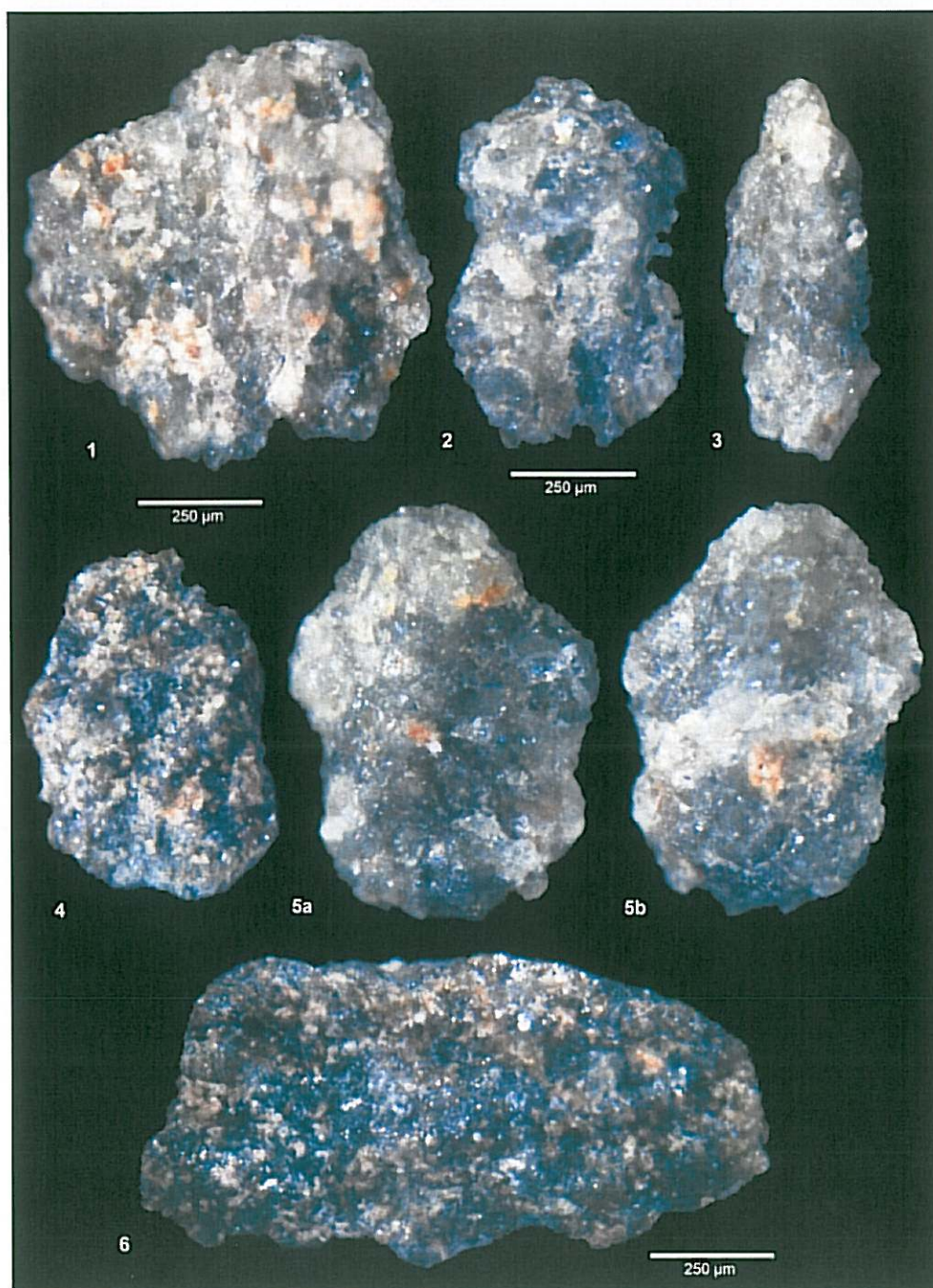


Plate .6. Microscopic photo of agglutinated foraminifera recovered from Well-C represent Hanadir shale Member of Qasim Formation: **1.** *Trochammina* sp; **2.** *Ammobaculites* sp; **3.** *Bulbobautilites* sp; **4, 6.** *Placopsilina* sp. **5a-b.** *Ammobaculites* sp.

3.4 BASIN MODELING

3.4.1 Numerical Simulation 1D Model

Petroleum resource assessment is the most highly visible and frequent integrate divers' extensive information on the geological, geochemical data. Petroleum system modeling incorporates geoscience data in ways that strengthen the assessment process and results are presented visually and numerically. Petroleum system quantify the petroleum system (Magoon and Dow, 1994) The primary purpose of constructing 1D model is to reconstruct the geological history at three selected wells (A, B, and C) in the Northwest region of Saudi Arabia.

4.4.2 Input to Present Day Model

The sedimentary basin consists of sequences of stratigraphic layers, which have been deposited during events of geological time. Each layer is characterized by its own lithologic type, specific matrix density and porosity versus depth. In this study, the dominant lithologic type in all wells (A, B and C) is siliciclastic sequences. The input data is a crucial process to build numerical simulation 1D model. It requires to assigned lithologies, ages and ranges of erosions to those intervals. (Fig3.10)

The most important boundary conditions are heat flow (HF) (Mw/m^2), water surface interface temperature (SWIT) and Paleo-water depth (PWD). It is necessary to identify those parameters, because they are varying based on the period of the sediments get buried and basin type such as rifted basin or normal shelf. Heat flow and surface water temperature are parameters control the calibration of the model with other maturity data such as corrected bottom whole temperature and vitrinite reflectance (Fig3.11).

Different scenarios should be applied for boundary condition parameter to match with calibrated maturity data. The 1D model can be built easily using Ptromod software. However, the input data that used to build numerical simulation 1D model doesn't necessarily leads to agreement with measured data.

Main Input Data for Well-A									
Depth Input: <input checked="" type="radio"/> Top <input type="radio"/> Base <input type="radio"/> Thickness <input type="button" value="Assign from Well Pick"/>									
<input checked="" type="checkbox"/> Paleozoic Pre Hercynian									
Layer	Top [m]	Base [m]	Thick. [m]	Eroded [m]	Depo. from [Ma]	Depo. to [Ma]	Eroded from [Ma]	Eroded to [Ma]	Lithology
Paleozoic Pre Hercynian	-733	21	754	1500	411.00	320.00	320.00	317.00	Sandstone (typical)
SHARAWRA	21	343	322		436.00	425.00			Sandstone (typical)
QUSAIBA	343	1075	732		440.00	436.00			Shale (organic rich, typical)
QUSAIBA HOT SHALE	1075	1390	315		442.00	440.00			Shale (organic rich, typical)
RA'AN	1390	1464	74		461.00	456.00			Shale (organic lean, typical)
KAHFAH	1464	1680	216		468.00	461.00			Sandstone (typical)
HANADIR	1680	1776	96		472.00	468.00			Shale (organic rich, typical)
SAQ FORMATION	1776	1972	196		500.00	472.00			Sandstone (typical)
						500.00			

Figure 3.10: Main input data for well-A to create 1D numerical simulation model . It includes stratigraphic layers, thickness and range of crosssections.

Boundary Conditions for Well-A					
↓ Sort Tables		<input type="checkbox"/>	Auto SWIT	McKenzie HF ...	
<input type="checkbox"/>	<input checked="" type="checkbox"/>		<input type="checkbox"/>	<input checked="" type="checkbox"/>	
Age [Ma]	PWD [m]	Age [Ma]	SWIT [°C]	Age [Ma]	HF mW/m ²
320.00	-733	320.00	18.00	320.00	62.00
436.00	120	436.00	20.00	436.00	62.00
440.00	120	440.00	18.00	440.00	72.00
442.00	120	442.00	18.00	442.00	72.00
461.00	120	461.00	18.00	461.00	72.00
468.00	120	468.00	18.00	468.00	62.00
472.00	120	472.00	18.00	472.00	62.00
500.00	120	500.00	20.00	500.00	72.00

Figure 3.10: Boundary conditions for well-A to create 1D numerical simulation model. It includes stratigraphic layers ages, paleo-water depth, surface interface temperatures and heat flow.

CHAPTER FOUR

DISCUSSION

4.1 HANADIR SHALE ROCK-EVAL PYROLYSIS

4.1.2 Quality of Organic Matter of Well-A

Twenty eight cuttings and cores samples recovered from (7882 - 8196.5 ft.) representing 314 ft. thick section of the Hanadir from well A. All samples are subjected to Rock-Eval pyrolysis to evaluate Hanadir source rock generative potential and maturity. The lithology of the Hanadir varies from light to dark gray occasionally olive green, laminated, fissile; abundant of graptolite and trilobite; predominantly argillaceous. Some observed graded silty laminae in lower part of the core and pyrite in part. Hanadir were deposited in an open marine shelf environment below storm wave base. (Senalp et al., 2001). The presence of storm indicates circulation and oxygenation of bottom water. The Rock -Eval pyrolysis results were loaded into GeoLog software to conduct a proper interpretation of Rock -Eval and TOC data (Figure 4.1). It also required to know the hole condition in order to evaluate if there is a mixing or caving of lithology within the studied layer.

The direct measurements form Rock-Eval Pyrolysis that related to quantity of organic matter are total organic carbon (TOC wt. %) , remaining hydrocarbon potential (S₂ mg HC/g Rock) and hydrogen index (HI mg HC/g TOC). Hanadir total organic carbon (TOC) values are fluctuating from (0.37 – 2.98 wt. %) with average (TOC) is about (1

wt. %). It suggests poor to very good quality of organic matter. Total organic carbon is not a stand-alone Rock-Eval measurement to evaluate hydrocarbon potential therefore, the geochemical parameter that used to evaluate Hanadir source rock generative potential is provided in (Table 4.1)

For a correct evaluation of hydrocarbon generative potential, total organic carbon must be combined with remaining hydrocarbon potential (S_2 mgHC/g Rock) and hydrogen index (HI). The values of the remaining hydrocarbon potential (S_2) are extending between (0.05-0.72 %). Additionally, hydrogen index (HI) results are showing low values, they are ranging between (8 – 69 mg HC/g Rock). The combination of total organic carbon (TOC), remaining hydrocarbon potential (S_2) and hydrogen index (HI) is suggesting hydrocarbon of Hanadir in well-A is lean to marginal generative potential. (Fig4.2).

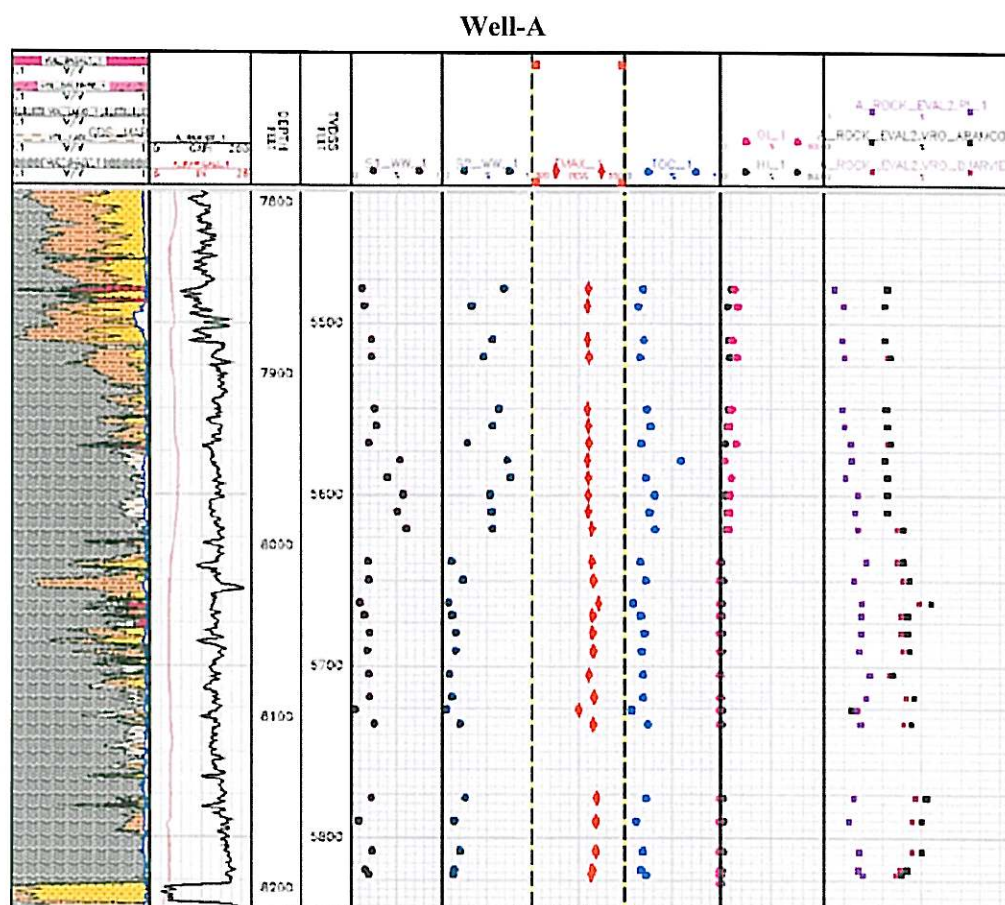


Figure 4.1: Geochemical log of Rock-Eval and TOC results from well -A. it includes calculated vitrinite reflectance in the last column.

Rock-Eval Parameter	Max	Min	Average
HI (mg HC/g TOC)	69	8	28
OI(mg CO ₂ /g TOC)	98	25	57
TOC (wt. %)	2.98	0.37	1.10
PI	0.29	0.72	0.50
S ₁ (mg HC/g Rock)	0.61	0.05	0.25
S ₂ (mg HC/g Rock)	0.72	0.05	0.32
T _{max} (°C)	479	427	458.5

Table 4.1: Geochemical parameter used to evaluate Hanadir source rock generative potential.

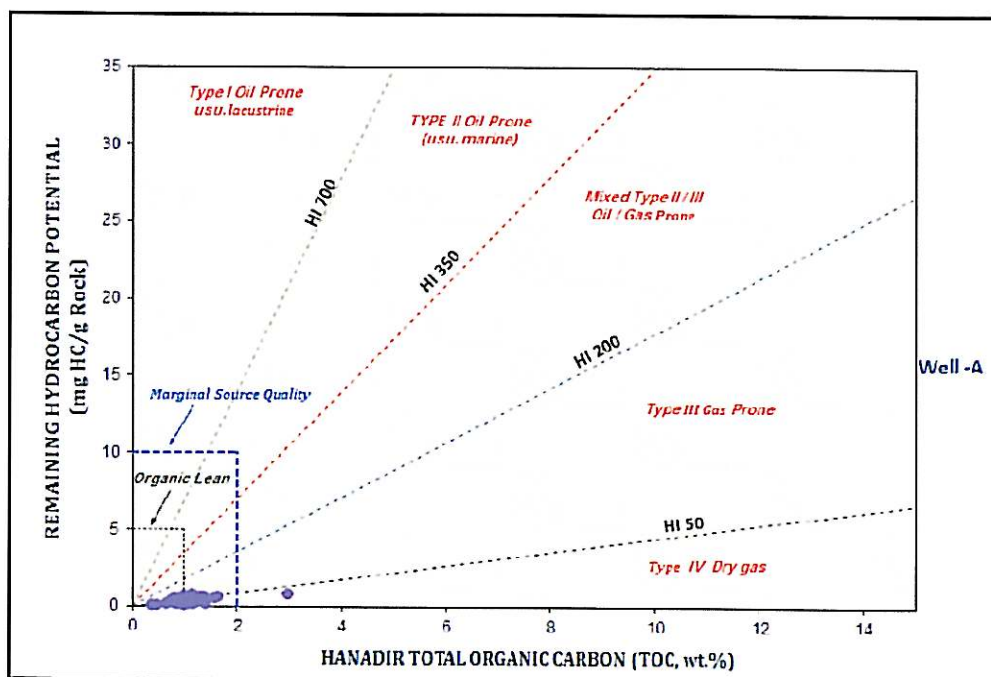


Figure 4.2: A plot of remaining hydrocarbon potential (S2) against total organic carbon (TOC) indicating lean to marginal source rock potential of Hanadir for Well-A.

4.1.3 Type of Organic Matter and Thermal Maturity of Well-A

Generally type of organic matter can be described by using plot of (OI) versus (HI) with support of microscopy and elemental analysis the plot of (OI) versus (HI) indicates the organic matter has pathways of kerogen type (III) or (IV) (Fig4.3). Kerogens type (III) and (IV) doesn't reflect the original type of kerogen of Hanadir, because kerogen type (III) indicate gas prone derived from higher land plant while, higher land plants doesn't exist during Ordovician, and it is evolved during Silurian time. In this study, describing type of organic matter of Hanadir is challenging task, because the organic matter of the Hanadir is representing a high level of thermal maturation. Another method to estimate maturity is plotting hydrogen index (HI) versus T_{max} , it indicates maximum release of hydrocarbons from cracking of kerogen occurs during pyrolysis at range of (450-480) °C reflecting mature to overmature level of thermal maturation. (Fig 4.4) .The origin kerogen type of the Hanadir remains under speculative interpretation, due to uncertainty in distinguishing the types of kerogen pathways have organic matter gone through to reach that high level of thermal maturation.

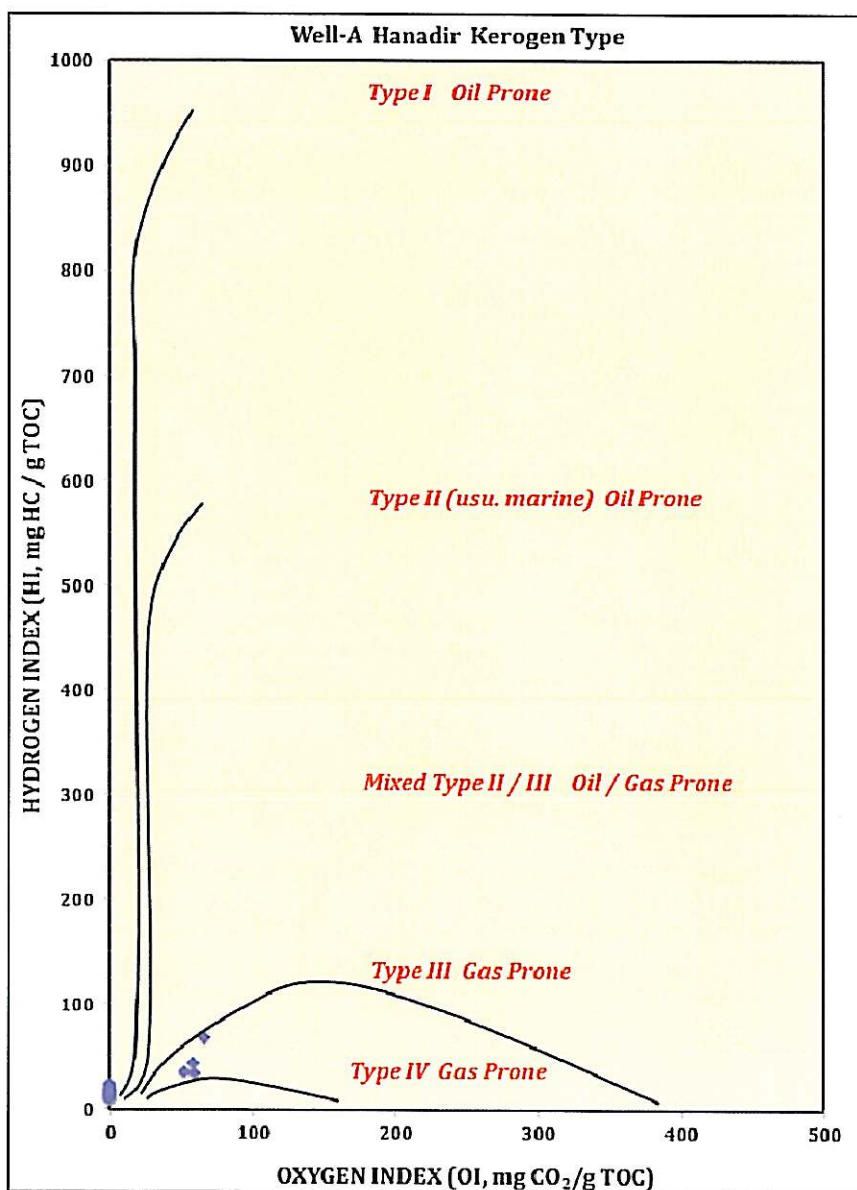


Figure 4.3: A plot of a pseudo Van Kervelen diagram of a hydrogen index against oxygen index. It suggests the kerogen type Hanadir shale is krogeron III or IV, but this is not the case. Type III or IV kerogen represent the last stage of maturation and it is difficult to determine the original type of kerogen reached to that late stage of thermal maturation.

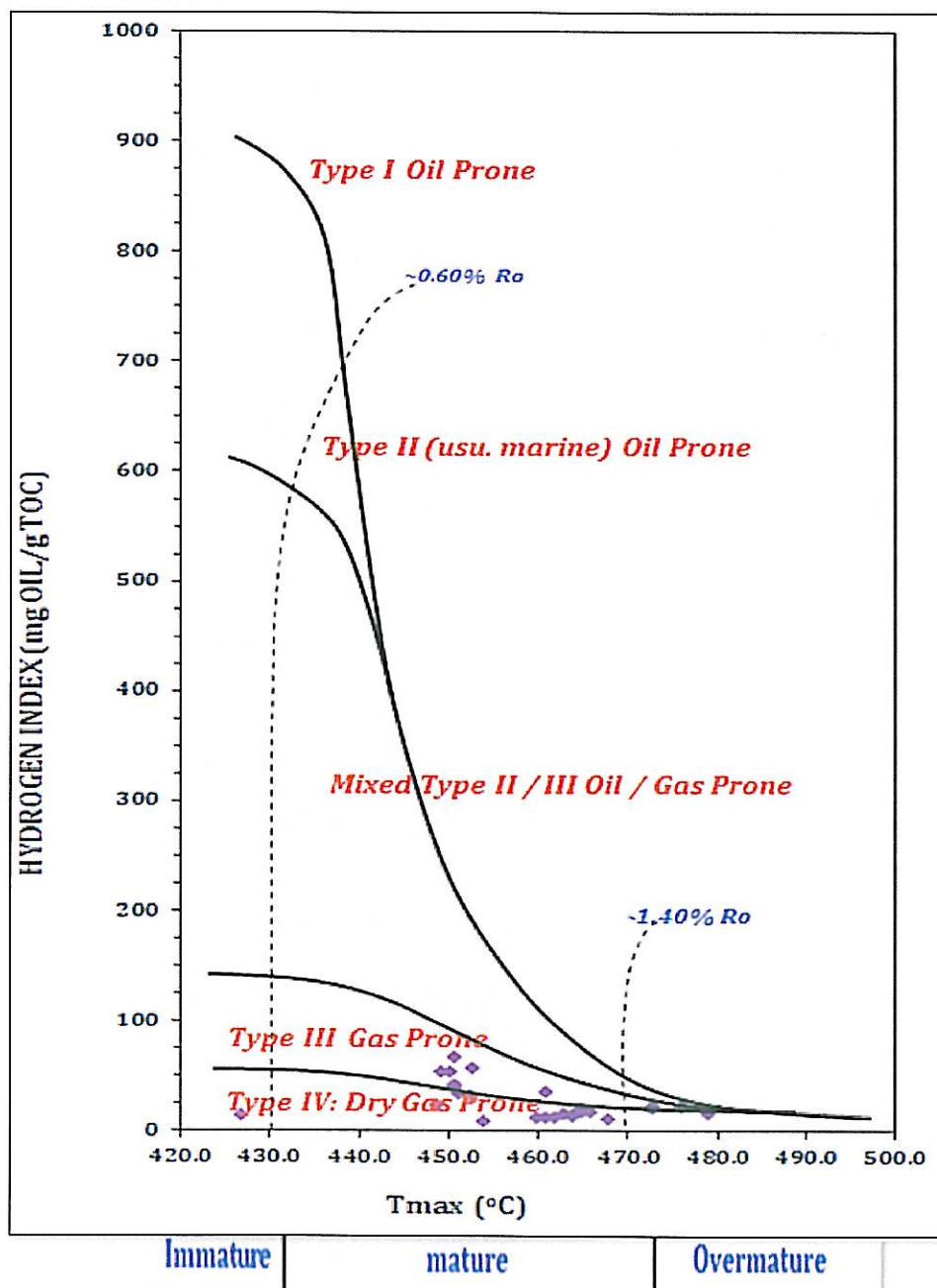


Figure 4.4: A plot of hydrogen index against T_{max} . It suggests the organic matter of the Hanadir is highly mature.

4.1.2 Quality of Organic Matter of Well-B

Twenty-four cuttings and cores samples recovered from (7516 - 7849 ft.) correspond to 333ft of thick interval of the Hanadir from well B. All samples are subjected to Rock-Eval pyrolysis to evaluate Hanadir source rock generative potential and maturity. The Rock-Eval pyrolysis results were loaded into GeoLog software for purpose of data correlation and interpretation (Fig 4.5). The total organic carbon of the Hanadir is ranging from (0.42 – 1.39 %) and suggesting poor to good quality of organic matter. The values of remaining hydrocarbon potential (S2) of the Hanadir is ranging between (0.20-0.39 %) additionally, hydrogen index (HI) values is between (21 – 81 mg HC/g Rock). Both results of (S2 and HI) confirming poor to lean generative potential (Fig 4.6). Geochemical parameter that used to evaluate the Hanadir source rock generative potential is provided in (Table 4.2).

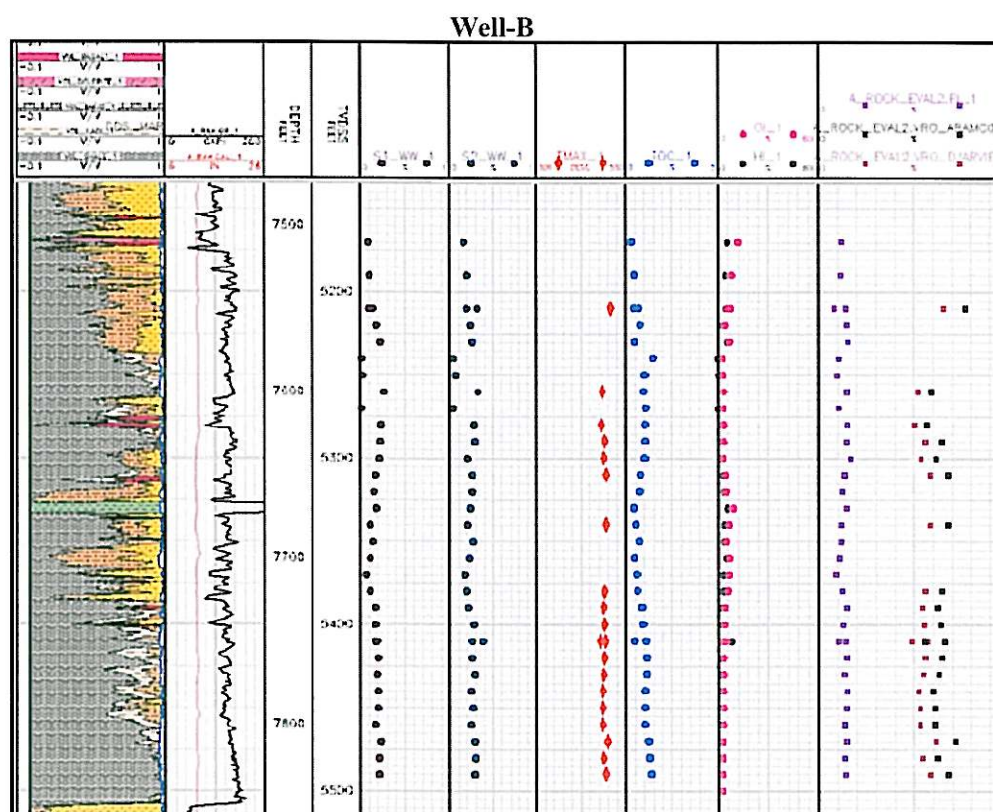


Figure 4.5: Geochemical log of Rock-Eval and TOC results from well -B.it includes calculated vitrinite reflectance in the last column.

Rock-Eval Parameter	Max	Min	Average
HI (mg HC/g TOC)*100	81	21	31
OI(mg CO ₂ /g TOC)	76	28	42
TOC (wt. %)	1.39	0.42	0.42
PI	0.51	0.24	0.50
S ₁ (mg HC/g Rock)	0.10	0.27	0.19
S ₂ (mg HC/g Rock)	0.39	0.20	0.27
T _{max} (°C)	507	429	488.25

Table 4.2: Geochemical parameter used to evaluate Hanadir source rock generative potential.

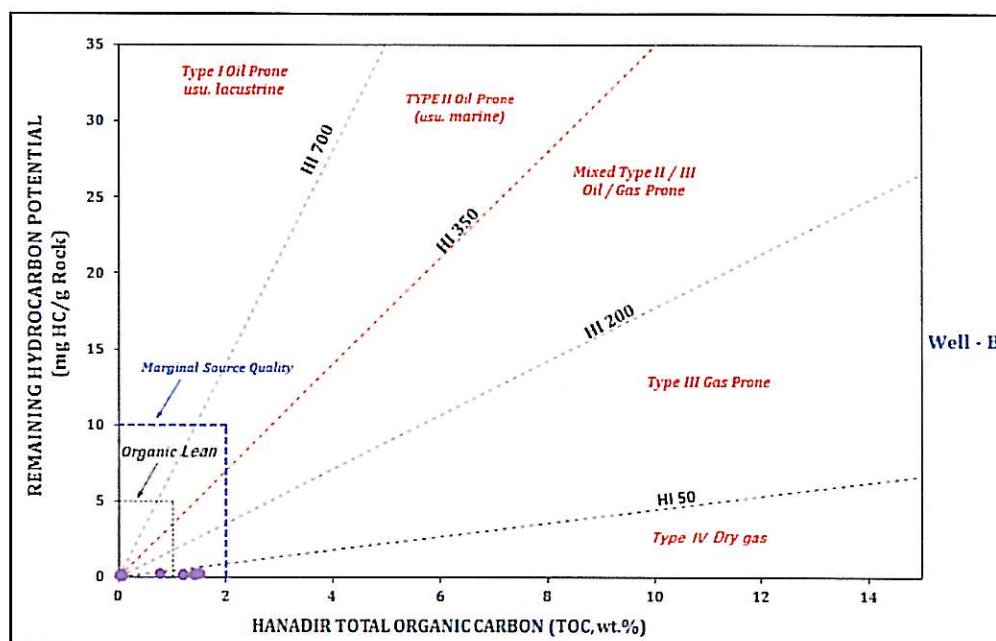


Figure 4.6: A plot of remaining hydrocarbon potential (S₂) against total organic carbon (TOC) indicating lean to marginal source rock potential of Hanadir shale for Well-B

4.1.3 Type of Organic Matter and Thermal Maturity of Well-B

Based on the plot of a pseudo Van Krevelen diagram (OI) and (HI) indicate that well-B relatively has higher thermal maturation than well-A, that makes the determination of kerogen type is impossible to achieve. A similar result was observed in well-B. The kerogens type (III) and (IV) doesn't reflect the original type of kerogen of Hanadir (Fig4.7). The plot hydrogen index (HI) versus T_{max} indicates maximum release of hydrocarbons from cracking of kerogen occurs during pyrolysis at 480 °C is reflecting high level of thermal maturation. (Fig 4.8).

The origin kerogen type of Hanadir remains under speculative interpretation, due to difficulty to differentiate the type of kerogen that have gone through that high level of thermal maturation. Additionally the predicted vitrinite reflectance equivalent indicates (VRe) the thermal maturity exceeds (1.4 %). Prominently Rock-Eval results obtained from well-A and well-B confirmed Handadir source rock is in the gas- generation stage or beyond as indicated from the present day very low HI and high T_{max} values.

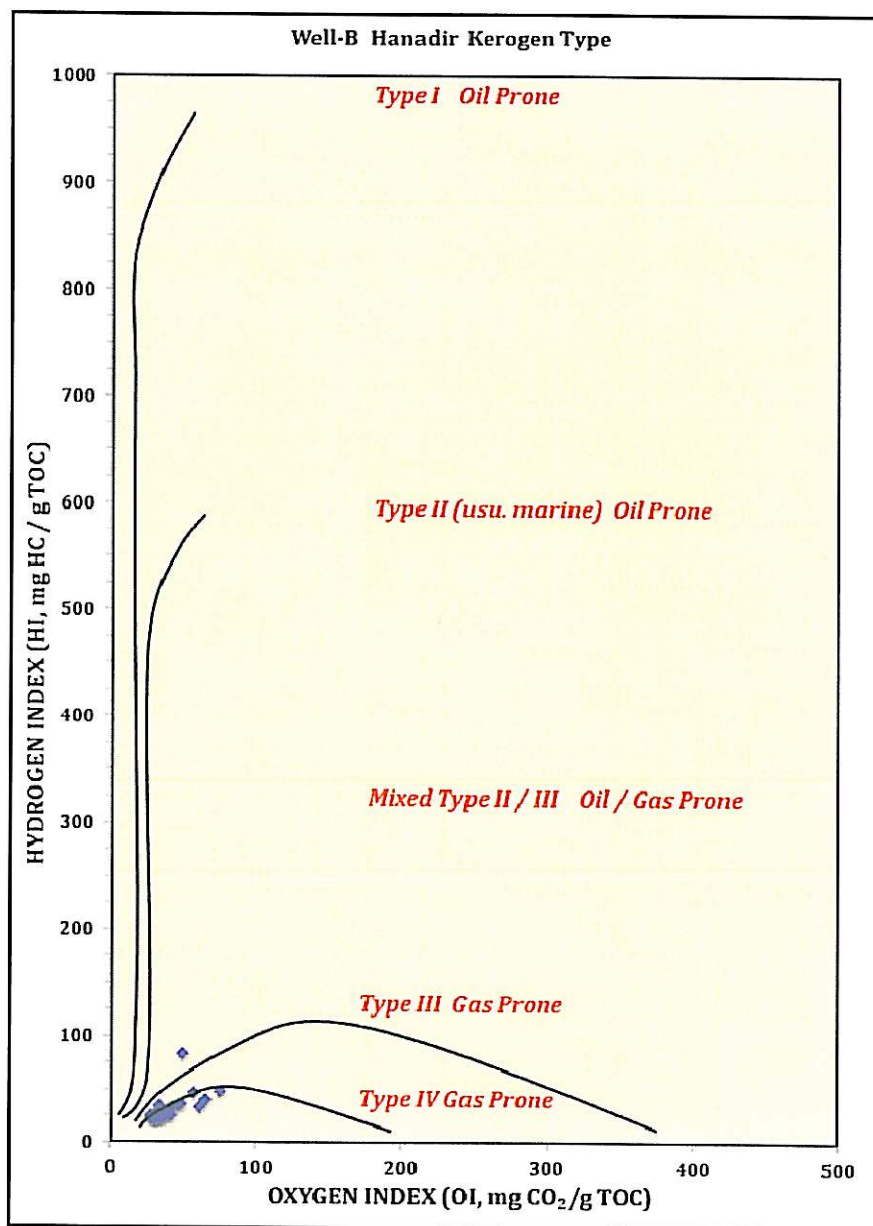


Figure 4.7: A plot of pseudo Van Kervelen diagram a hydrogen index against oxygen index. It suggests the kerogen type Hanadir shale is Kerogen III or IV, although the this suggestion is not true , because type III or IV kerogen represent the last stage of maturation and it is difficult to determine the original type of kerogen reached to that late stage of thermal maturation.

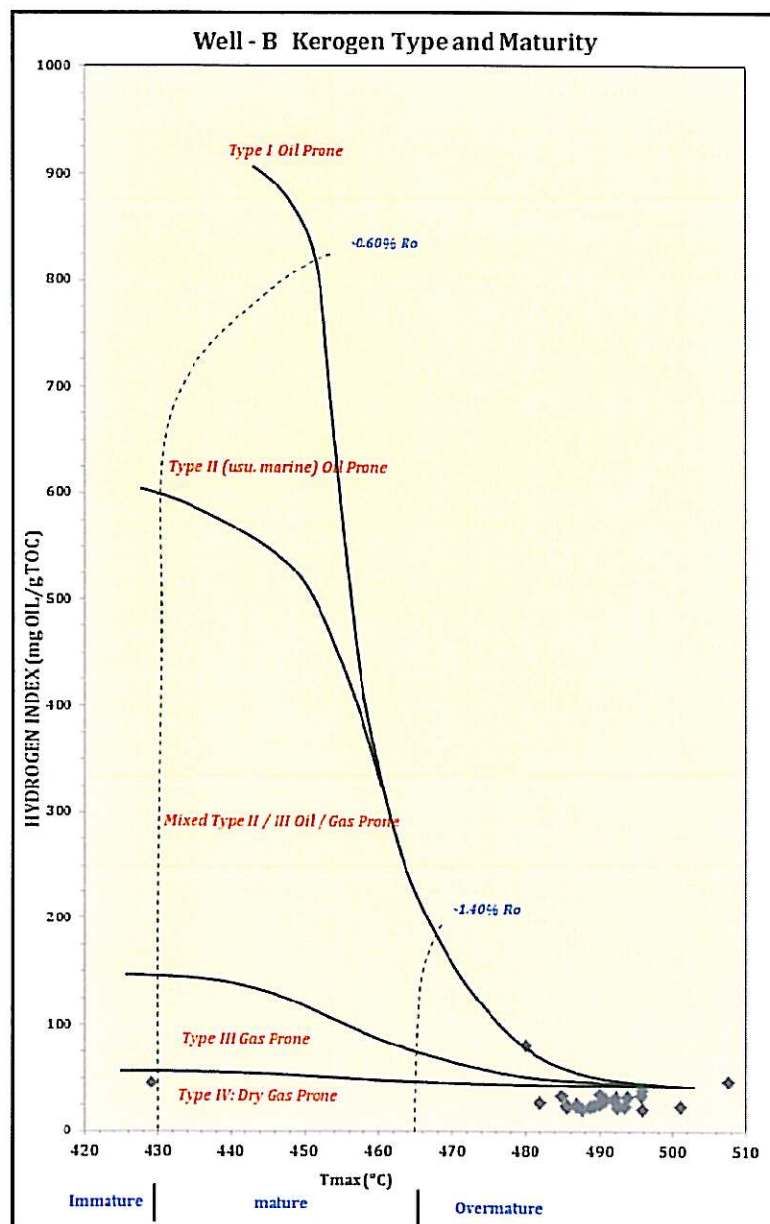


Figure 4.8: A plot of hydrogen index against T_{max} to estimate the thermal maturation of organic matter of Hanadir. It suggests the organic matter of Hanadir in well-B is highly mature than well-A.

4.1.3 Quality of Organic Matter of Well-C

Seventeen cuttings samples recovered from depth (6510ft - 6870 ft.) represent a thickness of 360ft of Hanadir from well C. All samples are subjected to Rock-Eval pyrolysis to evaluate Hanadir source rock generative potential and maturity. (Fig 4.9). Hanadir total organic carbon (TOC) values are fluctuating from (0.037 – 1.50 wt. %) with average (TOC) is about (0.4 %). It suggests poor to fair quality of organic matter. Also the values of oxygen index (OI) suggest that the organic matter has been oxidized which imply there is no hydrocarbon potential in this well. The geochemical parameter that used to evaluate Hanadir source rock generative potential is provided in (Table 4.3)

Rock-Eval Parameter	Max	Min	Average
HI (mg HC/g TOC)*100	425	10	31
OI(mg CO ₂ /g TOC)	925	61	455
TOC (wt. %)	1.50	0.03	0.40
PI	0.59	0.41	0.51
S ₁ (mg HC/g Rock)	0.27	0.10	0.16
S ₂ (mg HC/g Rock)	0.39	0.20	0.27
T _{max} (°C)	504.5	293	350

Table 4.3: Geochemical parameter used to evaluate Hanadir source rock generative potential.

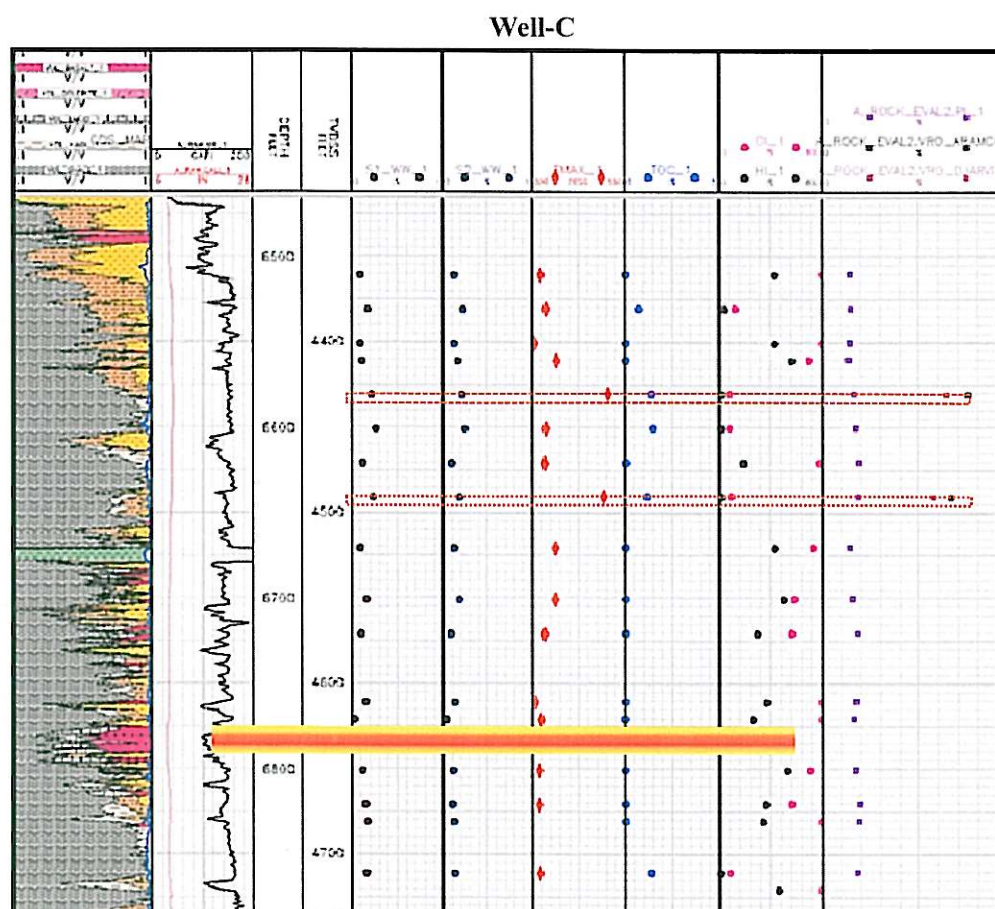


Figure 4.9: Geochemical log of Rock-Eval and TOC results from well-C. It includes calculated vitrinite reflectance in the last column. The dashed lines representing two samples that may not be affected by contamination. The orange color bar corresponds to igneous intrusion identified based on log readings.

4.1.4 Possible Effect of Contamination Observed in well-C

Hanadir in well-C potentially has been affected by contamination of drilling fluids. The most severely affected Rock-Eval parameters by contamination are (S1, T_{max}, and PI). Commonly the effect of contamination show in S1 peak greater than (S2 mg HC/g rock), extraordinary high production index (PI) value, and lower reading of T_{max} compared to adjacent samples. In addition the bimodal S2 peak can be recognized from available pyrogram (Peters, 1986). High values of production index (PI), lower values of T_{max}, and possible bimodal for S2 peak was noticed; all those parameters are in agreement with presence of contamination in the well-C, except there are no substantial high values noticed for S1. Two samples were noticed with high T_{max} (494 and 505 °C) and may not affect by contamination.

Source rock of Hanadir in well-C is originally poor to non-generative potential and lately affected by contamination, also the values of oxygen index (OI) suggest that the organic matter has been oxidized which imply there is no hydrocarbon potential in this well.

As result the effect of contamination in very poor to marginal source rock most likely is not increasing the reading of S1. Additionally, the conversion of organic matter indicates that most of the samples were exposed to contamination except for two samples were in the very high mature zone. The possible interpretation of these two samples may survive from the effect of contamination and exposed to igneous intrusion. (Fig 4.10).

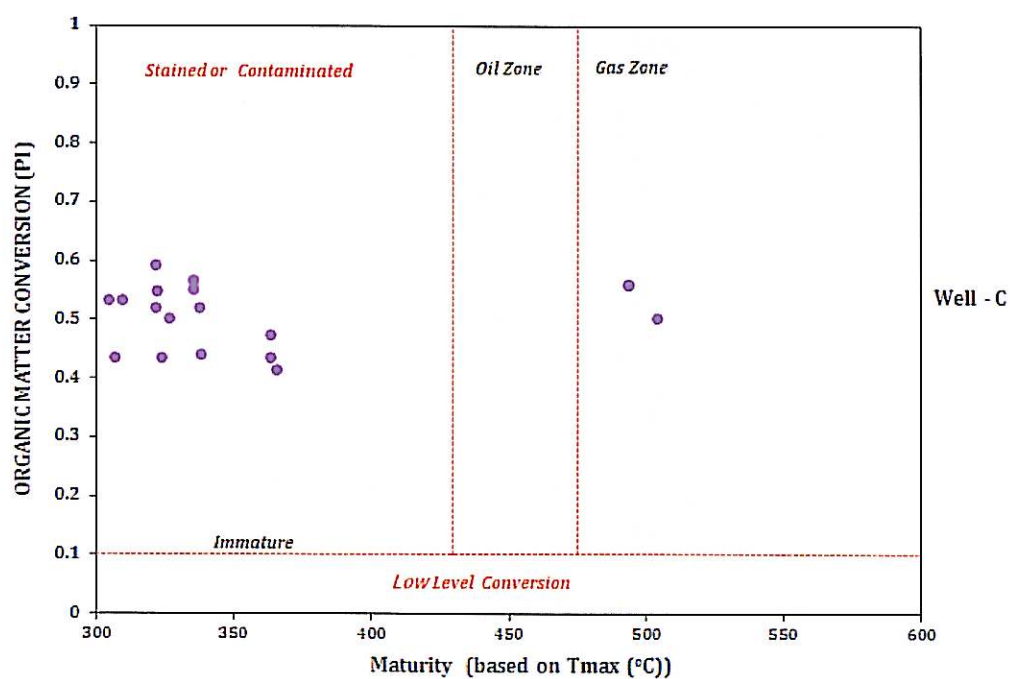


Figure 4.10: A plot of organic matter conversion suggesting the most of samples has been affected by contamination. The values of PI exceed more than 0.1 and lowering the T_{max} less than 430 $^{\circ}C$, except two samples indicating high level of thermal maturity, which may be affected by igneous intrusion.

Additional evidence supporting the argument of contamination is a bimodal histogram of T_{\max} is reflecting low and extremely high temperatures. If the most of the samples not exposed to contamination they will be gone through high maturity between, the predicted T_{\max} will be between (400 -470 $^{\circ}\text{C}$), the two over-mature samples may reflect the effect of igneous intrusion (Fig4.11)

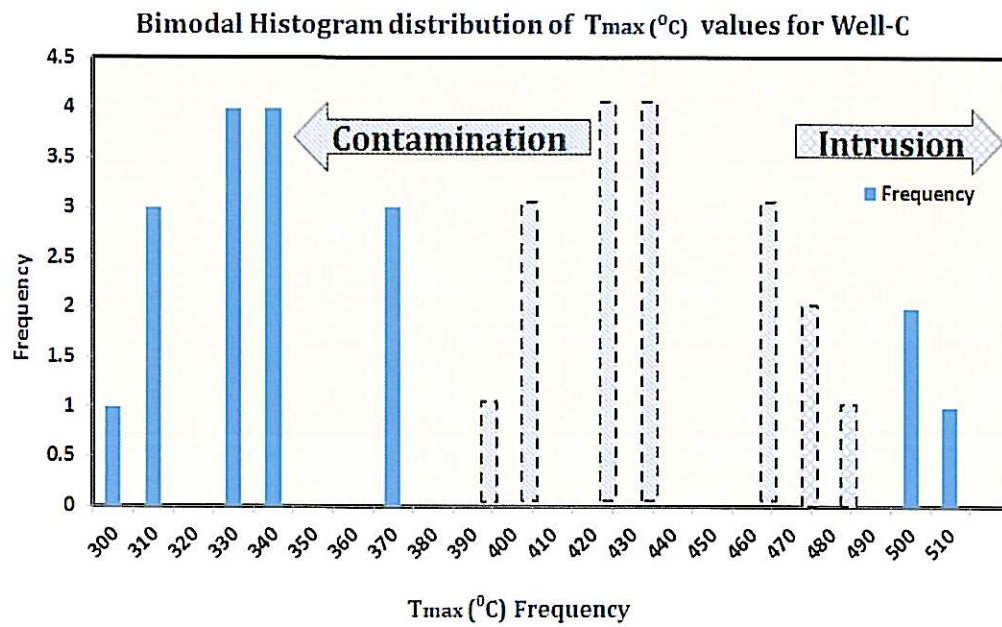


Figure 4.11: Bimodal histogram of T_{\max} showing two different temperatures low, and anomalously high values. The majority of the samples were affected by contamination, the dashed line predicting the T_{\max} if the samples were not affected by contamination. The two samples with extremely high temperature may reflect the effect of igneous intrusion.

4.2 ELEMENTAL ANALYSIS

Cole, 1994 conducted an analysis of Iron –sulfur-carbon (Fe-S-C) for some marine source rock samples from Qasim formation in northwest Saudi Arabia. The location of the study is exactly on the location of the current study (Fig 4.12). The analysis concludes that almost of all of the samples used in the analysis are plotted towards Iron apex which indicates these samples were deposited under oxic condition. Few samples from Hanadir shale showing they were deposited in anoxic-dysoxic conditions (Fig 4.13). Prevailed oxygenated bottom waters coupled with low organic productivity during the deposition of Hanadir member in well C, ultimately resulted in accumulation of poor to marginal generative potential.

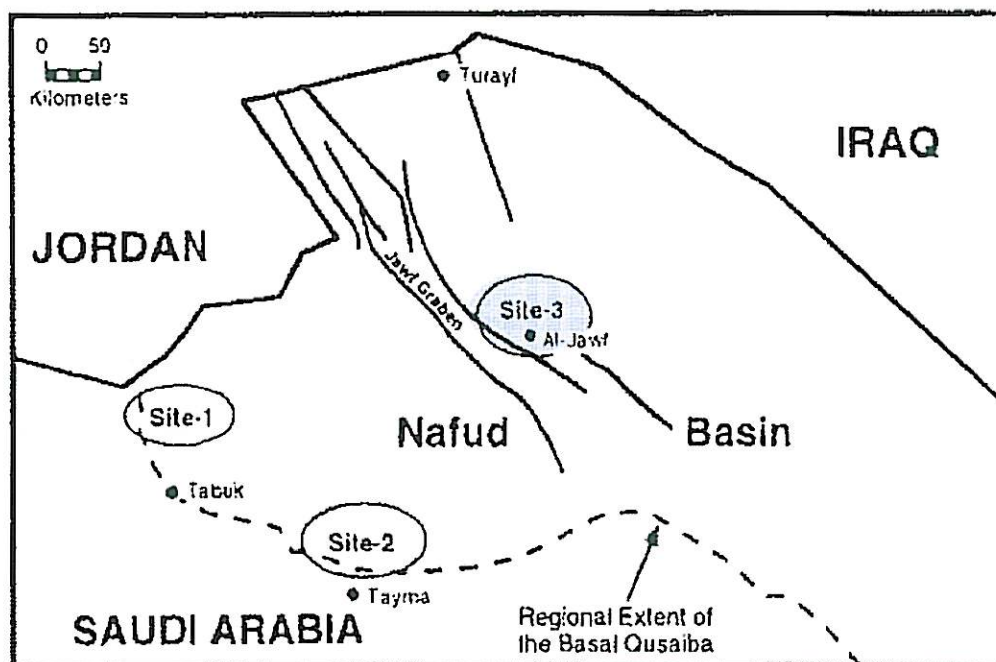


Figure 4.12: location map showing site 3 where source rock samples from Qasim Formation including Hanadir member, were collected for Fe-S-C analysis (Cole.,1994)

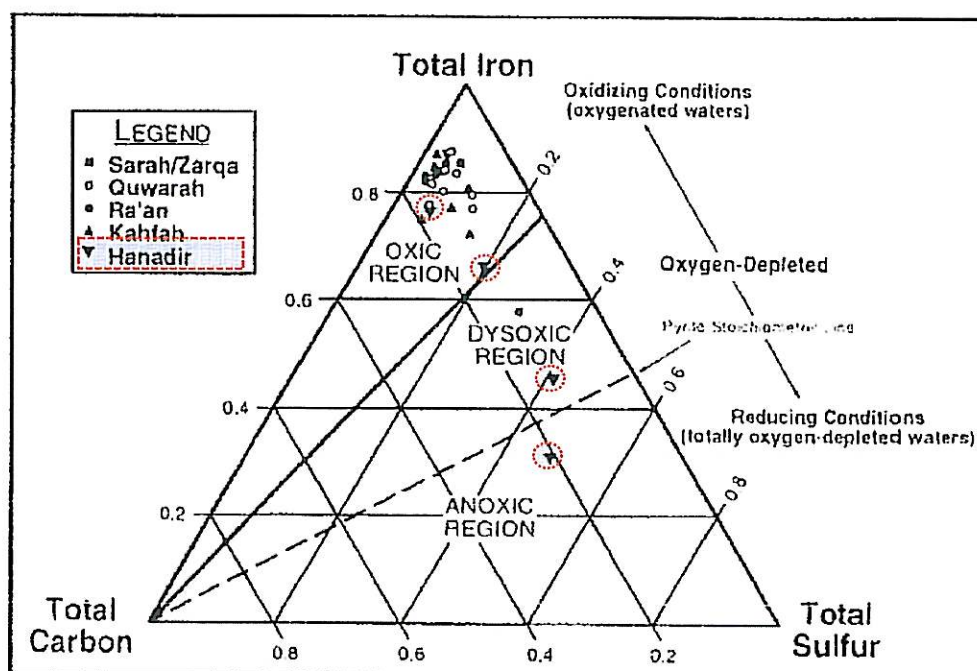


Figure 4.13: results of iron-sulfur-carbon (Fe-S-C) analysis at ternary plot for Qasim formation including Hanadir member in the northwest Saudi Arabia. Almost of the samples were plotted toward Iron (Fe) apex which indicates they were deposited in oxic conditions, except few samples from Hanadir (in red circle) showing they were deposited in range of anoxic-oxic conditions that confirm Hanadir in well C was not deposited totally in anoxic condition it may be seasonally exposed to dysoxic condition as indicated by result of oxygen index (OI) from rock – eval analysis (after Cole., 1994)

4.3 MICROPALAEONTOLOGY

The depositional environment of Hanadir shale member of the Qasim Formation was described by (Senalp et al., 2001) as predominately argillaceous sediments were deposited from suspension in open-marine shelf environment below storm wave base. (Kaminski et al., 1993) conducted a study to examine and document deep water agglutinated foraminifera in response to oxygen levels and organic carbon contents in modern restricted California borderland dysoxic basin. The study concluded that the deep water agglutinated foraminifera from seasonally dysoxic environments are mainly contained foraminifera such as *Reophax* and *Psammosphaera* and has been observed as large-sized taxa in some Catalina basin. The most severely dysoxic organic rich basin had foraminifers that were strongly dominated by small, flattened, tapered shapes.

The faunal change takes place when oxygen values of bottom water fall to 0.2 ml/l. In contrast with well oxygenated (oxic) condition, the foraminifera contain a variety of different morphogroups with more habitat space. (Fig 4.14) The most recent agglutinated forms were recovered from Hanadir during the progress of this study suggests that the organic matter of the Hanadir in well C was not preserved completely in anoxic bottom water conditions; it may have been exposed seasonally to dysoxic and oxic conditions as confirmed the presence of oxidization by results of rock-eval pyrolysis of high value of oxygen index OI.

The descriptions of recovered agglutinated foraminifera are small and medium-large sized taxa with elongated rounded, flattened and tapered chamber may reflect seasonal dysoxic conditions. The best predominant agglutinated forms represent dysoxic

environments are *Psammosphaera sp* and *Placopsilina* (Fig 4.15). Some observed *Placopsilina* are growing attached to something, most probably on organic matter to get more oxygen when the depositional condition becomes severely dysoxic. The SEM pictures showing micro porosity evolved around the suture for attached forms (plate 6 and 7). The total organic carbon value corresponds to that condition is (0.76 TOC wt. %).

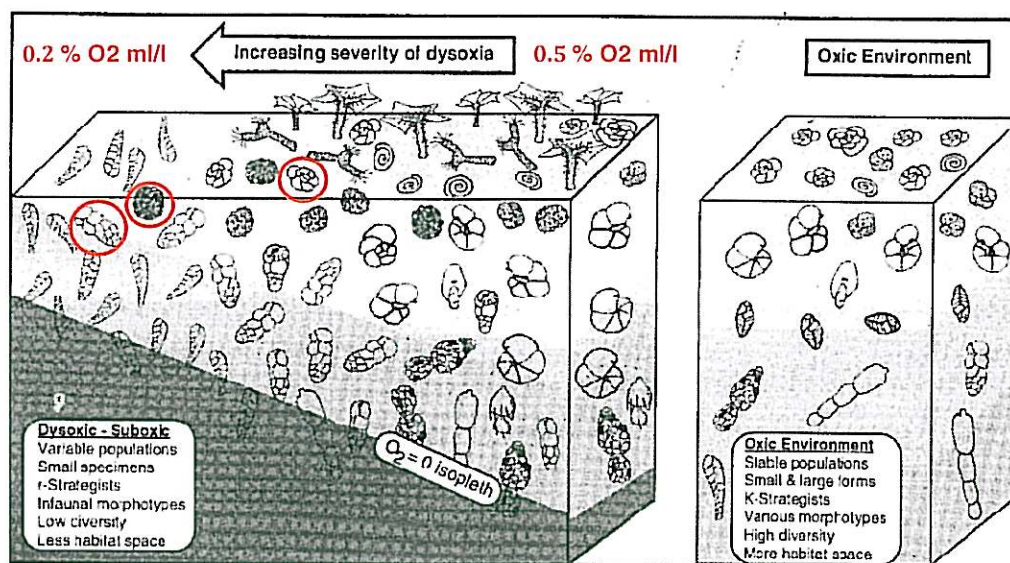


Figure 4.14: conceptual morphogroup model representing the response of agglutinated foraminifera to dysoxic conditions in the California Borderland basin (Kaminski et al., 1995) that can be applied to the Hanadir source rock where *Psammosphaera* sp and *Placopsilina* were adapted to low oxygen content.

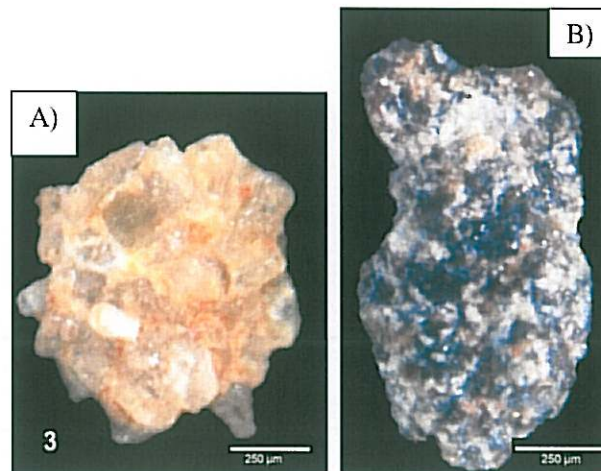


Figure 4.15: A) Showing recovered *Psammosphaera* sp. as elongated agglutinated foraminifera from Hanadir member in well- C reflecting dysoxic condition. B) *placopsilina* sp flattened and tapered chamber, the arrow indicate it may be lived attached to something, most probably organic material to exchange the oxygen when the percentage of oxygen become severely low

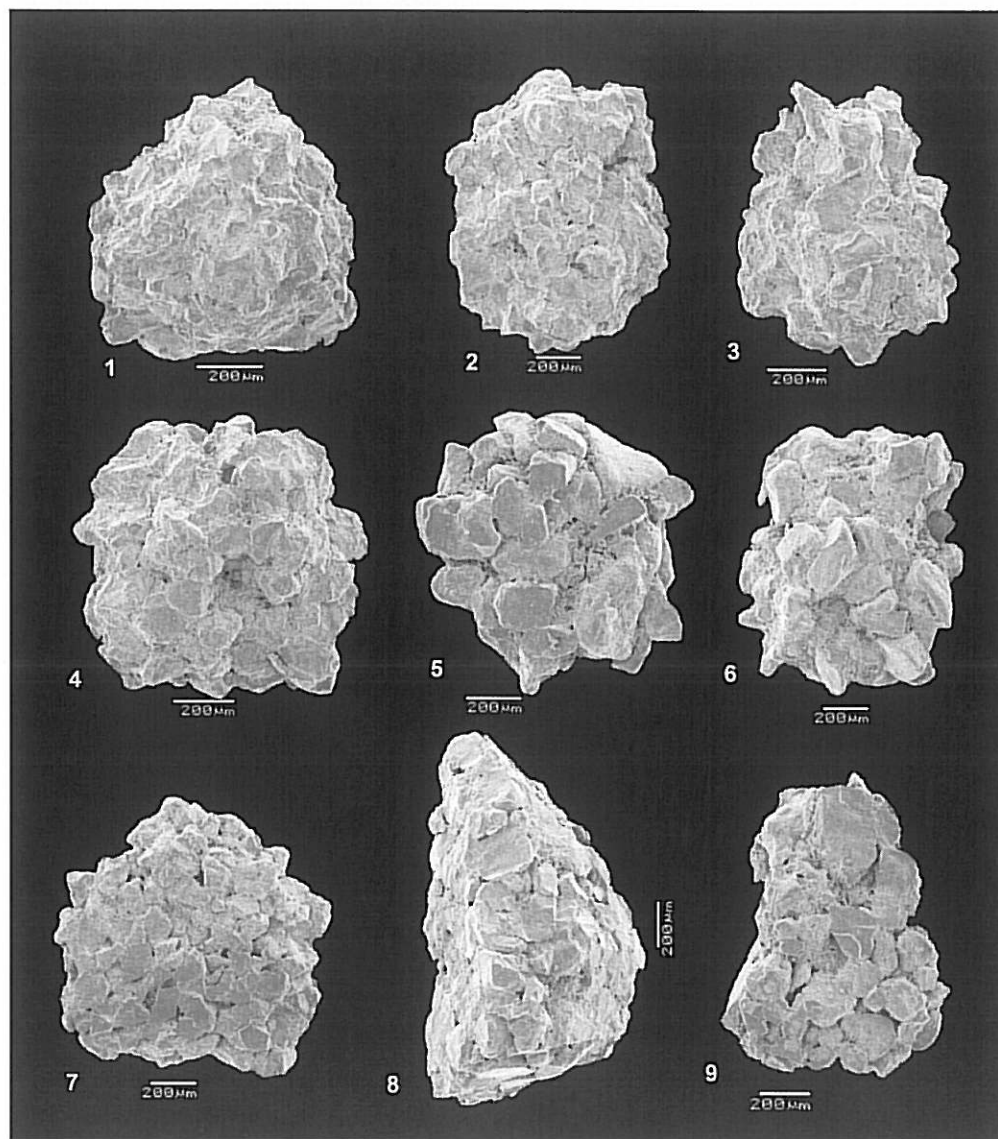


Plate 6: SEM photo showing the flat surface of attached foraminifera, notice samples number 4, 5, 7 and 9

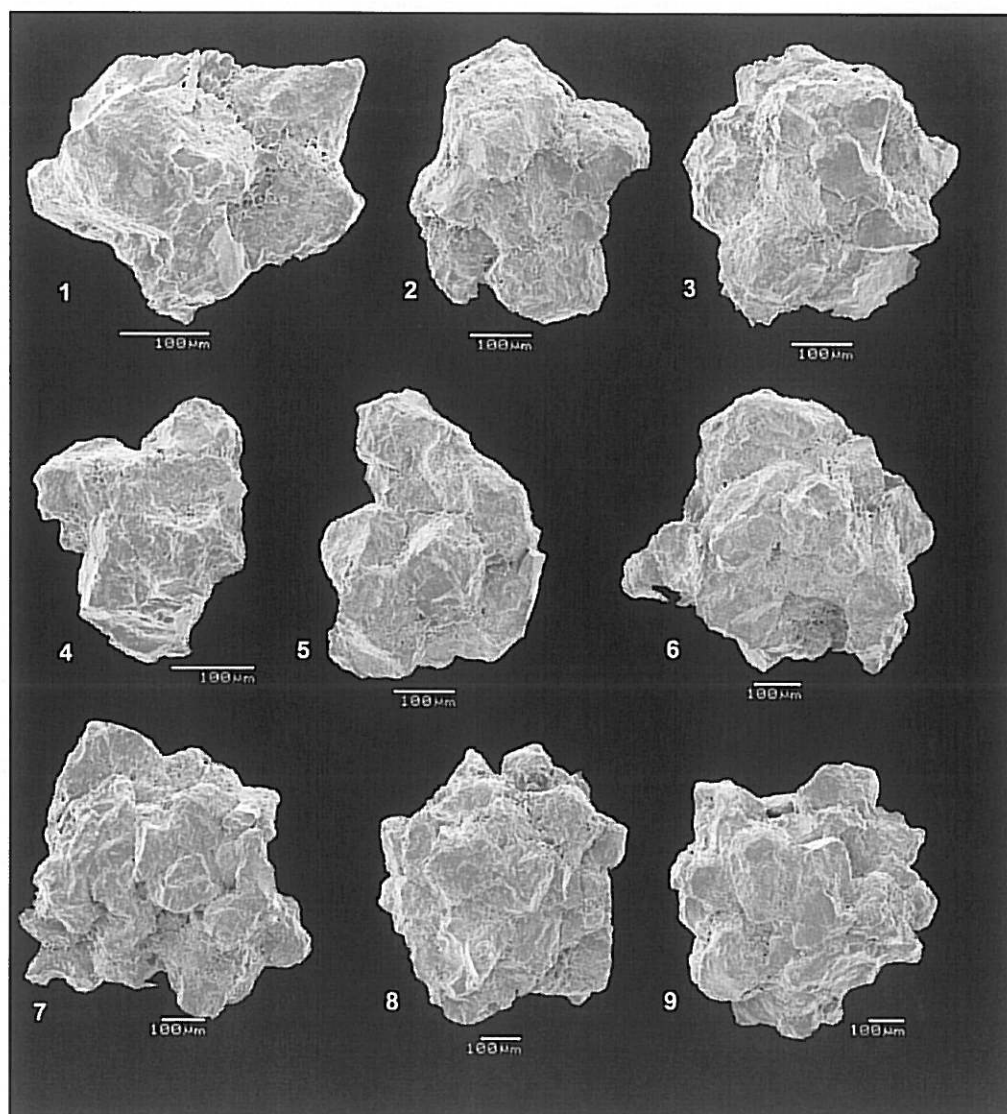


Plate7: SEM photo showing developed micro porosity around the suture may be was used as channel of transferring the oxygen to the organism left inside the chamber

4.3.1 New Approach to Predict Hanadir Kerogen Type

Identifying kerogen type of the Hanadir is an extremely challengeable process to accomplish; especially for source rock has gone through advance stage of thermal maturation. Organic petrography has been considered to utilize to identify kerogen type of the Hanadir . Unfortunately the analysis was not conducted due to inadequate amount of sample to carry out the analysis and the study of palynofacies taxa recovered and analyzed from Hanadir indicate thermal alteration index 3+ on Staplin scale which corresponds to values of vitrinite reflectance in the range of 1.3-1.5, i.e., over-mature source rock, consequently the kerogen type is problematic to recognized by this tool. Interestingly the challenge of determining kerogen type of the Hanadir can be overwhelmed indirectly by utilizing the relationship of depleted oxygen environment of agglutinated, benthic foraminifera and source rock organic facies (Fig 4.16)



Figure 4.16: Systematic approach that subjectively predicts the kerogen for advance thermal matured source rock. It optimizes the relationship of redox condition of agglutinated foraminifera and source rock organic facies

This approach indicates there some agglutinated foraminifera such as *Psammosphaera* and *placopsilina* species can be adapted with dysoxic environment. These two species survive when the Oxygen content decreased to reach up to 0.2 ml/l of water. Consistently the benthic foraminifera adapted also with the same content of oxygen at dysoxic environment (Fig 4.14). Gerard et al., 1983) predicted four organic facies based on relationship between oxygen content at dysoxic environment and benthic adapted to low oxygen condition. (Table 4.4)

Organic Facies	Kerogen Type	Oxygen Condition	Depositional Environment	Amount of Organic Matter	Presence of Fauna and remarks
1	Kerogen(I) (oil-prone)	Highly Reducing	Lacustrine/Marine	Up to 30%	Highly anoxic no benthic foraminifera
2	Kerogen(II) (oil-prone)	Anoxic-dysoxic	Lacustrine/Marine	1-10 %	Benthic foraminifera and worm burrows with Increasing dysoxic condition
3	Kerogen(III) (gas-prone)	Mildly oxic-anoxic	Continental-marginal marine, lagoonal	20%	Fairly abundant benthic foraminifera
4	Kerogen(IV) (non-source)	Oxic	Any environment	0.2 - 3%	Organic matter residence for long time in oxic-microbial degradation. Ventilated oceanic conditions, low sedimentation rate, such shallow high energy shelves

Table 4.4: summarize of four rock source organic facies identified based on relationship between oxygen content, benthic environment and depositional factors (Gerard, 1983). Hanadir source rock represents kerogen type (II). The organic matter of was not preserved in total anoxic bottom water condition, it may have been seasonally deposited in dysoxic environments.

The benthic foraminifera can survive when the percentage of oxygen reduced up to 1 ml/l taking in consideration sedimentation rate. The expected type of kerogen can be observed in dysoxic environment are type II or type III depend on the type of organic matter if it is derived from terrestrial or marine organic matter (Fig 4.17). Applying this approach using agglutinated and benthic foraminifera oxygen depleted environment to determine kerogen type of Hanadir source rock. Subjectively indicate that the organic matter of Hanadir source rock represent type II kerogen, because land plant (type III kerogen) was evolve after Silurian time. Also this result is consistent with regional Hanadir source rock equivalent in adjacent countries such as Syria, Jordan and Iraq.

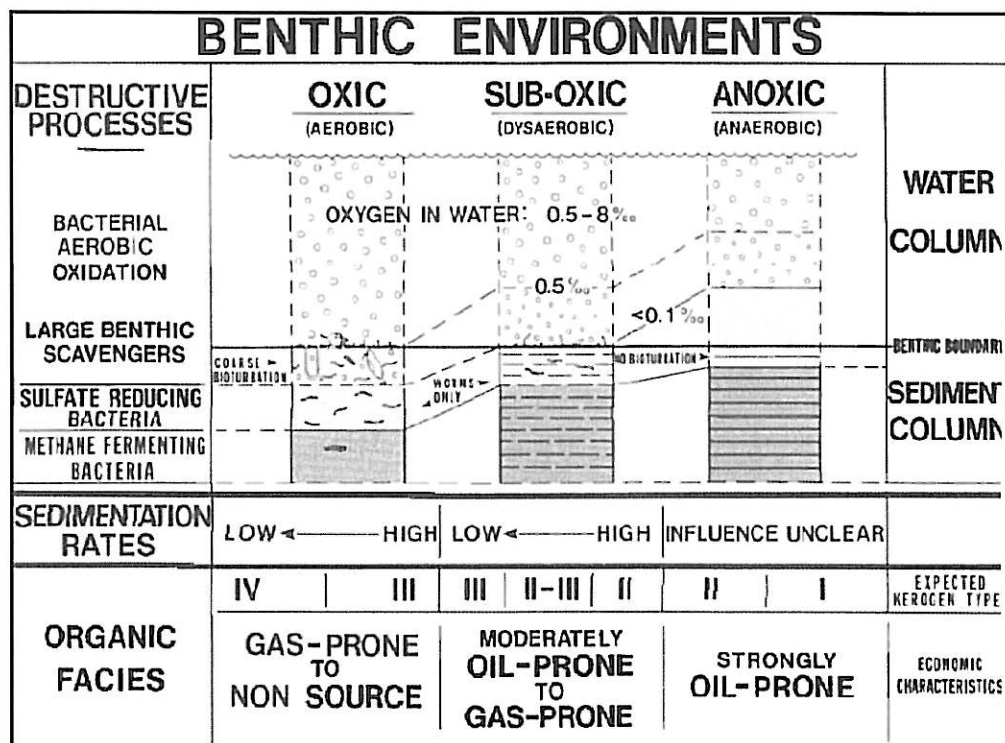


Figure 4.17: Organic facies identified based on relationship between depositional factors, keogen type and oxygen depleted settings favorable for source rock deposition (Gerard et al., 1983).

4.4 PALYNOLOGY

4.4.1 Palynology Samples Analysis and Thermal Maturation

The *Acritarchs* and *Chitinozans* analyses essentially used to provide information about the evolution of thermal maturation, they clearly confirmed the organic matter of Hanadir shale was exposed to high level of maturation ranging between 1.3-1.5 VRe. The palynology samples were from well (A, B and C). Table (4.5) showing the depth for palynology samples

Depth of Palynology Samples (ft.)					
Well -A	Sample Type	Well-B	Sample Type	Well-C	Sample Type
8103.7	core	7570	cuttings	6520	cuttings
8147.0	core	7620	cuttings	6570	cuttings
8191.6	core	7660	cuttings	6610	cuttings
8196.5	core	7710	cuttings	6650	cuttings
8199.8	core	7720	cuttings	6840	cuttings
		7740	cuttings	6850	cuttings
		7770	cuttings		
		7800	cuttings		
		7810	cuttings		

Table: 4.5: Depth of collected samples for palynology analysis

The analyzed samples contain abundant organic matter, structured and unstructured, of brown to dark brown in color, which can be attributed to a thermal alteration index of 3+ on Staplin color scale which corresponds to values of vitrinite reflectance in the range of 1.3-1.5, i.e., over-mature organic matter, in the dry gas generation window (Fig 4.18)(Staplin, 1969).The palynological assemblage includes moderately well preserved to poorly preserved chitinozoans and acritarchs (abundant) and cryptospores (rare).

The diversity of the assemblage is moderate (low in sample 8103.7), but it is probably underestimated because the poor preservation does not allow in many cases to recognize taxa down to species level. Depositional environment was normal marine, open shelf. The most commonly occurring taxa include:

Acritarchs:

Baltisphaeridium ternatum, *Frankea longiuscula*, *Michrystidium*
sp., *Stellechinatum celestum*, *Stelliferidium stelligerum*, *Stelliferidium striatulum*

Chitinozoans:

Acanthochitina sp., *Belonechitina* sp., *Cutichitina legrandi*, *Desmochitina mortoni*
Lagenochitina spp. *Linochitina pissotensis*, *Siphonochitina formosa*

The assemblage clearly demonstrates a Darriwilian (Llanvirn) age; it corresponds to the O2/O3 palynological zone as used by Saudi Aramco.

Plate 7: Typical palynofacies taxa recovered and analyzed from Hanadir Shale Indicate thermal alteration index 3+ on color scale of Staplin which corresponds to values of vitrinite reflectance in the range of 1.3-1.5, i.e., over-mature organic matter:

1. *Frankea longiuscula*
2. *Desmochitina mortoni*
3. *Acanthochitina* sp.
4. *Cutichitina legrandi*
5. *Stelliferidium stelligerum*
6. *Linochitina pissotensis*

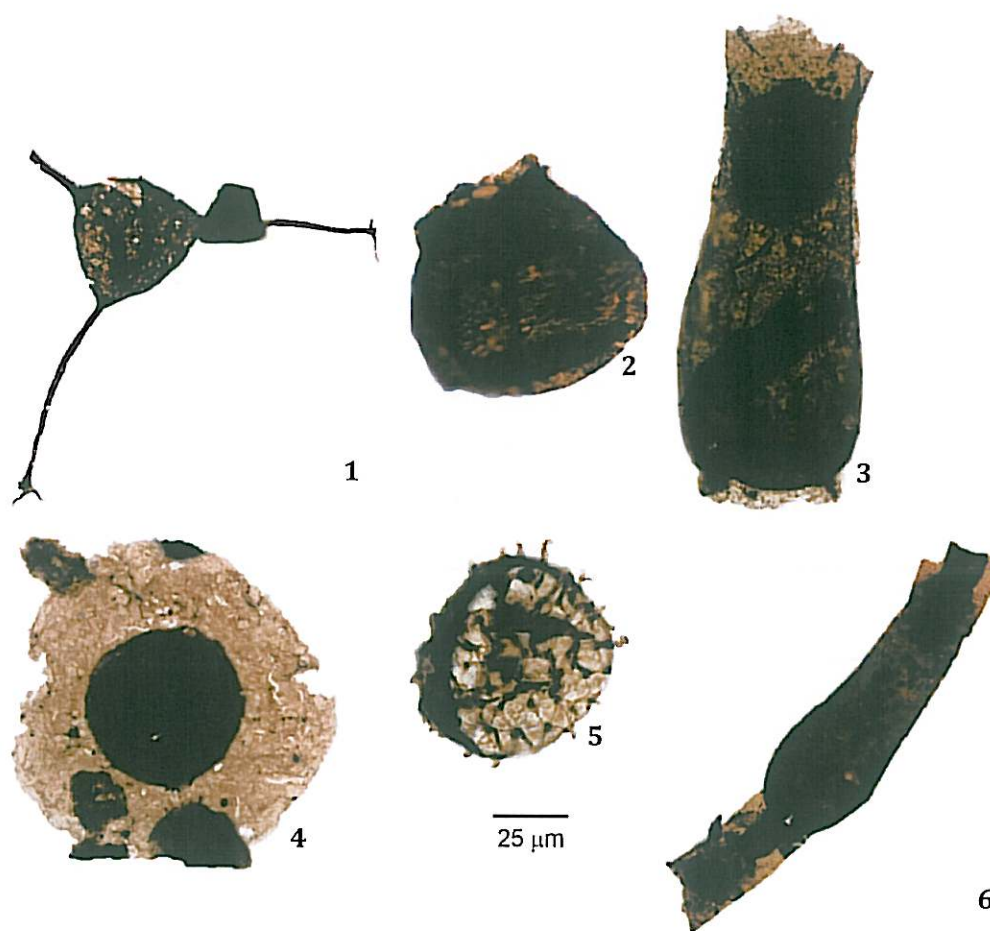


Plate 8: Representative palynofacies recovered from well (A and B) 1. *Frankea longiuscula*; 2. *Desmochitina mortoni* 3. *Acanthochitina* sp.; 4. *Cutichitina legrandi*; 5. *Stelliferidium stelligerum*; 6. *Linochitina pissotensis*.

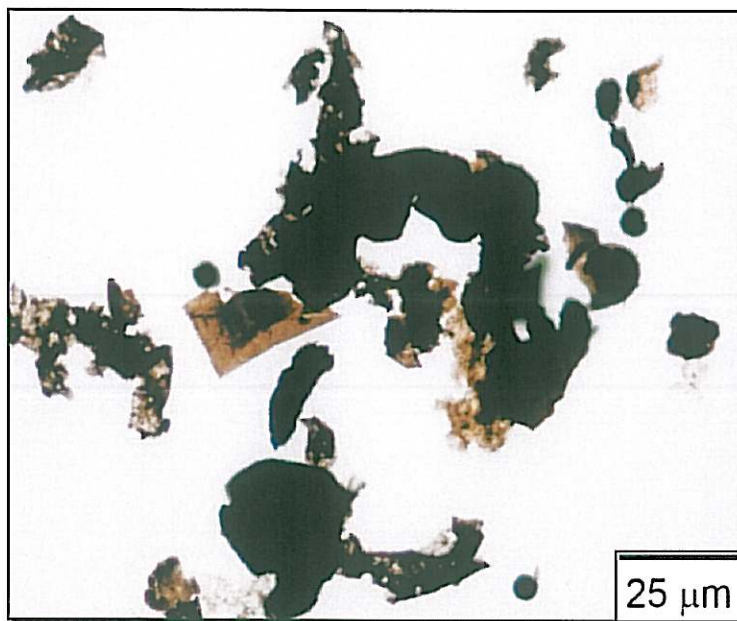


Plate 8: Typical palynofacies of the analyzed slides, with organic matter preservation indicating a thermal alteration index of 3+ on the color scale of Staplin (1980)


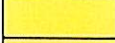

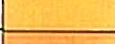
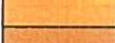






ORGANIC THERMAL MATURITY	COLOR OF FOSSIL SPORES/POLLEN	MUNSELL PRD. NO.	APPROXIMATE CORRELATION TO OTHER SCALES		COAL RANK	EXINITE FLUORESCENCE: AMOUNT AND COLOR
			TAI= 1-5	VITRINITE REFLECTANCE		
IMMATURE		17,391	1	0.2%	Peat	High to Medium; blue-green
		20,520	1+	0.3%	Lignite	High to Medium; green-white
		19,688	2-		Subbituminous	
		14,253	2	0.5%	Bituminous, High Vol. C Bituminous, High Vol. B Bituminous, High Vol. A	High to Medium; white-yellow
MATURE MAIN PHASE OF LIQUID PETROLEUM GENERATION		12,800	2+			High to Low; yellow
		12,424	3-	0.7%	Bituminous, Medium Vol.	Low; dark yellow to orange-brown
		15,816	3			No Fluorescence of Spores/Pollen Exines
		17,207	3+	1.3%	Bituminous, Low Vol.	
DRY-GAS OR BARREN		13,814A	4-	2.0%	Semi-anthracite	No Fluorescence of Spores/Pollen Exines
		19,365	4	2.5%	Anthracite	
			(5)			
	BLACK & DEFORMED					

Figure 4.18: Color of thermal alteration index where Hanadir represent 3+ in the color scale of Staplin (1980). It corresponds to values of vitrinite reflectance (VR) in the range of 1.3-1.5 % at late gas window.

4.5 BASIN MODELING

Burial history is one part of basin modeling study that was implemented on wells (A, B and C). Numerical simulation 1D model require a reasonable geological and thermal model that can be calibrated against measured maturity data such as present day bottom hole temperature and vitrinite reflectance values. It is important to achieve the most reasonable scenarios that can explain the basin evolution during geological time. Basin modeling concept has been used to evaluate source rock potentiality, temperature history and organic matter maturity (e.g. Lopattin, 1971; Ungerer et al., 1990; Yalcin et al., 1997). Petromod basin modeling software was utilized throughout this study.

4.5.1 Structural Restoration

Structural restoration is a crucial process to basin modeling, because it determines the evolution of geological structures during geological times. The backstripping is a simple method that decompact the layers using porosity versus depth relationships of only 2D or 3D balanced cross section. Creating a balanced cross section in the Northwest area of Saudi Arabia is not an easy task; especially if it was affected by different tectonic events of rifting, uplifting, and erosions. For example the Hercynian uplift is difficult to captured and interpreted from seismic lines. Based on personal communication with Aramco structural geologist (Dr. Hong B, Xiao) the Hercynian uplift is difficult to be picked from seismic lines and conduct restoration of the stratigraphic layers, because the

uplift ultimately diminished by Cretaceous erosion. The structural restoration was not applied on this study due to poor quality and coverage of seismic lines.

4.5.2 Calibration Data of Basin Models and Limitation

The calibrated data that goes to model can be classified into calibration parameters and uncertain calibration input parameters. The essential thermal calibration parameters are bottom hole temperature, vitrinite reflectance (VR_o), and T_{max} values. These parameters are utilized to search for best fitting model. For example, bottom hole temperatures (BHT) were corrected for well A which range from 98-140 $^{\circ}C/km$ and 55-170 $^{\circ}C/km$ at well B and 80-120 $^{\circ}C$ at well-C. Generally a good agreement between present day bottom hole temperature and vitrinite reflectance values has been observed in those wells. The most uncertain calibration input parameters is heat flow through time and thermal conductivity, uncertainty is due to generally poor knowledge of Paleozoic basement structure and composition in the Northwest area. Therefore different scenarios of heat flow have been taken in account.

4.5.3 Two Different Scenarios of Heat Flow

The first scenario of heat flow values (50-60 mW/m^2) was applied to wells (A, B and C). The results showing around 40% of miss matching between present day bottom hole temperature and vitrinite reflectance values. The second scenario suggests the heat flow should be increased to values of 62 -72 mW/m^2 . It revealed an excellent match for all wells (A, B and C). The second scenario achieved approximately 85% of agreement between present day bottom hole temperature and vitrinite reflectance values. Some geochemist and basin modelers may argue using 72 mW/m^2 heat flow is too high for the

Arabian plate, it is considered to be a stable platform influenced by compressive tectonic activities, therefore in such settings heat flow values are not extremely high. However, this assumption is exactly true anymore, due to the fact the selected wells of this study are located in extensional regimes where higher heat flows and heat flow differences are anticipated (Yalcin et al., 1997). Additionally, based on personal communication with X-Aramco basin modeler (Dr. Pierre J. Van Laer), the heat flow values of Arabian plate in some area confidently should be increased to 75 mW/m^2 . Furthermore, (Abu - Ali and Littke, 2005) have been applied value of 75 mW/m^2 heat flow in (SDGM, UTMN and JAWB) wells which are located in central Arabia.

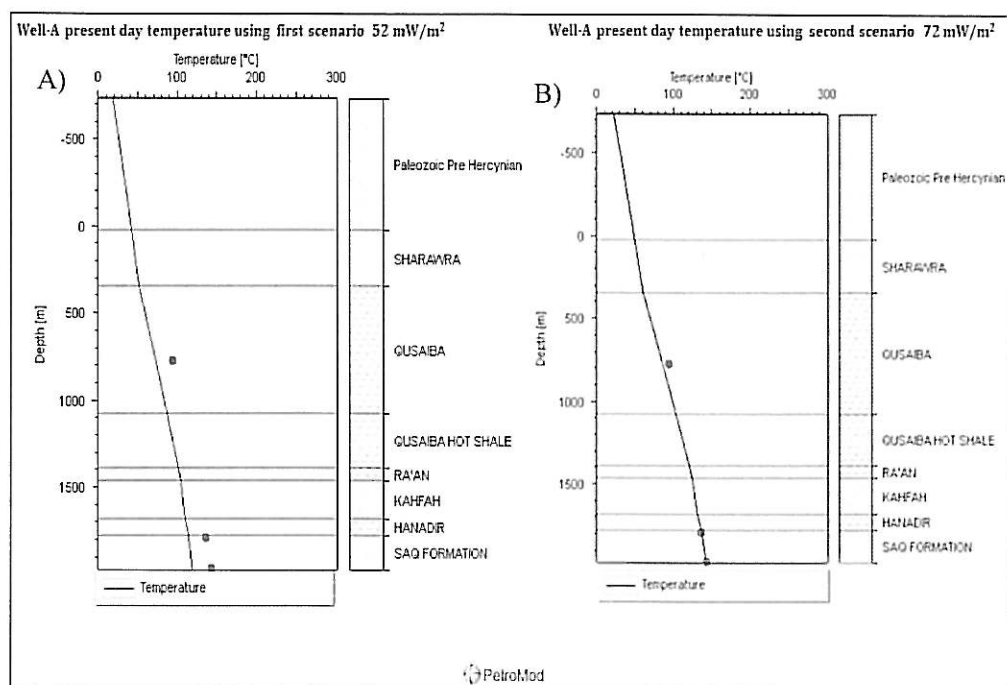


Figure 4.19: showing the compression between two scenarios for measured and predicted present day temperature. A) The first scenario showing miss match between present day bottom hole temperature and vitrinite reflectance values using 52 mW/m^2 of heat flow prediction. B) Second scenario showing excellent correlation between present day bottom hole temperature and vitrinite reflectance values using 72 mW/m^2 of heat flow prediction.

4.5.4 Thermal and Burial History of Well-A

The potential for Handir shale to generate hydrocarbons is controlled by their burial and thermal history. Figures 4.20 A and B displayed vitrinite and temperature data versus subsea depth in meters. The vitrinite data are shown in solid rectangles and represent graptolites reflectance. The temperature calibration are shown in solid circles and they were all corrected using the Horner method based on the original bottom - hole temperature. When the second scenario of heat flow is used, the vitrinite reflectance and temperature values are in good correlation. Hanadir maturity curve is shown in Figure 4.20 C. It shows on the y-axis vitrinite reflectance and on the x-axis is the geological time scale, it clearly illustrates the organic matter during the Ordovician time is not mature and it enters early mature to late mature stage during Silurian time. The thermal maturation of Hanadir is gradually increased till reach to over-mature stage at the present day (1.5 % VR). The burial history curve of well-A is shown in (Fig 4.21). The well was modeled with a heat flow value of 72 mW/m^2 , the maximum burial depth is attained in during Silurian and Devonian. Hanadir temperature is around $100 - 120 ^\circ\text{C}$ which may indicates rapid sedimentation rate and hydrocarbon generation. All integrated results obtained from Rock-Eval, basin modeling and kerogen thermal alteration index confirmed the Hanadir source rock is in gas generation or over-mature stage as indicated by low HI ,high T_{max} , high vitrinite reflectance and temperature measurements.

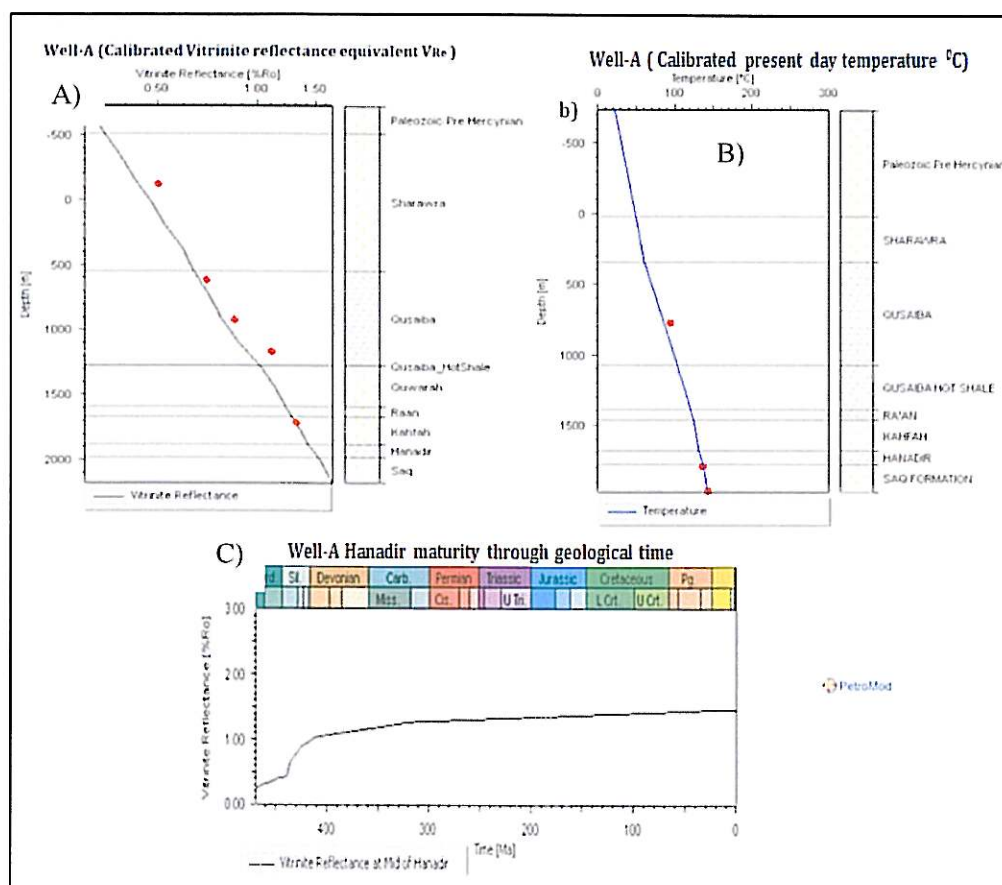


Figure 4.20: Temperature and vitrinite reflectance calibration for well-A. A) Showing very good calibration of predicted and measured vitrinite reflectance (VRe) model. B) Showing excellent correlation with present day temperature (°C), when applying heat flow scenario of (72 mW/m²). C) Predicted vitrinite reflectance (VR) showing increased Hanadir thermal maturation through geological time, it keeps increasing till reach high level of thermal maturity at present day.

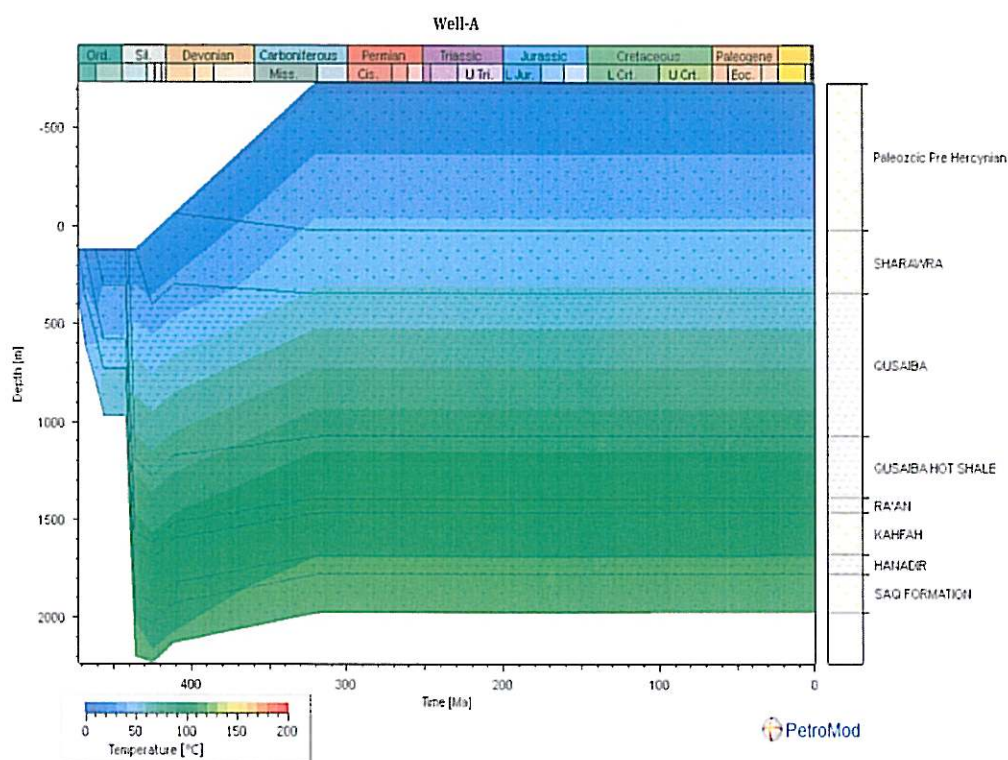


Figure 4.21: Burial history of well -A showing depth versus time for all geological layers. The well -A was modeled present day flow value of 72 mW/m^2 , the maximum burial depth is attained in during Silurian and Devonian. During the maximum burial, Hanadir temperature is around $100 - 120^\circ\text{C}$, which indicates rapid sedimentation rate and hydrocarbon generation

4.4.5 Thermal and Burial History of Well-B

Figures 4.22 A and B displayed vitrinite and temperature data versus subsea depth in meters. The vitrinite data are shown in solid rectangles and represent graptolites reflectance. The temperature calibration are shown in solid circles and they were all corrected using the Horner method based on the original bottom – hole temperature. When the second scenario of heat flow is used, the vitrinite reflectance and temperature values are in good correlation. Hanadir maturity curve is shown in Figure 4.22 C. It shows on the y-axis vitrinite reflectance and on the x-axis is the geological time scale, it clearly illustrates the organic matter during Ordovician time is not mature and it enters maturation stage during Middle Silurian time. The thermal maturation of Hanadir is gradually increased till reach to over-mature stage at the present day (1.5 % VR). The burial history curve of well-B is shown in (Fig 4.23). The well was modeled with a heat flow value of 72 mW/m^2 , the maximum burial depth is attained in during Silurian and Carboniferous. Hanadir temperature is around $140 - 170 ^\circ\text{C}$ which may indicate rapid sedimentation rate and hydrocarbon generation. In comparison the level of the thermal maturation of well-B is higher than observed in well-A.

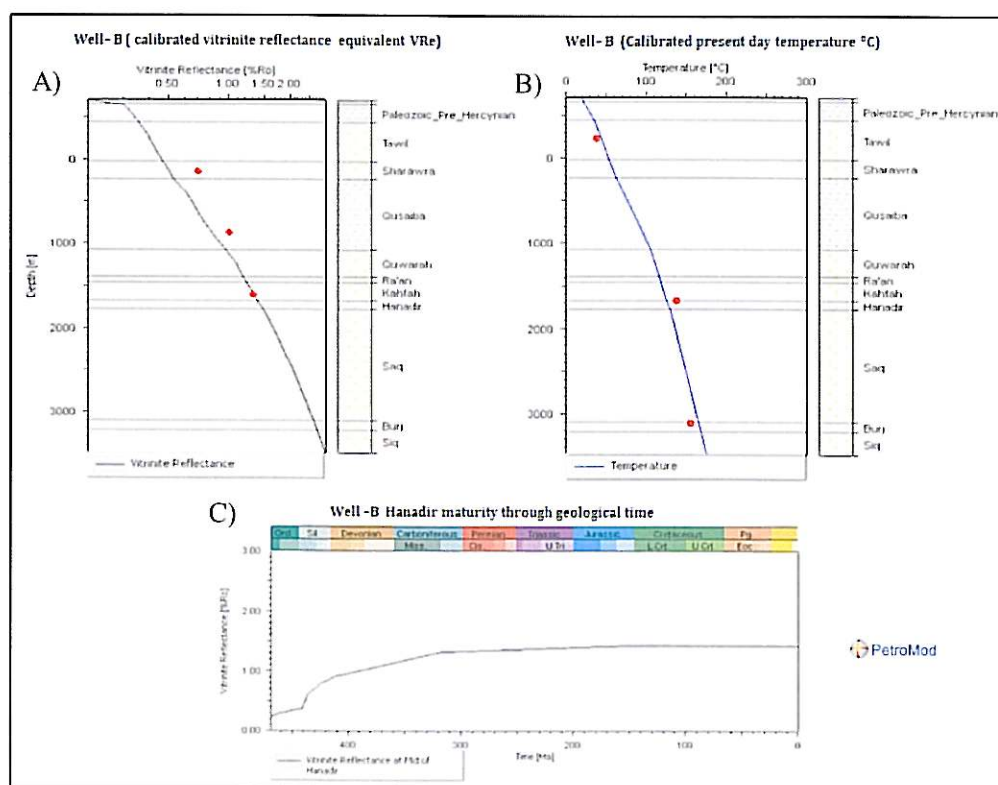


Figure 4.22: Temperature and vitrinite reflectance calibration for well-B. A) Showing good calibration of predicted and measured vitrinite reflectance (VRe) model. B) Showing very good correlation with present-day temperature ($^{\circ}\text{C}$) when applying heat flow scenario of (72 mW/m^2). C) Predicted vitrinite reflectance (VR) showing increased Hanadir thermal maturation through geological time.

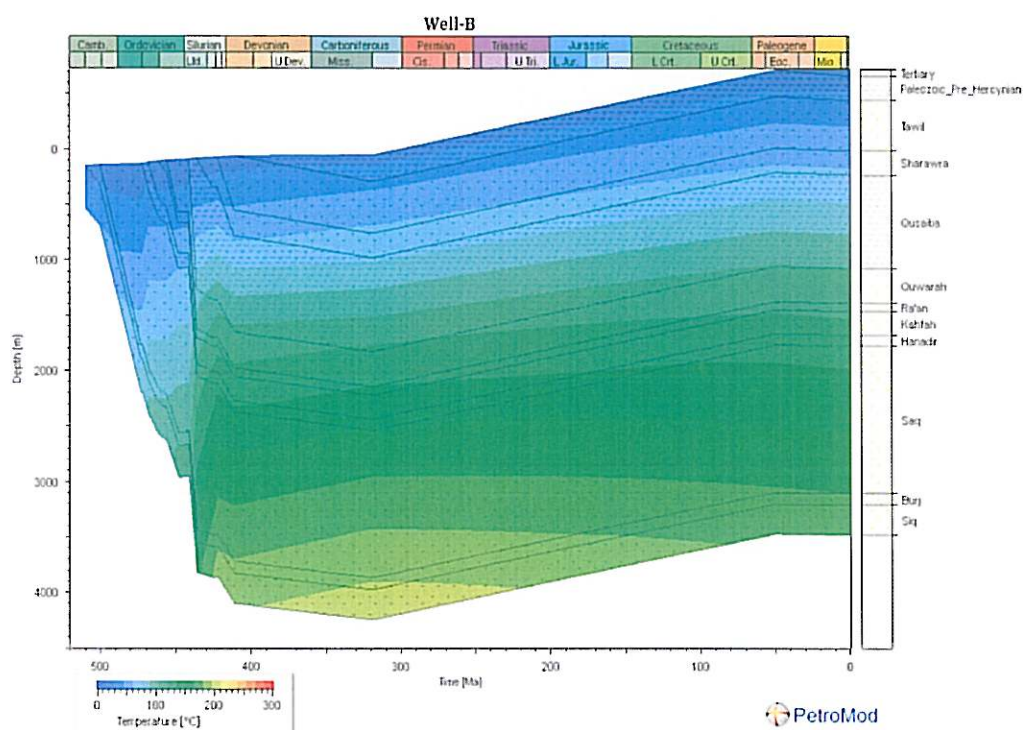


Figure 4.23: Burial history of well -A showing depth versus time for all geological layers. The well -A was modeled present day flow value of 72 mW/m^2 , the maximum burial depth is attained in during Silurian and Carboniferous. During the maximum burial, Hanadir temperature is around $140 - 170^\circ\text{C}$ which may indicate rapid sedimentation rate and hydrocarbon generation.

4.4.5 Thermal and Burial History of Well-C

The numerical simulation 1D model of Well-C has revealed distinctive results from other wells. The present day heat flow prediction of (62.42 mW/m^2) was applied to well-C which showed very good correlation with calculated present day temperature (Fig4.24). Localize basaltic sills has been reported from many wells in the Northwest of Saudi Arabia, also it has been reported from Qusaiba and Quwarah of well-C. Lithology based-log calculation from well-C was used to identify basaltic sill that was encountered in the middle of the Hanadir member. This localized intrusion possibly occurred during volcanism and rifting at late Devonian time (Sharland et al., 2000)

Figures 4.24 A and B displayed vitrinite and temperature data versus subsea depth in meters. When the second scenario of heat flow is applied, the temperature values are in good correlation.

In well-C there is no available graptolite reflectance measurement. However, the increased of thermal maturity has been noticed at the zone of intrusion.it increased dramatically from 0.5 % VR before the intrusion to 1.3% VR at the zone of intrusion. (Fig 4.24 B). All sills may have a local effect on rocks immediately above and below them; although the intrusion assumed to have negligible effect on regional heat flow. Burial history model suggests that the sediments were deposited at maximum burial depth, although the predicted temperature and vitrinite reflectance are indicating minimal effect of hydrocarbon thermal maturation (Fig 4.25)

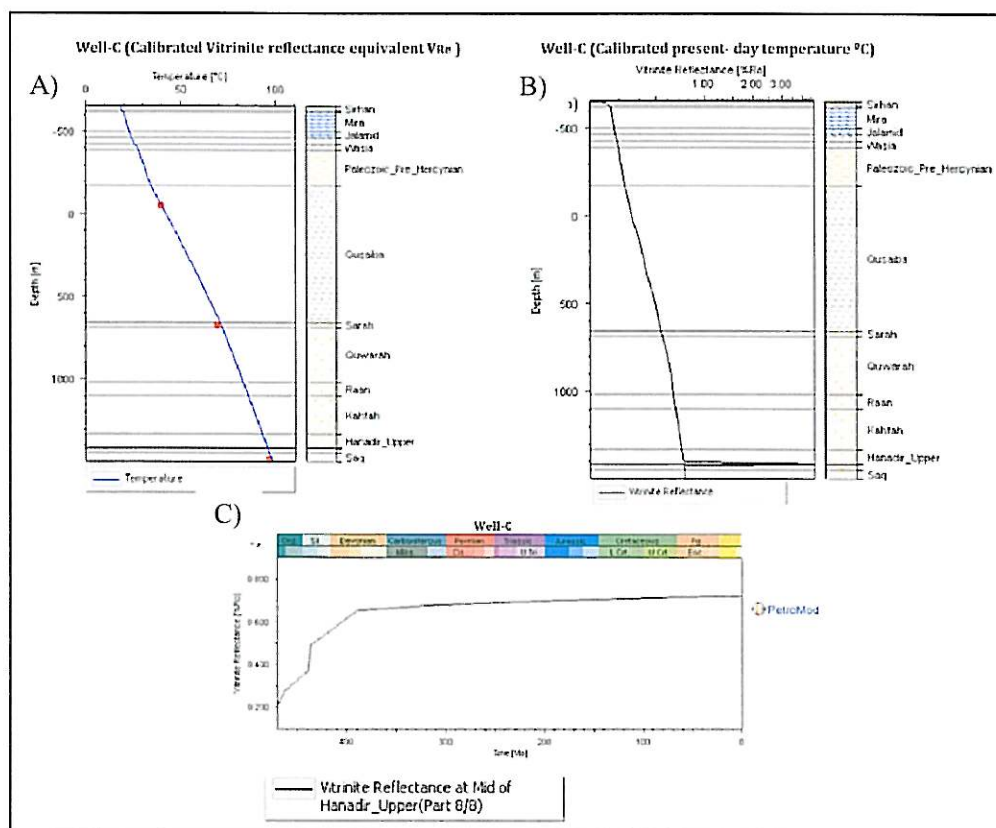


Figure 4.24: A) Showing the close calibration of predicted and measured vitrinite reflectance (VRe) model. (B) Showing excellent correlation with present-day temperature ($^{\circ}\text{C}$) applying heat flow scenario of (62.42 mW/m^2). C) Showing the non-calibrated vitrinite reflectance equivalents (VRe), the result of this model is not conclusive due to lack of vitrinite calibration data.

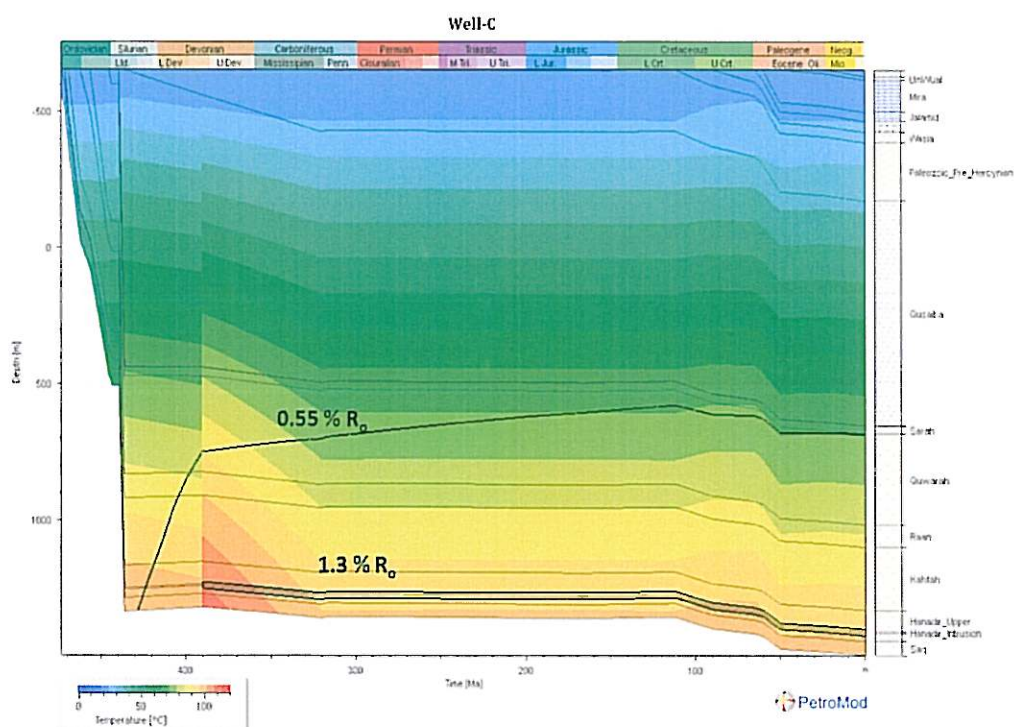


Figure 4.25: numerical simulation of 1D model showing the basin evolution, where the basin had reached the maximum burial depth during (Silurian-Devonian) ages, the high temperature prediction has been affected by zone of intrusion , the isotherm lines are ranging between (0.55 - 1.3 VRe) , which indicate increasing of thermal maturity of hydrocarbon in contact with igneous intrusion.

The Rock- Eval pyrolysis results suggest that well – C has been affected by contamination which caused low values of T_{max} , high values of PI, and SI. Possibly the two samples with high values of T_{max} (494 and 507 °C) were only the two samples survived from contamination effect and may reflect the actual values of T_{max} . (Fig 4.26 A). Also the values of oxygen index (OI) suggest that the organic matter has been oxidized which imply the source rock preservation conditions was not optimal as indicated by *Psammosphaera* and *placopsilina* species that were adapted to dysoxic conditions.

The zone of intrusion is highlighted with orange color bar, the zone of intrusion was identified based on lithology based-log calculation and recognized igneous fragments shown in (Fig 4.26 A and C). This zone apparently was affected by two different effects. One effect was igneous intrusion during late Devonian time and the second one was contamination which was lately introduced by drilling additives.

Igneous intrusion definitely has a great impact on source rock that in contact with that intrusion. This intrusion can be imagined as a natural pyrolysis phenomenon that caused rapid thermal cracking of organic matter to produce hydrocarbon. The hydrocarbon at the zone of intrusion is spent and nothing left to produce, due to high temperature of intrusion. In addition to predicted vitrinite reflectance confirmed over-mature stage of thermal maturity at zone of intrusion (Fig 4.26 A and B).

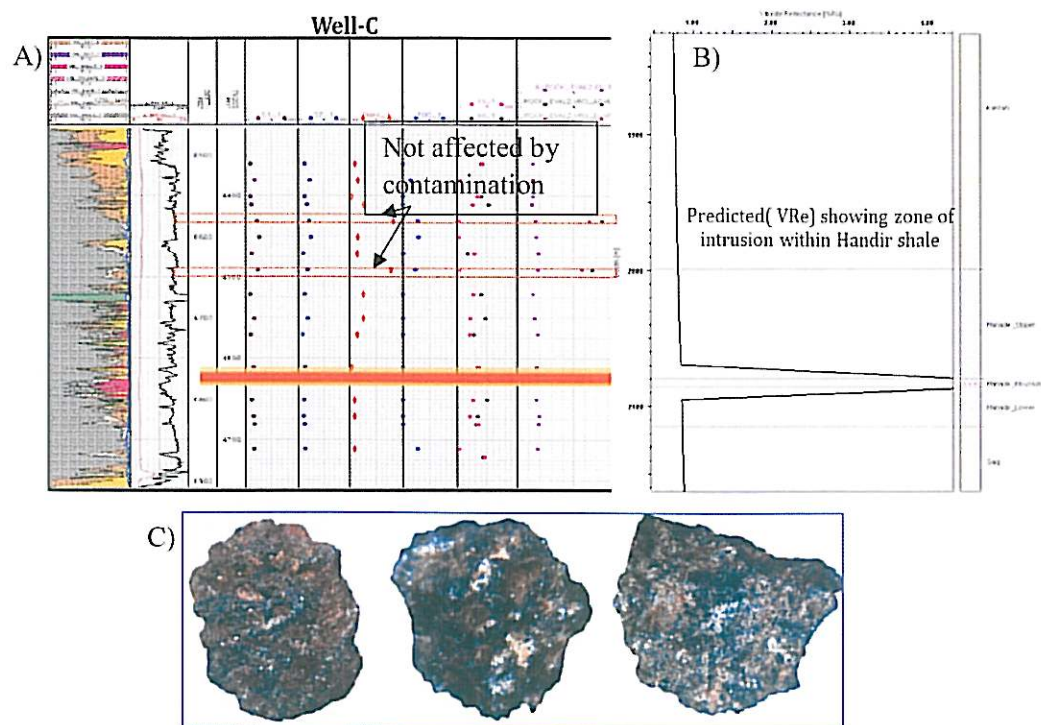


Figure 4.26: (A showing the integrated interpretation of igneous intrusion identified by lithology-log derived calculation in the middle of Hanadir shale. B) Showing increased predicted vitrinite reflectance values of (0.7 – 4 % VR) as indication of extremely high level of thermal maturation at the zone of intrusion. C) Photo of recognized igneous fragments from cutting samples has igneous intrusion features

CONCLUSIONS

The organic matter of Hanadir member in wells A and B is preserved in anoxic conditions, where in well C it was not preserved in total anoxic bottom water conditions; it may be exposed seasonally to dysoxic and oxic conditions. As oxygenated bottom waters, coupled with low organic productivity in well C, it ultimately resulted in accumulation of poor to marginal generative potential. Geochemically the present day organic matter of Hanadir can be correlated with present day organic matter of Hiswa formation in Jordan because they both are highly mature type II kerogen with range of total organic carbon between 0.05 -2.98% (TOC) in Hanadir and 0.5 -1.5% (TOC) in Hiswa Formation and consider to be the main source of gas in Jordan. Furthermore all integrated results obtained from Rock-Eval of wells A and B indicates the source rock of the Hanadir is in gas generation window as indicated by low HI ,high T_{max}, high vitrinite reflectance and present day temperature which implies Hanadir member is possibly another candidate Paleozoic source rock to be the main source of gas in Northwest of Saudi Arabia.

Rock-Eval pyrolysis is insufficient tool to determine type of kerogen, especially for highly mature source rock. Interestingly the challenge of determining kerogen type of the Hanadir can be overwhelmed indirectly by utilizing the relationship of depleted oxygen environment of agglutinated, benthic foraminifera and source rock organic facies. Accordingly, this approach indicates that Hanadir source rock represents type II

kerogen; it is also regionally consistent with Hanadir source rock equivalents in adjacent countries such as Syria, Jordan and Iraq.

Values of (60-72 mW/m²) was the best heat flow scenario was applied to create 1D models and show very good match between vitrinite reflectance and present day bottom hole temperature values. Distinctively a localized igneous intrusion was encountered within Hanadir shale at Well-C. This intrusion can be imagined as a natural pyrolysis phenomenon that caused rapid thermal cracking of organic matter to produce hydrocarbon. The hydrocarbon at the zone of intrusion possibly is spent and nothing left to produce.

RECOMMENDATIONS

- This study was conducted on three selected wells close to Al-Jawf graben. It is first step for extensive geochemical study. It will have a great impact on exploration activities if further geochemical study is conducted toward Jalamid area, where thick sediments of Qasim Formation is considered to be existed. It may reveal very optimistic results for Handir source rock potential.
- Recovered subsurface cuttings and cores samples are not enough to get the complete picture about depositional environment and abundance of agglutinated foraminifera, it will be beneficial if a similar study is applied on Hanadir outcrop section to establish a correlation and examine the diversity between agglutinated foraminifera from subsurface with one recovered from outcrops.
- The fundamental process is to establish agglutinated foraminifera diversity curve and identify exactly the maximum flooding surface (MFS) within Hanadir.
- Agglutinated foraminifera are a good tool to identify the depositional environment through the taxa description and their response to an oxygen depleted environment. It is extremely important to integrate this tool with the source rock Rock-Eval pyrolysis tool, to able to determine the poor and excellent source rock quality.
- Create structural restoration model is an essential to support the basin modelers to understand evolution of geological structures through geological times.

REFERENCES

- Abu Ali and Ralf Littke 2005. Paleozoic petroleum system of Saudi Arabia: a basin modeling approach. *GeoArabia*, v.10, p.131-168.
- Al-Laboun, A. 1986. Stratigraphy and Hydrocarbon Potential of the Paleozoic Succession in Both Tabuk and Midyan Basins, Arabia. *American Association of Petroleum Geologists Bulletin*, v. 40, p. 373-397.
- Al-Laboun, AA. 1993. Lexicon of Paleozoic and lower Mesozoic of Saudi Arabia, Part 1. Lithostratigraphic Units, Nomenclature Review. Al-Hudhud Publishers, Riyadh, Saudi Arabia 509 p.
- Al-Hajri, S 1995. Biostratigraphy of the Ordovician chitinozoa of northwestern Saudi Arabia. In Owens, H., Al-Tayyar, J.G.L.A. Van der Eem and S. Al-Hajri (Eds.), *Paleozoic palynostratigraphy of the Kingdom of Saudi Arabia, review of Paleobotany, Special Issue*, v.89, no.1/2 p.27-48.
- Al-Sharhan, A .S. and A.E.M. Narin, 1997. *Book of sedimentary basins and petroleum geology of the Middle East*
- Aqrabi, A.A.M., 1998, Paleozoic stratigraphy and petroleum system of the western and southwestern deserts of Iraq: *GeoArabia*, v.3, p.229-247.

Al-Hajri, S., Owens, B., 2000. Sub-surface palynostratigraphy of the Palaeozoic of Saudi Arabia. In: Al- Hajri, S., Owens, B. (Eds.), *Stratigraphic Palynology of the Palaeozoic of Saudi Arabia*. Special Geoarabia Publication 1, Gulf Petrolink, Bahrain, pp. 10–17

Al-Hadidy, A. 2007. Paleozoic stratigraphic lexicon and hydrocarbon habitat of Iraq. *Geoarabia*, v.12, no.1, pp. 63-130.

Clark-Lowes, D.D. 1980. Sedimentology and mineralization potential of the Saq and Tabuk Formations, Al-Qasim District. Imperial College of Science and Technology, Cover Rock Contract, Open-File Report CRC/1C-7, Saudi Arabian Deputy Ministry for Mineral Resources, Open-File Report DGMR-767, 88 p.

Cherchi, A. & Schroeder, R. 1984/1985. Middle Cambrian Foraminifera and other Microfossils from SW Sardinia. *Italian Paleontological Society*, v. 23, no.19, p.149-160.

Cole Gary A. 1994. Graptolite-Chitinozoan Reflectance and Its Relationship to Other Geochemical Maturity Indicators in the Silurian Qusaiba Shale, Saudi Arabia. *Energy & Fuels* v. 8, p. 1443-1459.

Clark-Lowes, D.D. 2005. Arabian glacial deposits: recognition of palaeovalleys within the Upper Ordovician Sarah Formation, Al Qasim district, Saudi Arabia. *Proceedings of the Geologist's Association*, 116, 331–347.

Cornford 2004., *The petroleum system Encyclopedia of Geology*. Elsevier, Oxford, p.268-294.

- El-Khayal, A.A., Romano, M., 1985. Lower Ordovician trilobites from the Hanadir Shale of Saudi Arabia. *Palaeontology* 28, 401–412.
- Helal, A.H. 1965. General geology and lithostratigraphic subdivision of the Devonian rocks of the Jaufarea, Saudi Arabia. *Neues Jahrbuch fur Geologie und Palaeontologie, Monatshefte* 9, p. 527–551.
- Konert, G., Afifi, A.M., Al-Hajri, S.A., de Groot, K., Al Naim, A.A., and Droste, H.J. The Paleozoic stratigraphy and hydrocarbon habitat of the Arabian Plate, in *Petroleum Provinces of the Twenty-first Century*, M.W. Downey, J.C. Threet, and W.A. Morgan, eds., The Pratt Conference II, AAPG Memoir no. 74.
- Lopatin, N.V. 1971. Temperature and geologic time as factors in coalification. *Akad. Nauk SSSR Izvestiya, Seriya Geologicheskaya*, v.3, p. 95-196 (in Russian).
- Loeblich, A.R. & Tappan, H.N. 1987. Foraminiferal genera and their classification. Van Nostrand Reinhold Company, 2 v., 970 pp., 847 pl., New York.
- Le Nindre Y.M., D. Vaslet, J. Le Metour, J. Bertrand and M. Halawani, 2003. Subsidence modeling of the Arabian Platform from Permian to Paleogene outcrops. *Sedimentary Geology*, v. 11, no.3, p. 325-338
- McClure, H.A. 1978. Early Paleozoic glaciation in Arabia. *Palaeogeography, Palaeoclimatology, Palaeoecology*, v. 25, p. 315–326.
- McClure, H.A. 1988. Chitinozoan and acritarch assemblages, stratigraphy and biogeography of the early Paleozoic of northwest Arabia. *Review of Paleobotany and Palynology*, v. 56, p. 41–60.

McGillivray, J.G., and M.I. Husseini 1992. The Paleozoic petroleum geology of central Arabia. AAPG Bull., v. 76, p 1473–1490.

Magoon, L.B. and W.G. Dow 1994. The petroleum system. In: Magoon and Dow (Eds.), The petroleum system from source to trap. American Association of Petroleum Geologists Memoir 60.

Nestell, G., Heredia, S., Mestre, A., Beresi, M., Gonzalez, M., 2011, The oldest Ordovician foraminifers (*Oepikodus evae* conodont Zone, Floian) from South America. *Geobios*. v. 44, p 601–608.

Peters, K.E., 1968, Guidelines for evaluating petroleum source rock using programmed pyrolysis: AAPG Bulletin, v. 70, p. 318–329

Paris, F., Elaouad-Debbaj, Z., Jaglin, J.C., Massa, D., Oulebsir, L., 1995. Chitinozoans and Late Ordovician glacial events on Gondwana. In: Cooper, J.D., Droser, M.L., Finney, S. (Eds.), *Ordovician Odyssey*, Short papers Seventh International Symposium on the Ordovician System, Society of Economic Paleontologists and Mineralogists, Fullerton, CA, p. 171–176.

Paris, F., Bourahrouh, A., Le H'e, A., 2000a. The effects of the final stages of the Late Ordovician glaciation on marine palynomorphs (chitinozoans, acritarchs, leiosphaeres) in well N1-2 (NE Algerian Sahara). *Review of Palaeobotany and Palynology* 113, 87–104.

Paris, F., Verniers, J., Al-Hajri, S., 2000b. Ordovician chitinozoans from Central Saudi Arabia. In: Al-Hajri, S., Owens, B. (Eds.), *Stratigraphic Palynology of the Palaeozoic of Saudi Arabia*. Special GeoArabia Publication 1, Gulf PetroLink, Bahrain, pp. 42–56.

Staplin, F.L., 1969. Sedimentary organic matter, organic metamorphism, and oil and gas occurrence. *Bull. Can. Petrol. Geol.*, v. 17, p. 47-66.

Senalp, M., and A.A. Al-Duaiji 1996. Stratigraphy and sedimentology of the storm and tide-dominated shallow marine siliciclastic members of the Qasim Formation, Qasim region, Saudi Arabia. 2nd Middle East Geosciences Conference, GEO'96, Abstracts. *GeoArabia*, v. 1, no. 1, p. 192.

Senalp, M. and A. Al-Laboun. 1996. Stratigraphy and Age of the Glacial Deposits in Qasim Region, Central Arabia. *GeoArabia Middle East Petroleum Geosciences*, v. 1, no. 1, p. 192-193.

Sharland, P.R., R. Archer, D.M. Casey, R.B. Davies, S. Hall, A. Heward, A. Horbury and M.D. Simmons 2001. *Arabian Plate Sequence Stratigraphy*. *GeoArabia Special Publication SP-2*, Gulf PetroLink, Bahrain, 371 p., with 3 charts.

Senalp, M., Al-Duaiji, A.A., 2001. Qasim Formation: Ordovician storm-and tide dominated shallow-marine siliciclastic sequences, Central Saudi Arabia. *GeoArabia* 6, 233–268.

Scott.D.B, Medioli .F and Braund.R., 2003. Foraminifera from the Cambrian of the Nova Scotia: The Oldest Multichambered Foraminifera. *Micropaleontology* v. 49, no.2 p. 109-126.

Ungerer, P., J. Burrus, b. Doligez, P.Y. Chenet and F. Bessis 1990. Basin evolution by integrated two-dimensional modeling of heat transfer, fluid flow, hydrocarbon generation, and migration. American Association of Petroleum Geologists Bulletin v.74,p.309-335.

Vaslet, D., Kellogg, K.S., Berthiaux, A., Le Strat, P., Vincent, P.-L., 1987. Explanatory notes to the geologic map of the Baq'a Quadrangle, Kingdom of Saudi Arabia. Geoscience Map GM-116C, scale 1:250,000 Sheet 27F. Deputy Ministry for Mineral Resources, Ministry of Petroleum and Mineral Resources, Kingdom of Saudi Arabia, 1–45.

Vecoli, M., 1999. Cambro-Ordovician palynostratigraphy (acritarchs and prasinophytes) of the Hassi-R'Mel area and northern Rhadames Basin, North Africa. *Palaeontographia Italica* 86, 1–112.

Yalcin, N.M., R. Littke and R.F.Sachsenhofer 1997. Thermal history of sedimentary basins. In, Welte, D.H. et al. (Eds.), *Petroleum and basin evolution*, Springer, Berlin, P.71-168.

APPENDIX

Well A Rock- Eval data														
Depth	Formation	Sample Type	(S1)	(S2)	(Tmax)	S3	TOC	HI	OI	PI	BF-TOC	S2/S3	*VreJV	*VreGU
7850	Hanadir Shale	Cuttings	0.13	0.69	450.9	0.85	1.00	69	85	0.16		0.81	0.96	0.99
7860	Hanadir Shale	Cuttings	0.15	0.33	448.7	0.75	0.73	45	103	0.31		0.44	0.92	0.94
7880	Hanadir Shale	Cuttings	0.23	0.56	449.3	0.77	1.04	54	74	0.29		0.73	0.93	0.95
7890	Hanadir Shale	Cuttings	0.23	0.46	452.7	0.79	0.81	57	98	0.33		0.58	0.99	1.03
7920	Hanadir Shale	Cuttings	0.26	0.63	450.4	0.81	1.18	53	69	0.29		0.78	0.95	0.98
7930	Hanadir Shale	Cuttings	0.28	0.56	450.7	0.79	1.38	41	57	0.33	1.4	0.71	0.95	0.98
7940	Hanadir Shale	Cuttings	0.20	0.28	452.6	0.82	0.87	32	94	0.42		0.34	0.99	1.03
7950	Hanadir Shale	Cuttings	0.54	0.72	448.9	0.82	2.98	24	28	0.43	1.11	0.88	0.92	0.94
7960	Hanadir Shale	Cuttings	0.40	0.76	450.9	0.75	1.13	67	66	0.34	1.4	1.01	0.96	0.99
7970	Hanadir Shale	Cuttings	0.57	0.53	451.4	0.95	1.59	33	60	0.52		0.56	0.97	1.00
7980	Hanadir Shale	Cuttings	0.51	0.55	450.8	0.76	1.30	42	58	0.48		0.72	0.95	0.99
7990	Hanadir Shale	Cuttings	0.61	0.56	460.9	0.85	1.62	35	52	0.52	1.46	0.66	1.14	1.22
8009.1	Hanadir Shale	Core	0.19	0.10	461.0	0.40	0.83	12	48	0.66		0.25	1.14	1.23
8020	Hanadir Shale	Core	0.20	0.23	465.0	0.45	1.13	20	40	0.47		0.51	1.21	1.32
8033.2	Hanadir Shale	Core	0.10	0.07	479.0	0.25	0.47	15	53	0.59		0.20	1.46	1.65
8040.5	Hanadir Shale	Core	0.15	0.11	464.0	0.28	0.84	13	33	0.58		0.39	1.19	1.30
8050.7	Hanadir Shale	Core	0.21	0.15	464.0	0.45	1.07	14	42	0.58		0.33	1.19	1.30
8061	Hanadir Shale	Core	0.18	0.15	465.0	0.22	0.92	16	24	0.55		0.68	1.21	1.32
8075	Hanadir Shale	Core	0.20	0.08	454.0	0.35	1.00	8	35	0.71		0.23	1.01	1.06
8088	Hanadir Shale	Core	0.21	0.11	468.0	0.25	1.01	11	25	0.66		0.44	1.26	1.39
8095.7	Hanadir Shale	Core	0.05	0.05	427.0	0.25	0.37	14	68	0.50		0.20	0.53	0.43
8103.9	Hanadir Shale	Core	0.26	0.20	466.0	0.45	1.23	16	37	0.57		0.44	1.23	1.34
8147	Hanadir Shale	Core	0.23	0.26	476.0	0.75	1.16	22	65	0.47		0.35	1.41	1.58
8160.4	Hanadir Shale	Core	0.09	0.14	473.0	0.55	0.64	22	86	0.39		0.25	1.35	1.51
8178	Hanadir Shale	Core	0.24	0.20	473.0	0.72	1.00	20	72	0.55		0.20	1.35	1.51
8188.9	Hanadir Shale	Core	0.16	0.14	463.0	0.76	0.89	16	85	0.53		0.18	1.17	1.27
8191.6	Hanadir Shale	Core	0.20	0.13	460.0	0.76	1.16	11	66	0.61		0.17	1.12	1.20
8196.5	Hanadir Shale	Core	0.20	0.17	462.0	0.76	1.41	12	54	0.54		0.22	1.16	1.25

Well B Rock-Eval data														
Depth	Formation	Sample Type	S1	S2	Tmax	S3	TOC	HI	OI	PI	BF-TOC	S2/S3	*VreJV	*VreGU
7550	Hanadir Shale	Cuttings	0.10	0.32	429	0.40	0.69	46	58	0.24		0.8	0.56	0.48
7550	Hanadir Shale	Cuttings	0.15	0.20	507.7	0.32	0.42	48	76	0.43		0.6	1.98	2.32
7560	Hanadir Shale	Cuttings	0.19	0.24	493.8	0.33	0.76	32	43	0.44		0.7	1.73	1.99
7600	Hanadir Shale	Cuttings	0.27	0.33	484.9	0.33	0.97	34	34	0.45		1.0	1.57	1.79
7620	Hanadir Shale	Cuttings	0.24	0.20	481.9	0.35	1.04	27	34	0.46		0.8	1.51	1.71
7630	Hanadir Shale	Cuttings	0.23	0.29	492.3	0.36	1.05	28	34	0.44		0.8	1.70	1.96
7640	Hanadir Shale	Cuttings	0.22	0.21	487.7	0.33	1.02	21	32	0.51		0.6	1.62	1.85
7650	Hanadir Shale	Cuttings	0.18	0.26	495.7	0.37	0.79	33	47	0.41		0.7	1.76	2.04
7660	Hanadir Shale	Cuttings	0.16	0.26	490.1	0.37	0.75	35	49	0.38		0.7	1.66	1.91
7680	Hanadir Shale	Cuttings	0.12	0.21	495.8	0.36	0.54	39	67	0.36		0.6	1.76	2.04
7720	Hanadir Shale	Cuttings	0.12	0.20	492.2	0.39	0.63	32	62	0.38		0.5	1.70	1.96
7730	Hanadir Shale	Cuttings	0.18	0.22	489.4	0.38	0.89	25	43	0.45		0.6	1.65	1.89
7740	Hanadir Shale	Cuttings	0.18	0.28	490.8	0.39	0.94	30	41	0.39		0.7	1.67	1.92
7750	Hanadir Shale	Cuttings	0.18	0.39	480	0.24	0.48	81	50	0.32		1.6	1.48	1.67
7750	Hanadir Shale	Cuttings	0.20	0.26	493.5	0.36	1.10	24	33	0.43		0.7	1.72	1.99
7760	Hanadir Shale	Cuttings	0.21	0.26	492.4	0.41	1.15	23	36	0.45	1.29	0.6	1.70	1.96
7770	Hanadir Shale	Cuttings	0.20	0.29	490.1	0.43	1.14	25	38	0.41		0.7	1.66	1.91
7780	Hanadir Shale	Cuttings	0.21	0.25	485.6	0.39	1.06	24	37	0.46		0.6	1.58	1.80
7790	Hanadir Shale	Cuttings	0.21	0.27	486.9	0.40	1.05	26	38	0.44		0.7	1.60	1.83
7800	Hanadir Shale	Cuttings	0.18	0.25	486.8	0.37	1.04	24	36	0.42		0.7	1.60	1.83
7810	Hanadir Shale	Cuttings	0.24	0.29	501.1	0.40	1.24	23	32	0.45		0.7	1.86	2.16
7820	Hanadir Shale	Cuttings	0.22	0.30	488.8	0.41	1.29	23	32	0.42	1.5	0.7	1.64	1.88
7830	Hanadir Shale	Cuttings	0.22	0.29	495.9	0.40	1.39	21	29	0.43	1.84	0.7	1.77	2.04
7840	Hanadir Shale	Cuttings	0.24	0.33	485.6	0.38	1.35	24	28	0.42		0.9	1.58	1.80

Well C Rock-Eval data														
Depth	Formation	Sample Type	S1	S2	Tmax	S3	TOC	HI	OI	PI	BF-TOC	S2/S3	*Vre JV	*Vre GU
6510	Hanadir Shale	Cuttings	0.10	0.13	324.0	0.34	0.04	325	850	0.43		0.38		
6530	Hanadir Shale	Cuttings	0.18	0.23	338.4	0.73	0.77	30	95	0.44		0.32		
6550	Hanadir Shale	Cuttings	0.10	0.13	307.0	0.28	0.04	325	700	0.43		0.46		
6560	Hanadir Shale	Cuttings	0.12	0.17	366.0	0.21	0.04	425	525	0.41		0.81		
6580	Hanadir Shale	Cuttings	0.22	0.22	504.5	0.87	1.41	16	62	0.50	1.4	0.25	1.92	2.24
6600	Hanadir Shale	Cuttings	0.27	0.25	338.0	0.92	1.50	17	61	0.52	1.47	0.27		
6620	Hanadir Shale	Cuttings	0.13	0.10	336.0	0.41	0.07	143	586	0.57		0.24		
6640	Hanadir Shale	Cuttings	0.24	0.19	494.0	0.88	1.19	16	74	0.56	1.68	0.22	1.73	2.00
6670	Hanadir Shale	Cuttings	0.10	0.13	364.0	0.22	0.04	325	550	0.43		0.59		
6700	Hanadir Shale	Cuttings	0.17	0.19	364.0	0.22	0.05	380	440	0.47		0.86		
6720	Hanadir Shale	Cuttings	0.11	0.09	336.0	0.17	0.04	225	425	0.55		0.53		
6760	Hanadir Shale	Cuttings	0.16	0.14	310.0	0.36	0.05	280	720	0.53		0.39		
6770	Hanadir Shale	Cuttings	0.04	0.04	327.0	0.34	0.02	200	1700	0.50		0.12		
6800	Hanadir Shale	Cuttings	0.13	0.12	322.0	0.16	0.03	400	533	0.52		0.75		
6820	Hanadir Shale	Cuttings	0.16	0.11	322.0	0.17	0.04	275	425	0.59		0.65		
6830	Hanadir Shale	Cuttings	0.18	0.13	293.0	0.35	0.05	260	700	0.58		0.37		
6860	Hanadir Shale	Cuttings	0.17	0.14	322.7	0.95	1.41	10	67	0.55	1.36	0.15		
6870	Hanadir Shale	Cuttings	0.16	0.14	305.0	0.37	0.04	350	925	0.53		0.38		

VITA

Assad Hadi Ali Ghazwani was born in Riyadh, Kingdom of Saudi Arabia. He joined King Abdulaziz University (KAAU) in 2000. He earned his B.Sc. degree in Petroleum Geology in 2004. He obtained training opportunities with Saudi Aramco through summer training program (2003 and 2004). In September 2004, he joined Saudi Aramco. He started the Master degree program at KFUPM in 2007. He was certified expert trainer in July, 2008 from Gulf Board Human Development. He joined Aramco specialist development program (SDP) in 2009. During (2010-2011), he became a member of the executive committee of Dhahran Geological Society (DGS) as responsible for public relations. He was the first Geochemist participate in basin and petroleum system dynamics program with Jacobs University in Bremen, Germany. During his master degree research project he discovered the oldest Paleozoic agglutinated foraminifera in the Arabian plate so far with support from Dr. Mikael Kaminski; this discovery was documented and presented to international workshop of agglutinated foraminifera (IWAF-9) during Sept, 2012 at University of Zaragoza, Spain. He received his Master degree in Geology in November 2012.

Address: Saudi Aramco, Dhahran 31311, P.O. Box 1063, Saudi Arabia

E-mail: assad.gazwani@aramco.com